NASA CR-120823

STRESS CORROSION CRACKING AND FATIGUE CRACK GROWTH STUDIES PERTINENT TO SPACECRAFT AND BOOSTER PRESSURE VESSELS

THE **BOEING** COMPANY

Prepared For

NATIONAL AERONAUTICS AND SPACE ADMINISTRATION

NASA Lewis Research Center

Contract NAS 3-12003

Gordon T. Smith, Project Manager

1. Report No. NASA CR-120873	2. Government Accession No.	3. Recipient's Catalog No.
4. Title and Subtitle Stress Corrosion Cracking and Fatigue Crack Growth Studies Pertinent to Spacecraft and Booster Pressure Vessels		5. Report Date December 1972
		6. Performing Organization Code
7. Author(s) L.R. Hall and R.W. Finger		8. Performing Organization Report No. D180-15018-1
		10. Work Unit No.
9. Performing Organization Name and Address The Boeing Company – Aerospace Group Research and Engineering Division Seattle, Washington		11. Contract or Grant No. NAS3-12003
		13. Type of Report and Period Covered Contractor Report
12. Sponsoring Agency Name and Address National Aeronautics and Space Administration Lewis Research Center Cleveland, Ohio		
		14. Sponsoring Agency Code

15. Supplementary Notes
Project Manager, Gordon T. Smith, Materials and Structures Division NASA Lewis Research Center, Cleveland, Ohio 44135

16. Abstract

This experimental program was divided into two parts. The first part evaluated stress corrosion cracking in 2219-T87 aluminum and 5Al-2.5 Sn (ELI) titanium alloy plate and weld metal. Both uniform height double cantilever beam and surface flawed specimens were tested in environments normally encountered during the fabrication and operation of pressure vessels in spacecraft and booster systems. The second part studied compatability of material-environment combinations suitable for high energy upper stage propulsion systems. Surface flawed specimens having thicknesses representative of minimum gage fuel and oxidizer tanks were tested. Titanium alloys 5Al-2.5 Sn (ELI), 6Al-4V annealed, and 6Al-4V STA were tested in both liquid and gaseous methane. Aluminum alloy 2219 in the T87 and T6E46 conditions was tested in fluorine, a fluorine-oxygen mixture, and methane. Results were evaluated using modified linear elastic fracture mechanics parameters.

17. Key Words (Suggested by Author(s)) Stress Corrosion Cracking 2219-T87 Aluminum 5Al-2.5 Sn (ELI) Titanium Weld Metals Base Metals	Surface Flaws Fracture Mechanics	18. Distribution Statement Unclassified, unlimited		
19. Security Classif. (of this report) Unclassified		20. Security Classif. (of this page) Unclassified	21. No. of Pages	22. Price* $3.00

NASA-C-168 (Rev. 6-71)

PREFACE

This report describes an investigation of stress corrosion cracking in metal tank materials performed by The Boeing Company from July 1968 to May 1971 under Contract NAS 3-12003. The work was administered by Mr. Gordon T. Smith of the NASA Lewis Research Center.

Boeing personnel who participated in the investigation include J. N. Masters, project leader; L. R. Hall, principal investigator; R. W. Finger, research engineer. Program support was provided by A. A. Ottlyk, non-hazardous environment testing; H. M. Olden, C. C. Mahnken and G. E. Vermilion, hazardous environment testing; L. Albertin, titanium welding; C. W. Bosworth, aluminum welding; E. C. Roberts, metallurgical support; and D. G. Good, technical illustrations and art work.

The information contained in this report is also released as Boeing Document D180-15018-1.

CONTENTS

CONTENTS (Cont'd)

SYMBOLS AND ACRONYMS

K_I Opening mode stress intensity factor

K_{IE} Fracture toughness obtained from tests of surface flawed specimens

K_{ISCC} Threshold stress intensity factor below which stress corrosion cracking does not occur

K_{cr} Critical stress intensity factor at which unstable crack propagation initiates

a   Crack depth of semi-elliptical surface flaw; crack length in double cantilever beam specimen; one-half crack length in center cracked specimen

a_i Value of 'a' at beginning of test

a_o Experimentally determined crack length increment added to actual crack length in double cantilever beam specimens to account for the effect of arm rotation on compliance

a_f Value of 'a' at termination of test

b   Specimen width for double cantilever beam specimens

b_n Crack width in double cantilever beam specimen

2c   Crack length at specimen face for semi-elliptical surface flaw

E   Young's modulus

h   One half specimen depth of double cantilever beam specimen

I   Moment of inertia of double cantilever beam specimen arm = $bh^3/12$

P   Load applied to test specimen

SYMBOLS AND ACRONYMS (Con't.)

ϕ Complete elliptical integral of the second kind corresponding to the modulus $k = \left[(c^2 - a^2) / c^2 \right]^{1/2}$

σ Uniform tensile stress acting perpendicular to plane of crack

σ_{ys} Uniaxial tensile yield stress

Q $\phi^2 - 0.212 (\sigma/\sigma_{ys})^2$

t Gage area thickness of test specimen

W Gage area width of test specimen

μ Poisson's ratio

M_K Scalar factor depending on a/t and $a/2c$ used to account for effect of stress free back specimen surface on stress intensity factor for surface flaws

SCC   Stress corrosion cracking

WR
WT
RW
RT   Crack propagation directions (See Figure 2-16)

SF   Surface flaw

DCB   Double cantilever beam

TM   Test medium

MEK   Methyl Ethyl Ketone

MA   Mill Annealed

LIST OF FIGURES

LIST OF FIGURES (Cont'd)

LIST OF FIGURES (Cont'd)

LIST OF FIGURES (Cont'd)

LIST OF TABLES

LIST OF TABLES (Cont'd)

LIST OF TABLES (Cont'd)

SUMMARY

This experimental program is one in a series of programs undertaken to develop and refine methods for estimating minimum performance capabilities of metallic pressure vessels with emphasis being placed on aerospace applications. The resulting methods reflect the knowledge that crack-like defects in new structure can grow under the influence of loads and environment to a size sufficiently large to initiate failure, and are based on fracture strength and subcritical crack growth data from tests of pre-cracked specimens. Previous programs were devoted to studies of fatigue and sustained load subcritical crack growth in the environments of ambient air, liquid nitorgen, and liquid hydrogen. This program was directed to a study of stress corrosion cracking (SCC) in metallic alloys. Results were evaluated using modified linear elastic fracture mechanics parameters so that effects of SCC can be properly accounted for in estimates of minimum performance capabilities of metallic pressure vessels. The experimental work was divided into two parts.

The first part of this program was undertaken to evaluate SCC in both parent and weld metal 2219-T87 aluminum and 5Al-2.5 Sn (ELI) titanium alloys. Each alloy was tested in environments encountered during the fabrication and operation of aerospace pressure vessels including cleaners, dye penetrants, fuels, oxidizers, and pressurizing gases. Both uniform height double cantilever beam and surface flawed specimens were tested in most environments. The 5Al-2.5 Sn (ELI) titanium alloy was susceptible to SCC in a number of environments. The susceptibility was found to depend on crack propagation direction and loading procedure; the RW direction was less susceptible than the WR direction and specimens loaded in air prior to being placed in the test environment were less susceptible than were specimens that were loaded while the crack was exposed to the test environment. For the 2219-T87 aluminum alloy, test durations were not sufficiently long to allow strong indications of either the presence or lack of SCC to develop. However, some evidence of SCC was noticed in 3-1/2 percent Na Cl solution, trichloroethylene, and dye penetrant. There also was evidence that SCC can be more pronounced in surface flawed than in equal thickness through-the-thickness cracked specimens.

The second part of this program was a compatibility study for material/
environment combinations suitable for high energy upper stage propulsion
systems. Material/environment combinations tested included: 2219-T87
aluminum alloy in both liquid and gaseous fluorine, fluorine-oxygen mixture,
and methane; 2219-T6E46 aluminum alloy in liquid and gaseous fluorine and
fluorine-oxygen mixture; and titanium alloys 5Al-2.5 Sn (ELI), 6Al-4V
annealed and 6Al-4V STA in both liquid and gaseous methane. All tests were
conducted using surface flawed specimens having thicknesses representative
of minimum gage fuel and oxidizer tanks. No evidence of SCC could be
detected in any of the material/environment combinations with a SCC velocity
detection sensitivity of 10^{-5} in/hr (7×10^{-8} cm/sec).

1.0 INTRODUCTION

Stress corrosion cracking (SCC) has been a contributing factor in numerous failures of aerospace structures. As a result, considerable effort is being directed to characterization of SCC in metallic alloys. Most investigations have used macroscopic experimental observations to investigate the phenomenology of SCC. Such observations have shown that SCC behavior can be related to the stress intensity factor that is defined by modified linear elastic fracture mechanics theory.

Pressure vessel design methods have been developed (1)* for assuring that crack-like defects will not grow sufficiently to initiate failure during the operational life of pressure vessels. Present design methods are most effective when applied to pressure vessels in which critical flaw sizes at proof stress levels are less than the thickness of the vessel wall. The methods become decreasingly effective as fracture toughness increases and/or thickness decreases. The approach is based on interpretation of results of a successful proof test combined with subcritical crack growth data obtained from tests of precracked laboratory specimens. Test data are correlated and related to full size structure behavior using modified linear elastic fracture mechanics parameters.

This program was initially directed to a study of SCC in metallic alloys with the intent of evaluating the results using linear elastic fracture mechanics parameters. By doing so, it was intended to establish methods whereby SCC could be properly accounted for in estimates of minimum possible pressure vessel lives within the framework of Reference 1. The program was later expanded to include long duration tests of material/environment combinations suitable for high energy upper stage propulsion systems.

---

* Numbers in parenthesis refer to references at end of report.

This experimental program had two objectives. The first objective was to evaluate the combined effects of load and environment on SCC susceptibility of 2219-T87 aluminum and 5Al-2.5 Sn (ELI) titanium alloy base and weld metal. Each alloy was tested in environments encountered during fabrication and operation of pressure vessels in spacecraft and booster systems including cleaners, dye penetrants, fuels, oxidizers and pressurizing gases. Both uniform height double cantilever beam and surface-flawed specimens were tested under invariant loadings to determine ranges of threshold stress intensity values over which SCC would not be expected to cause significant crack growth.

The second objective was to study compatibility of material/environment combinations suitable for high energy upper stage propulsion systems. Material/environment combinations tested included: 2219-T87 aluminum alloy in both liquid and gaseous fluorine, fluorine/oxygen mixture, and methane; 2219-T6E46 aluminum alloy in liquid and gaseous fluorine and fluorine/oxygen mixture; and titanium alloys 5Al-2.5 Sn (ELI), 6Al-4V and 6Al-4V STA in both liquid and gaseous methane. All tests were conducted using surface-flawed specimens having thicknesses representative of minimum gage fuel and oxidizer tanks. Test durations ranged from 10 to 500 hours.

This experimental program is the fifth in a series of programs (2, 3, 4, 5) designed to provide methods and data for fracture control in metallic pressure vessels. Two initial programs (2, 3) defined methods for predicting minimum pressure vessel fatigue performance capabilities using tests of 2219-T87 aluminum, 2014-T62 aluminum, 5Al-2.5 Sn (ELI) titanium and 6Al-4V (ELI) titanium alloy surface-flawed specimens. The ensuing programs (4, 5) defined sustained load flaw growth characteristics of 2219-T87 aluminum and 5Al-2.5 Sn (ELI) titanium alloys in air, liquid nitrogen, and liquid hydrogen, and the effects of combined bending and tension stresses, weld-induced residual stresses, and stress fields adjacent to circular holes on fracture and fatigue growth of partially embedded flaws.

4

The remainder of this report is organized in two separate sections. Each section describes materials and procedures and presents results, discussions, and conclusions relating to a single phase of the program. Section 2 describes the investigation of stress corrosion cracking in 2219-T87 aluminum and 5Al-2.5 Sn (ELI) titanium alloys. Section 3 covers compatibility studies of material/environment combinations pertinent to high energy upper stage propulsion systems.

2.0 INVESTIGATION OF STRESS CORROSION CRACKING IN 2219-T87 ALUMINUM AND 5A1-2.5Sn(ELI) TITANIUM ALLOYS

The tests described in this section were undertaken to evaluate the combined effects of load and environment on stress corrosion cracking (SCC) susceptibility of 2219-T87 aluminum and 5A1-2.5Sn(ELI) titanium alloy base and weld metals. The test program for each alloy is summarized in Tables 2-1, 2-2 and 2-3. Each alloy was tested in environments encountered during the fabrication and operation of pressure vessels in spacecraft and booster systems including cleaners, dye penetrants, fuels, oxidizers, and pressurizing gases. Both double cantilever beam (DCB) and surface flawed (SF) specimens were tested under invariant loads. The DCB specimen was tested because of the resultant economy and convenience. The SF specimen was tested because it is the best available model of a common failure origin in aerospace pressure vessels and it was desired to compare results of the SF specimen tests with the cheaper DCB specimen tests. Tests of SF specimens in room air, liquid nitrogen and liquid hydrogen were included to allow a direct comparison between the alloy heats tested in this program with those similarly tested in a previous program (4).

It was originally planned to test only the transverse direction for the aluminum alloy and the longitudinal direction for the titanium alloy, and to load all DCB specimens in air prior to exposing them to the test environment. During the performance of the tests outlined in Tables 2-1 and 2-2, it was discovered that the transverse direction of the titanium alloy was more susceptible to SCC than was the longitudinal direction, and that the procedure of loading DCB specimens in air inhibited subsequent SCC in other environments. Accordingly, the supplemental tests outlined in Table 2-3 were added to the program. In the supplemental tests, both the longitudinal and transverse directions were tested and all specimens were loaded in the test environment.

The effect of SF specimen thickness on SCC susceptibility of the 5A1-2.5Sn(ELI) titanium alloy was investigated by conducting the tests summarized in Table 2-4.

For each thickness (0.20, 0.10 and 0.05 inch or 0.51, 0.25 or 0.13 cm), three tests were performed. One load-unload test was conducted in argon gas to evaluate the effect on flaw growth of the loading ramp used to apply the sustained loads. Two subsequent sustained load tests were conducted in methanol to evaluate thickness effects on SCC susceptibility.

2.1   Materials

Both 2219-T87 aluminum and 5A1-2.5Sn(ELI) titanium alloys were tested. The 2219-T87 plate stock, 1.0 by 48.0 by 144.0 inches (2.5 x 121.9 x 365.8 cm), was purchased from a single heat lot in the T87 condition per BMS 7-105C (equivalent to MIL-A-8920 (ASG) specification). Specification limits on chemical composition and mechanical properties measured at The Boeing Company are listed in Tables 2-5 and 2-6, respectively. Mechanical properties are plotted against temperature in Figure 2-1. The 5A1-2.5Sn(ELI) plate stock, 0.375 by 36.0 by 72.0 inches (0.95 by 91.4 by 182.9 cm), was purchased in the mill annealed condition per MIL-T-9046E. The plates were reannealed in an argon atmosphere within enclosed retorts using a 1550F (1117K), 8 hour, retort cool treatment. The resulting mechanical properties measured at The Boeing Company are listed in Table 2-6 and plotted against temperature in Figure 2-2. Certified ingot composition is given in Table 2-5.

Both aluminum and titanium welds were prepared using the GTA process. Aluminum welds were tested in the as-welded condition. Titanium welds were stress relieved at 1250F (950K) for one hour in an inert atmosphere. Mechanical properties determined at The Boeing Company for both aluminum and titanium welds are listed in Table 2-6 and are plotted against temperature in Figures 2-1 and 2-2, respectively.

Fracture toughness values for the aluminum and titanium alloy plate and titanium welds are summarized in Table 2-7; data for the aluminum alloy plate are plotted in Figure 2-3 and for the titanium alloy plate and welds in Figure 2-4. None of the reported values were obtained per ASTM standards (6) for plane strain fracture toughness tests. It has been shown (5),

8

however, that SF specimen fracture data agree with plane strain fracture toughness data obtained from ASTM recommended tests for 2219-T87 aluminum alloy plates at temperatures ranging from 72F (295K) to -423F (20K), and for 5Al-2.5Sn(ELI) titanium alloy plate at -423F (20K). For 5Al-2.5Sn(ELI) titanium alloy plate at -320F, SF specimen fracture toughness values were found (5) to exceed plane strain fracture toughness values obtained in accordance with the ASTM methods (6).

The plate material tested in this program was obtained from the same heats and rolling batches as were materials tested in a companion program (5). Since SF fracture toughness values had been previously established, only a limited number of fracture toughness tests were conducted in this program. Data from both sources are included in Table 2-7. Fracture toughness values obtained from DCB specimen tests are less than those for SF specimens at least partially because of the anisotropy of the parent plate. Appendix B includes detailed descriptions of the DCB specimen tests.

2.2   Procedures

2.2.1   Welding

All welds were prepared using the GTA welding process. Detailed weld settings are included in Appendix C and general procedures are described below.

2219-T87 Aluminum Procedures - Weld panels, 1.0 by 24 by 48 inches (2.5 by 61.0 by 121.9 cm) for SF specimens and 1.0 by 8 by 48 inches (2.5 by 20.3 by 121.9 cm) for DCB specimens, were prepared by joining two identical panel halves. The square butt faying edges were wiped clean with MEK, draw filed, scraped, and wrapped with aluminum foil. Panels were handled with lint free gloves throughout the preweld and welding operations. Time delay between weld preparation and welding was less than six hours. Panels were welded in the vertical position with a three pass procedure including one continuous tack pass and one penetration pass from each side. No remelt or repair passes were used. Radiographs showed that weld quality was excellent.

5Al-2.5Sn(ELI) Titanium Procedures - Weld panels, 0.35 by 12 by 36 inches
(0.89 by 30.5 by 91.4 cm) for SF specimens and 0.35 by 3.5 by 36 inches
(0.89 by 8.9 by 91.4 cm) for DCB specimens were prepared by joining two
identical panel halves. One edge of each panel half was machined straight
and parallel within ± 0.005 inch (± 0.013 cm) with a surface finish of
RMS 63 or better, providing a square butt joint configuration. The top
and bottom panel surfaces were scraped over a width of 0.5 inch (1.3 cm)
from the faying plane just prior to welding, and the mating surfaces were
wiped clean with MEK. Panels were welded in the downhand position in a
controlled atmosphere weld chamber. After the panel components were aligned,
the chamber was sealed, evacuated to a pressure of 1×10^{-5} mm Hg, and
backfilled with welding grade argon gas to atmospheric pressure. Panels
were then welded using a two pass procedure, including one penetration
pass from each side. The first and second passes resulted in 100 and
90 percent penetration without any measurable underfill along the edges of
the weld bead. Radiographs showed that weld quality was excellent.

2.2.2   Specimen Preparation

Double cantilever beam (DCB), surface-flawed (SF), and mechanical property
specimens were used to accomplish program objectives. Specimen configu-
rations used for each series of tests are summarized in Appendix C.

Loading holes in all specimens were drilled and reamed using jigs in which
holes had been located to a tolerance of ± 0.001 inch (± 0.025 mm). Grips
were drilled using the same jigs in order to effect accurate fits between
specimen and grip.

The surfaces of all SF specimens were machined flat and parallel after
specimen blanks had been cut from plate stock or weld panels. Specimens
containing welds were machined just enough to clean up the weld.

Various side groove geometries were used for DCB specimens in order to
force the crack to grow in the original crack plane. Aluminum alloy base

metal specimens were fabricated with semicircular shaped grooves having a depth of 10 percent of the specimen thickness. All other specimens contained Vee shaped side grooves having a root radius of 0.01 inch (0.025 cm) and an included angle of 60 degrees. Side groove depths were equal to 10 and 15 percent of the specimen thicknesses for the aluminum weld and titanium alloy DCB specimens, respectively. Side groove geometries were selected on the basis of results of an initial series of tests directed to an evaluation of the effects of side grooves on crack growth in DCB specimens. Results of these tests are included in Appendix B.

All surface flaws were prepared by growing fatigue cracks from starter slots. Starter slots were produced using an electrical discharge machine and 0.06 inch (0.15 cm) thick circular electrodes; electrode tips were machined to a radius of 0.003 inch (0.008 cm) and an included angle of less than 20 degrees. Fatigue cracks were grown at 72F (295K) in room air using tension-tension fatigue cycles with an R value of 0.06, frequency of 1800 cpm (30 Hz), and peak stresses of 12 and 25 ksi (83 and 172 MN/m^2) for the aluminum and titanium alloy specimens, respectively.

All DCB specimens were precracked by growing fatigue cracks from the ends of starter slots. The tips of the 0.125 inch (0.317 cm) wide milled starter slots were machined with an included angle of 60 degrees and a root radius of 0.003 inch (0.008 cm) using an electrical discharge machine. Fatigue cracks were grown to a length of about 0.10 inch (0.25 cm) using peak cyclic loads of 1500, 2000, and 2500 pounds (6672, 8896, and 11,120 N) for titanium, aluminum weld, and aluminum base metal DCB specimens, respectively.

All specimens were cleaned after having been precracked. Aluminum alloy specimens were vapor degreased and titanium alloy specimens were alkaline cleaned. All cleaned specimens were handled with white gloves and sealed in plastic bags until tested. Aluminum alloy specimens tested in fluorine or FLOX were further cleaned immediately prior to testing using the procedure detailed in Appendix E.

11

2.2.3   Testing

<u>Surface Flawed Specimens</u> – All specimens were tested in tensile test machines
after the surface cracks had been flooded with the test medium and brought
to the correct temperature.

Test media were contained either in small sealed cups clamped to the speci-
men over the crack cavity, or in enclosed cryostats surrounding the entire
test specimen.   All media except LN_2, LH_2, and GH_2 at -423F (20K) were
contained in cups.   A typical cup and clamping bar is shown in Figure 2-5.
Teflon seals were used except in fluorine and FLOX where metal seals were
used.   The remaining environments were contained in cryostats surrounding
the entire specimen.

Test temperatures were obtained by submerging the cups and/or test speci-
mens in a medium at the desired temperature.   Tests at 72F (295K) were
conducted in an enclosed air conditioned laboratory.   Tests in helium and
hydrogen gas at ambient temperatures were conducted out of doors over a
temperature range of 40 to 60F (278 to 289K).   No measurement of speci-
men temperature was made.   Tests at -320F (78K) and -423F (20K) were
conducted in liquid nitrogen and liquid hydrogen baths at ambient pressure,
respectively.   Finally, tests in gaseous hydrogen at about -423F (20K)
were performed by submerging the lower half of the specimen in liquid
hydrogen within an enclosed cryostat.   The liquid level was kept slightly
more than 1 inch (2.5 cm) below the crack by an automatic liquid level
control system triggered by liquid level sensors.

Several environments including GH_2, GO_2, He, F_2, OF_2 and FLOX were
obtained from pressurized bottles that were used as the source of both
test medium and pressure.   All other environments were pressurized with
welding grade argon gas.

Specimens tested in environments other than those containing fluorine were
exposed to the test medium prior to the application of load. For environments
containing fluorine, the following procedure was used:

1) Install specimen and environment chamber in the test machine and passivate
   with test medium at ambient temperature;
2) Purge and pressurize system with helium gas;
3) Load specimen to 70 percent of maximum test load;
4) Tighten pressure cups until leaks are halted;
5) Introduce test environment;
6) After environment is stabilized, load specimen to maximum test load.

At the conclusion of all sustained load tests, specimens were subjected to
fatigue loadings to delineate the flaw periphery, and were then loaded to
failure.

DCB Specimens - DCB specimens were loaded by forcing a pin-like wedge into the
central loading hole of the DCB specimens as illustrated in Figure 2-6. The
pins were inserted using a bench vise and the maximum stress intensity factors
were controlled by micrometer measurements of deflection across the slotted
end of the specimen using procedures described in Appendix B. For titanium
specimens, a cap was used to prevent lateral deflection of the specimen arms
during loading.

For tests listed in Tables 2-1 and 2-2, specimens were loaded in room air and
placed in a test chamber that had been cleaned, then filled with the test
medium prior to loading of specimens. For tests listed in Table 2-3, specimens
were loaded with the crack tip submerged in the test environment. The chambers
were sealed using a flanged top containing an O-ring seal, then pressurized.

Test temperatures were controlled by submerging the test chambers in either
air, liquid nitrogen, or liquid hydrogen at ambient pressure. Tests at 72F
(295K) were conducted within an enclosed air conditioned laboratory in which
specimens, environments, and test chambers were stored prior to testing.

Tests in hydrogen and helium gas at ambient temperatures were conducted out of doors over a temperature range of 40 to 60F (278 to 289K). Actual specimen temperatures were not monitored. Tests at -320F (78K) were conducted with the test chambers submerged in liquid nitrogen under ambient pressure. For tests in hydrogen gas, the test chambers were purged with helium gas, submerged in liquid nitrogen for fifteen minutes, then backfilled with hydrogen gas. For tests in F_2, OF_2, and FLOX, the chambers were purged with helium gas, passivated with the media in gaseous form, and then submerged in liquid nitrogen. The test media were added to the test chambers as required to maintain the desired pressure until the chambers were filled with liquid. Test duration was measured from the time at which the test chambers became filled with liquid. Tests in helium gas at -423F (20K) were conducted with the test chambers submerged in liquid hydrogen.

Three DCB specimens were simultaneously tested in each environment. For non-hazardous environments, specimens were individually removed from the test environment after successively longer periods of exposure ranging from about 20 to 250 hours. For hazardous environments, all specimens were removed at one time.

After each specimen had been removed from the test environment, the micrometer deflection across the slotted end of the specimen was remeasured, loading pins were removed, and the specimen was pin loaded in a test machine to the load required to effect the same micrometer deflection as that measured at the end of the test.

This load was used in the calculation of stress intensity factor at the time each test was terminated. The specimen was then subjected to fatigue cycles to delineate the crack front before being loaded to failure.

Mechanical Property Specimens – Tests were conducted using a strain rate of 0.005/minute until yield strength had been exceeded; the strain rate was then increased to 0.02/minute until failure.

14

2.2.4   Interpretation of Results

Crack growth was observed in all sustained load tests of both DCB and SF specimens. In some specimens, crack growth occurred only during the loading ramp of the sustained load profiles. In other specimens, crack growth occurred both during the loading ramp and subsequent sustained load. Hence, a procedure had to be developed to distinguish time dependent crack growth from crack growth that occurred during the loading process. In general, this could be accomplished by visual observations of the fracture surface, using a 30x microscope. When significant time dependent growth occurred, two distinct bands of crack growth were noted on the fracture surface. The first band was due to crack growth that occurred during the loading ramp; the second band was due to SCC that occurred during the sustained load period. In addition, the fracture surfaces of all sustained load specimens were compared to those of specimens that had been subjected only to the loading ramp of the sustained load profile.

Results were evaluated in terms of the stress intensity factor defined by linear elastic fracture mechanics theory. Stress intensity factors for DCB specimens were calculated using the semi-empirical equation

$$K_1 = \frac{2P}{b} \left(\frac{b}{b_n} \right)^{1/2} \left[\frac{3(a + a_o)^2 + h^2}{(1 - \mu)^2 h^3} \right]^{1/2} \tag{1}$$

where P is applied load, b is specimen width, b_n is crack width, a is crack length, a_o is an experimentally determined increment of crack length, 2h is the specimen height, and μ is Poisson's ratio. Values of a_o were found to be 0.90 and 0.78 inch (2.29 and 1.98 cm) for aluminum and titanium alloy specimens, respectively. Methods and data used to evaluate a_o are described in Appendix B.

Stress intensity factors for most SF specimens were calculated using the equation (Ref. 8).

$$K_1 = 1.1\sigma \sqrt{\pi a/Q} \tag{2}$$

where σ is a uniform tensile stress acting perpendicular to the plane of the crack; a and Q are defined in Figure 2-7. Equation 2 is applicable for elastic stress levels and surface cracks with depth to length (a/2c) and depth to plate thickness (a/t) ratios less than one-half (8). Equation 2 was used exclusively except for tests undertaken to evaluate the effect of SF specimen thickness on SCC susceptibility. In the excepted tests, flaw depths exceeded one-half the specimen thickness and stress intensity was calculated using the equation

$$K_I = 1.1 \ M_K \sigma \ \sqrt{\frac{\pi \ a}{Q}} \tag{3}$$

where M_K is a factor that accounts for the effect on stress intensity of the back specimen face. Values of M_K were taken from Figure 57 in Reference 9. The referenced M_K values were experimentally evaluated using tests of 0.20 inch (0.51 cm) thick Ti-5Al-2.5Sn(ELI) alloy SF specimens at -320F (78K) and -423F (20K).

2.3   Results and Discussion

Raw data for all environmental survey tests are included in Tables A1 through A12 in Appendix A. The raw data are summarized in Figures 2-8 through 2-15 which show the stress intensity factors at both the beginning and end of the longest duration sustained load test conducted in each test environment. The initial stress intensity factors are denoted by circles and the final stress intensity factors are denoted by triangles. When no SCC was observed in a given test, the stress intensity factors are represented by open symbols. When SCC was observed, solid symbols are used. Note that stress intensity factors decreased during DCB specimen tests since the specimens were subjected to constant opening mode deflections; stress intensity factors increased during SF specimen tests under constant applied loadings. Other test details are also summarized in Figures 2-8 through 2-15 including: test duration, crack propagation direction (see Figure 2-16), loading environment (either room air or test medium), specimen type (DCB or SF), and test environment.

16

2.3.1 Discussion of Titanium Alloy Results

Both 5A1-2.5Sn(ELI) titanium base metal and weld metal underwent SCC in several environments as noted in Figures 2-8 through 2-11. The severity of susceptibility to SCC was found to depend on environment, crack propagation direction, and loading environment (air or test medium). There were indications that susceptibility can also be influenced by material condition (plate or weld) and specimen type (SF or DCB).

Effects of Test Environment

The Ti-5A1-2.5Sn(ELI) plate and welds were susceptible to SCC in the environments of methanol, methanol plus two percent (by volume) distilled water, dye penetrant (ZL-2A), 3-1/2 percent sodium chloride solution (salt water), ethanol plus two percent (by volume) distilled water, and distilled water. The base metal underwent crack propagation in hydrogen gas at ambient temperatures. The weld metal was prone to SCC in methyl ethyl ketone and ethanol. No SCC was observed in either base or weld metal in the 72F (295K) environments of argon, air, acetone, and helium, or in the cryogenic environments of liquid nitrogen and liquid hydrogen. An indication of the relative aggressiveness of the environments that promoted SCC can be obtained from Figures 2-8 through 2-11 by comparing values of stress intensity factors at test termination in the various environments. For DCB tests, SCC susceptibility is inversely related to the value of the terminal stress intensity factor which is at or near the K_{Iscc} value. For example, base metal DCB specimens that were loaded in the test medium (WR direction tests in Figure 2-8) show that methanol, dilute methanol, and salt water are equally aggressive environments. Dye penetrant, dilute ethanol, and distilled water were progressively less aggressive.

The absolute values of environmentally induced crack growth observed in each of the susceptible environments are summarized in Figure 2-17 and Table 2-8. Fracture faces of selected specimens are shown in Figure 2-18. The amounts of SCC observed in base metal DCB specimen tests were substantial in aggressive environments, e.g., 2.05 inches (5.21 cm) during 116 hours of exposure to salt water. Large amounts of SCC were also observed for base metal tests in the environments of dye penetrant, dilute methanol, and methanol.

The dilute alcohol environments were tested in view of prior test results (10) showing that addition of water to methanol in amounts exceeding about one percent by volume could markedly increase time to failure for smooth titanium foil specimens. Typical smooth specimen test results (10) are included in Figure 2-19 for pure titanium (CP35A), and Ti-6Al-4V. In the precracked specimen tests conducted in this program, the addition of two percent by volume of distilled water to methanol moderately reduced SCC susceptibility in both weld metal and base metal DCB tests (see RW direction/load-in-air tests in Figures 2-8 and 2-10). Base metal SF specimen test results were essentially identical in the pure and dilute methanol environments, whereas the rate of cracking in weld metal DCB tests was slowed by the addition of water. It remains to be seen whether additions of greater amounts of water would further inhibit SCC in precracked specimens. A synergistic effect was noted in both base and weld metal tests in the environment of dilute ethanol. For base metal, the effect was noted in DCB specimen tests (WR direction/loaded in test medium) in Figure 2-8; for tests having nearly equal durations, the dilute ethanol promoted more SCC than either of the pure ethanol or distilled water environments. A similar effect was noted in the SF specimen tests for the weld metal (Figure 2-10).

Cracking susceptibility of 5Al-2.5Sn(ELI) titanium base metal in ambient hydrogen gas environments was found to be pressure dependent, i.e., cracking was observed at 100 psig (689.5 kN/m^2 gage pressure) but not at 30 psig (689.5 kN/m^2 gage pressure) as shown in Figure 2-9. Williams (11) found that the cracking tendencies of Ti-5Al-2.5Sn(ELI) in hydrogen gas was dependent on both pressure and temperature. The tests conducted in this program were of short duration (24 hours for the DCB and 10 hours for the SF specimens) and there is a possibility that longer duration tests would have resulted in more cracking. Tests of precracked titanium alloy specimens in hydrogen gas have shown that for initial stress intensity factors less than the critical value, rapid cracking to failure occurs only after some finite time period or incubation period, as schematically illustrated in Figure 2-20. The test durations in this program may not have been sufficiently longer than the corresponding incubation periods to result in maximum cracking.

18

Results for tests in LN$_2$ and LH$_2$ are similar to those previously reported by Lorenz (3). In LH$_2$, Lorenz determined a threshold stress intensity factor from ten hour duration tests equal to or greater than 90 percent of the plane strain fracture toughness of 52 ksi$\sqrt{in}$ (57 MN/m$^{3/2}$). In this test program, the ten hour threshold stress intensity factor in LH$_2$ was greater than ninety percent of the corresponding fracture toughness of 70 ksi$\sqrt{in}$ (77 MN/m$^{3/2}$). In LN$_2$, Lorenz found that threshold stress intensity was sensitive to applied stress level. For stresses in excess of 85 percent of the tensile yield stress, the ten hour threshold stress intensity factor was 82 percent of the fracture toughness of 71 ksi$\sqrt{in}$ (78 MN/m$^{3/2}$); for stresses less than the above value, the threshold stress intensity was very nearly equal to the fracture toughness. In this investigation, sustained load tests were conducted at stress levels equal to seventy percent of the tensile yield stress and the ten hour threshold stress intensity factor was greater than ninety percent of the fracture toughness value of 84 ksi$\sqrt{in}$ (92 MN/m$^{3/2}$).

No attempt will be made to quote K$_{Iscc}$ values for any of the material/environment combinations tested in this program. Fundamentally oriented investigations of SCC in titanium alloys (12) have shown that true threshold stress intensity factors below which no SCC will occur do not appear to exist for many material/environment combinations. Rather, SCC progresses at continually decreasing rates at the lower stress intensity levels as schematically shown in Figure 2-21. It is yet to be determined what happens at very low stress intensity factors. There are some material/environment combinations for which there does appear to be a true K$_{Iscc}$, e.g., titanium alloys in aqueous solutions. Figure 2-21 also shows how stress intensity factor - SCC velocity relationships can be divided into three regions, one at low and one at high stress intensity factors (Regions I and III) in which velocity is strongly dependent on stress intensity factor, and an intermediate region (Region II) in which velocity is independent of stress intensity factor.

Effect of Crack Propagation Direction
Susceptibility of the 5Al-2.5Sn(ELI) titanium alloy plate was dependent on crack propagation direction. The WR direction (See Figure 2-16) was more susceptible than the RW direction in distilled water, dilute ethanol, dye penetrant (ZL-2A), salt water and dilute methanol. The WR direction was not tested in pure methanol.

In the salt water environment, cracking in the RW specimen deviated from the original crack plane and progressed in the WR direction. Similar results have been reported (12) for numerous other titanium alloys. Variations in SCC behavior with crack propagation direction are due to texturing (preferential grain orientation) in the plate materials (12). In α alloys, cracking occurs near the basal plane so that the lining up of the susceptible planes in the crystals increases SCC susceptibility. However, a pole figure for the 5Al-2.5Sn(ELI) plate material tested in this program showed no detectable texturing.

Effects of Loading Environment

The amount of cracking observed in the base metal tests was found to be strongly influenced by loading environment. Base metal DCB specimens that were loaded in laboratory air prior to being placed in the test medium were less susceptible to SCC than were specimens that were loaded and tested without removal from the test medium. This result was obtained from tests in distilled water, dilute ethanol, dye penetrant, salt water, and dilute methanol as shown in Figure 2-8. Similar results have been reported elsewhere (13,14) and are thought to be due to the very rapid oxidation of the fresh crack surfaces generated during the exposure to room air.

Comparison Between Base and Weld Metal Behaviors

The relative SCC resistance of 5Al-2.5Sn(ELI) titanium base and weld metal can be evaluated using the SF specimen test results as summarized in the upper part of Figure 2-17. In general, SCC velocities in the weld metal specimens tended to be less than those in the base metal specimens. For example, the base and weld metal specimens failed after 0.008 and 0.17 hours of exposure to salt water, respectively. Similar results were obtained in methanol and dilute methanol. On the other hand, there were two environments (ethanol and MEK) in which SCC was observed in the weld metal, but not in the base metal. On the basis of the foregoing observations, there did not seem to be a great deal of difference between SCC resistance of the weld and base metals tested in this program. The DCB specimen results shown in the lower part of Figure 2-17 show the weld metal to be superior to base metal in terms of SCC resistance. However, the SCC resistance of the weld metal in DCB specimens was probably enhanced by loading the specimens in room air.

20

On the basis of fundamental investigations of SCC in titanium alloys (12), it
was concluded that 5Al-2.5Sn(ELI) titanium weld metal should have SCC resistance
equal or superior to the base metal. Welding is a β process and since the 5Al-2.5
Sn(ELI) alloy contains iron (a β phase stabilizer), the weld metal could take on
some of the superior SCC characteristics exhibited by β processed material.
Furthermore, the grains should be more randomly oriented in a cast weld structure
than in a hot rolled plate and this should improve SCC resistance since prefer-
ential grain orientation can have a strong detrimental effect on SCC resistance.

Effects of Specimen Type

Neither the base metal nor weld metal data allow a good comparison between SCC
behavior determined from tests of SF and DCB specimens. It had been originally
planned to test SF specimens using initial stress intensity factor values both
slightly above and slightly below the K_{Iscc} value determined from the DCB
tests. The initial set of tests were conducted using DCB specimens loaded
in air and very little SCC was observed. It was then decided to test the
SF specimens at the highest stress intensity factor that could be generated
under conditions in which the elastic stress intensity factor determined
material behavior at the crack tip, i.e., about 65 ksi $\sqrt{in}$. It was later
realized that both crack propagation direction and loading medium had a
significant effect on SCC. There are some indications that SF specimens
resulted in greater SCC susceptibility than did the DCB specimens for the
material thickness tested. A comparison of average SCC velocities observed
in DCB and SF specimens for the RW and RT directions of the 5Al-2.5Sn(ELI)
plate material (using data in Figure 2-8) shows that the SCC velocities were
much higher in SF specimens than in DCB specimens for the environments of dye
penetrant and methanol. In dye penetrant, the average SCC velocity (crack
growth/test duration) in the DCB specimen that was loaded in environment was
3×10^{-3} inches/hour (2.1×10^{-6} cm/sec) at an average stress intensity factor
of 100 ksi $\sqrt{in}$. The corresponding velocity in the SF specimen was about
0.2 in/hr (0.14×10^{-3} cm/sec) at an average stress intensity factor of about
90 ksi $\sqrt{in}$. It is evident that the SCC velocity in the SF specimen was
considerably greater than in the DCB specimen even though the applied stress
intensity factors were lower. In dilute methanol, the average SCC velocities
were 3×10^{-3} in/hr (2.8×10^{-6} cm/sec) and 4.8×10^{-2} in/hr (3.4×10^{-5} cm/sec)
in the DCB and SF specimens, respectively; the corresponding average stress

intensity factors were 60 and 74 ksi$\sqrt{\text{in}}$, respectively. The average SCC velocities showed considerably better agreement in the dilute methanol than in the dye penetrant. Nevertheless, there did seem to be a tendency for SCC to be more pronounced in SF than in DCB specimens. Similar results were obtained in weld metal tests conducted in the environments of methyl ethyl ketone (MEK), salt water, methanol, and dilute methanol (see Figure 2-10). However, the weld metal results were not directly comparable since the DCB specimens were loaded in air and the SF specimens were loaded in the test medium.

It is reasonable to expect that differences in SCC susceptibility determined from tests of DCB and SF specimens could be observed. It has been previously demonstrated (15) that specimen thickness can have a marked effect on SCC susceptibility as determined from through-the-thickness cracked specimens. This is illustrated by the results included in Figure 2-22 for 6Al-4V and 8Al-1 Mo-1V titanium alloys. Thickness effects are believed to be due to changes in constraint to crack tip deformations as thickness changes, i.e., changes from plane stress to plane strain conditions. The SCC susceptibility increases as plane strain conditions are approached. Since less thickness is thought to be required to generate plane strain conditions in SF specimens than in through-the-thickness cracked specimens (5), there should be a range of thicknesses over which SF specimens would result in greater SCC velocities and lower apparent K_{Iscc} values than would through-cracked specimens of equal thickness. The 0.375 inch thick 5Al-2.5Sn(ELI) titanium alloy plate tested in this program seemed to fall into this thickness range.

Surface Flawed Specimen Thickness Effects

Results of tests to investigate the effect of SF specimen thickness on SCC susceptibility are included in Figure 2-23 and Table 2-9. The impetus for these tests was provided by the observation that apparent threshold stress intensity values increase with decreasing through-the-thickness cracked specimen thickness as illustrated in Figure 2-22. In SF specimens, changes in constraint to crack tip deformations undoubtedly occur when specimen thickness is decreased to the extent that the ligament between crack tip and back specimen face becomes entirely enveloped by plastic deformations. It had been thought that decreased specimen thickness might decrease SCC susceptibility at surface cracks in a manner analogous to that observed for through-the-thick-

22

ness cracked specimens. As specimen thickness was decreased in the tests reported herein, the ratio of approximate maximum plane strain plastic zone dimension [$0.2 \, (K_I/\sigma_{ys})^2$] to uncracked ligament depth (t-a) increased from 0.2 to 0.6 to 0.8 as specimen thickness decreased from 0.20 to 0.10 to 0.05 inch (0.51 to 0.25 to 0.13 cm). Hence, it was believed that if surface flaw specimen thickness was a significant factor in SCC susceptibility, the effect would be observed in these tests.

Tests were conducted using the 5Al-2.5Sn(ELI) titanium/methanol material/ environment combination. For each of three specimen thicknesses (0.20, 0.10 and 0.05 inch or 0.51, 0.25 and 0.13 cm), three specimens were tested. Two specimens were sustain loaded in methanol to generate stress intensity factors at the crack tip both above and below 42 ksi $\sqrt{in}$ (46.2 MN/m$^{3/2}$), i.e., the minimum K level at which SCC was observed in the previously described DCB specimen tests (see Figure 2-8); one specimen was subjected in argon to a load-unload profile using the same loading ramp that was used in the prior sustained load tests.

In all tests, more crack depth growth was observed in the sustained load tests in methanol than in the load-unload tests in argon. Hence, it can be concluded that SCC occurred in all sustained load tests in methanol. A comparison of tests no. 3 and 5 in Figure 2-23 and Table 2-16 shows that significantly more crack depth growth was observed in the 0.10 inch (0.25 cm) thick specimen than in the 0.20 inch (0.51 cm) thick tests. For all thicknesses, considerable SCC was observed at initial stress intensity factors of 39 ksi $\sqrt{in}$. Hence, these tests yielded no indications that SCC susceptibility decreased with decreasing SF specimen thickness.

Both crack tip blunting and plastic flow could influence relative SCC suscepti- bility as SF specimen thickness is varied. Crack tip blunting should decrease susceptibility to nucleation of stress corrosion cracks and increased plastic flow could enhance SCC. At the present time, the effects of blunting and plastic flow on SCC are not well understood. Hence, it is not possible to predict what the SF specimen thickness effect should be. These tests tended to indicate that SCC susceptibility was enhanced by decreasing specimen thick- ness which leads to the speculation that the effects of increased plastic flow predominated in these tests.

23

Other Crack Growth Observations

Observations of crack depth growth in most titanium alloy SF specimens led to the undertaking of tests to evaluate crack depth growth characteristics during both rising loads and early stages of sustained loadings. Four series of tests were conducted with each series consisting of three identical SF specimens loaded to a predetermined peak load level; one specimen was immediately unloaded and the other two specimens were unloaded after either one or twenty hour exposures to the peak load. Specimens were then subjected to low stress fatigue cycles to delineate any crack growth that occurred during the prior testing. Both base metal and weld metal were tested in room air and argon gas. Results are summarized in the lower half of Table 2-10 and crack depth growth is plotted against test duration in Figure 2-24.

Only insignificant amounts of crack depth growth were observed in the weld metal specimens and results were not influenced by test medium. Larger amounts of crack depth growth were observed in base metal tests and results were influenced by test medium. In argon, crack depth growth values of 0.014 ± 0.002 inch $(0.36 \pm 0.05\text{mm})$ were noted regardless of test duration and it was concluded that crack growth occurred only during rising load in argon. In air, crack depth growth for the one and twenty hour duration tests averaged 0.025 inch (0.63mm) as compared to the value of 0.006 inch (0.15mm) for the load-unload test. Hence, it appeared that crack depth growth in air occurred during both rising load and the early part of the subsequent invariant load.

The only firm conclusion that can be drawn from the titanium alloy results in Figure 2-24 is that crack growth can occur during the loading ramp of a sustained load test and must be accounted for in interpreting sustained load test results. It is not clear why the air and argon results differed. Indications of transient crack growth followed by crack growth arrest were evident in the air results but not in the argon data. Previous observations (3, 21) of transient crack growth have been made in chemically inert environments and are thought to be due to mechanical factors. On the other hand, data scatter could have resulted in false indications of transient crack growth and the discrepancy between crack depth growth values in air and argon may not have been influenced by environmental factors.

Crack growth was observed in a number of titanium weld metal DCB specimens tested in gaseous hydrogen and helium at ambient temperatures. Results are included in Table A10 in Appendix A. The amount of crack growth ranged from 0.05 to 0.25 inch (1.3 to 6.4mm). Since similar results were obtained in both helium and hydrogen, it was postulated that the crack growth was not assisted by the test media. Rather, it is thought that the crack growth was accentuated by the temperature drop between loading and test environments. Specimens were loaded in an enclosed building at about 70F (295K) and were then tested at outdoor temperatures ranging from 40 to 60F (278 to 289K). The temperature drop could have resulted in a decrease in fracture toughness accompanied by crack propagation.

2.3.2   Discussion of Aluminum Alloy Results

Indications of SCC in 2219 aluminum were observed in three of the environments tested in this program. Both 2219-T87 plate (WR direction) and 2219 as welded weld metal underwent what appeared to be SCC in salt water at 72F (295K). Traces of apparent SCC were noted in the plate material in trichlorethylene and dye penetrant (ZL-4B). No evidence of SCC was observed in the ambient temperature environments of room air, argon gas, distilled water, hydrogen gas, flourine gas, gaseous oxygen diflouride, and a gaseous flourine-oxygen mixture. There was an absence of SCC in the -320F (78K) environments of liquid oxygen, gaseous hydrogen, liquid flourine, liquid oxygen diflouride, and liquid flourine-oxygen mixture, and in the -423F (20K) environments of gaseous and liquid hydrogen.

Indications of SCC
Indications of SCC in the 2219-T87 plate tested in salt water are pictured in Figure 2-25. Specimen 55 was loaded in air using the same loading procedures that were used for specimens S-2 and S-4; this specimen was then immediately unloaded; crack growth due to the loading process can be seen on the fracture face. Specimens S-2 and S-4 were loaded in air then immersed in salt water for 50 and 262 hours, respectively. Crack growth on the fracture face of specimen S-2 resembles that on the face of specimen 55, both in magnitude and shape. It was concluded that the crack growth noted in specimen S-2 was due to the loading

process and that no SCC had occurred. Crack growth on the fracture face of specimen S-4 was composed of four distinct areas including; the initial fatigue crack, crack growth due to loading, a band of crack growth that appears to be SCC, and fatigue crack growth induced to mark the crack periphery at test termination. The maximum width of the apparent SCC band was 0.12 inch (0.30 cm) at the center of the specimen and the average apparent SCC velocity (band width/ test duration) was 4.6×10^{-4} in/hr (3.2×10^{-7} cm/sec). Specimen S-4 was examined metallographically and it was observed that the crack growth in the apparent SCC band was intergranular. Intergranular growth is characteristic of SCC in aluminum alloys. There was no evidence of grain boundary corrosion in the grains lying adjacent to the crack surface. In order to determine if the apparent SCC growth in specimen S-4 might have been due to intergranular corrosion that was relatively independent of stress intensity, two additional base metal DCB specimens were tested in salt water. Test procedures were identical to those for specimen S-4 except that one specimen was subjected to an opening mode deflection equal to fifty percent of that used to load S-4, and the second specimen was tested in an unstressed condition. Both specimens were exposed to salt water for 260 hours. After being pulled to failure, the fracture surfaces yielded no evidence of apparent SCC. It was concluded that the apparent SCC growth observed in Specimen S-4 was dependent on stress intensity factor.

The fracture faces of two weld metal DCB specimens tested in salt water are pictured in Figure 2-26. Small bands of apparent SCC are shown along the fronts of the initial fatigue cracks. The width of the apparent SCC band for specimen WS-3 was 0.03 inch (0.76 mm) and the average apparent SCC velocity was 7.3×10^{-5} in/hr (5.2×10^{-8} cm/sec). The corresponding stress intensity factor was 31 ksi $\sqrt{in}$ (34 $MN/m^{3/2}$). Figure 2-26 also illustrates the non-uniform pre-cracks that were typical of the weld metal DCB specimens.

Crack growth was observed on the fracture faces of all 2219 weld metal SF specimens. The absolute amounts of crack growth are summarized in Tables 2-10 and 2-11, and are plotted as a function of test temperature Figure 2-27. The fracture faces of two 2219 weld metal SF specimens are shown in Figure 2-28. Specimen WDP-1A was subjected to the loading ramp of the sustained load profile used to conduct the ambient temperature sustained load tests, and

was then unloaded; the specimen was subjected to low stress fatigue cycles to outline the crack growth that occurred during the prior loading. The features of the fracture surface do not show up well in Figure 2-26, but the growth that occurred during the rising load of the loading ramp was clearly outlined on the fracture surface. Specimen WS-1 was subjected to an invariant loading in salt water for a period of 24 hours. The amount of crack growth that occurred during the test is visible as a dark area on the fracture surface. At 72F (295K) all specimens other than WS-1 yielded crack depth growth values ranging from 0.03 to 0.045 inch (7.6 to 11.4 mm). Specimen WS-1 underwent a crack depth growth of 0.075 inch (19.1 mm). This result is certainly an indication that SCC may have occurred in Specimen WS-1. However, the authors feel that one test is an insufficient basis on which to judge the SCC susceptibility of 2219 weld metal. Assuming that SCC resulted in crack depth growth somewhere between 0.03 and 0.045 inch (7.6 and 11.4 mm) in specimen WS-1, the corresponding average SCC velocities are 1.3×10^{-3} and 1.9×10^{-3} in/hr (0.9 and 1.3×10^{-6} cm/sec).

The fracture faces of two 2219-T87 aluminum base metal specimens pictured in Figure 2-28 also contained indications of SCC. Specimen AD-1 was tested in dye penetrant and specimen AT-1 in trichloroethylene. Both specimens contained zones of apparent SCC in the WR direction as outlined by the arrows in the figure. The extent of each zone was greater than comparable crack growth observed in any other 2219-T87 base metal SF specimen tested at 72F (295K).

It is believed that the evidence of SCC noted in the 2219 aluminum tests reported herein is insufficient to establish the susceptiblity of the alloy to SCC. Only very small amounts of crack growth were observed and well defined procedures for identifying the nature of such small amounts of growth were lacking. More tests of longer duration are required to either substantiate or refute the evidence of SCC in 2219 aluminum observed in these tests.

Other Crack Growth Observations

Crack growth was observed in all aluminum alloy SF specimens tested in this program. Typical examples of surface crack growth are included in Figures 2-28 and 2-29.

To evaluate the characteristics of surface crack growth both during and immediately after the application of sustained loadings, three series of tests were undertaken. Each test series included three tests of identical SF specimens that were loaded to a predetermined peak load level and then were unloaded after either a zero, one, or twenty hour exposure to the peak load; 2219-T87 base metal specimens were tested in both room air and welding grade argon gas and 2219 weld metal specimens were tested in room air. At the conclusion of each test, specimens were subjected to fatigue loadings at 72F (295K) to delineate any crack growth that occurred during the test run. Results are summarized in Table 2-10 and crack depth growth is plotted against test duration in Figure 2-24.

The test results indicate that crack growth occurred only during rising loads and not during invariant loadings in both the 2219-T87 base metal (WT direction) and 2219 as-welded weld metal. This conclusion was based on the observation that the amount of crack growth was independent of test duration (within limits of normal data scatter) in both test environments.

Crack depth growth observed in 2219 weld metal SF specimens is summarized in Table 2-12 and plotted in Figure 2-27. The fracture faces in Figure 2-28 illustrate the characteristics of the observed crack growth. The scatter bands in Figure 2-27 include all crack depth growth measurements for sustained load tests conducted at either 22 or 25 ksi (151.7 or 172.4 MN/m^2) uniform applied stress levels. The individual circular data points represent crack depth growth measurements for specimens that were loaded at the same rate as were the sustained load specimens, then immediately unloaded. For the 22 ksi (151.7 MN/m^2) sustained load tests, consistent crack depth growth measurements were obtained in all environments except salt water. Because of this result, it was concluded that environments other than salt water did not promote SCC in the 2219 aluminum weld metal. The data points for the 22 ksi (151.7 MN/m^2) load-unload tests fall outside of the scatter band for the corresponding sustained load tests. This may have been due to data scatter. At -423F (20K), however, transient crack growth may have occurred after the loading process. Transient crack growth followed by crack growth arrest has been observed (3) during the early stages of sustained load tests of 2219-T87 base metal specimens. The low yield strength and high fracture toughness of 2219 as-welded weld metal should make it more prone to transient crack growth than base metal. At cryogenic temperatures, the sustained load tests yielded

28

significantly more crack depth growth than did the corresponding load-unload tests. It is believed that the additional crack growth observed in the sustained load tests was due to mechanical processes in the plastically deformed material at the crack tip and not SCC. It is difficult to believe that SCC would have occurred during the relatively short test durations in all cryogenic environments tested.

Crack growth during rising loads in 2219 as-welded GRA weld centerlines was found to be highly stress level dependent as illustrated in Figure 2-30 by data obtained from specimens loaded to various stress levels in ambient air. For stress levels above about 17 ksi (117 MN/m^2), crack growth was very sensitive to peak stress level. The actual yield strength of the weld metal was not measured, but it is believed to be about 16 ksi (110 MN/m^2) or less. Hence, all 2219 weld metal tests in this program were conducted using stress levels in excess of the true uniaxial weld metal yield stress. The data in Figure 2-30 show that rising loads to stress levels in excess of the actual yield strength can result in large amounts of crack extension.

Failure characteristics of cracked 2219 weld metal can be inferred from the data in Figure 2-30. It is evident that when failure stresses are well in excess of the yield stress, crack size does not undergo an abrupt instability at the failure load. Rather, crack dimensions start to increase once the yield stress is exceeded and continue to grow at an increasing rate until failure occurs. It is not clear whether failure is due to initiation of unstable crack propagation or to an exceedance of ultimate stress on the net section.

Comparison With Previously Reported Results
Other investigations have shown that 2219-T87 aluminum alloy plate is very resistant to SCC. The short transverse direction of one inch thick plate has been tested (16) both in an outdoor atmosphere and in a 3.5% NaCl solution with results shown in Figures 2-31 and 2-32. No SCC was detected in either set of tests with a detection sensitivity noted in the two figures. Figures 2-31 and 2-32 also include SCC velocity correlations for a number of 7000 and 2000 series aluminum alloys. When compared to the schematic SCC velocity-stress intensity factor correlation previously included in Figure 2-21, it can be seen that aluminum alloys do not exhibit Region III behavior. The plateau (Region II) velocities for the 2000 series alloys are all very close to 10^{-3} in/hr (7 x 10^{-7}

cm/sec), which agrees with the apparent SCC velocity observed for the WR
direction of the 1.0 inch (2.5 cm) thick plate tested in this investigation.
An electrochemical test has been developed for predicting the stress corrosion
performance of 2219 aluminum in the T851 and T87 tempers (17). The test requires
the measurement of the solution potential of an unstressed specimen in a mixture
of absolute methyl alcohol and carbon tetrachloride. Changes in potential for
2219 alloy plate as it is artificially aged from the T37 to T87 temper are shown
in Figure 2-33 along with smooth specimen stress corrosion data. These data also
show 2219-T87 aluminum alloy plate to be very stress corrosion resistant.

Previously conducted SF specimen tests (3) for 1.0 inch (2.5 cm) thick 2219-T87
plate in the environments of air, LN_2 and LH_2 have shown that crack growth under
sustained loads can occur in four stages including: (1) crack growth during
rising load; (2) initial transient crack growth; (3) crack acceleration; and
(4) unstable crack propagation or failure. The number of crack growth stages
occurring in any test is primarily dependent on the magnitude of the stress
intensity factor (K) applied to the crack tip. For low K values, no growth is
observed; for intermediate K values, growth during loading and transient crack
growth are observed followed by crack growth arrest; for high K values, all
stages of crack growth are observed resulting in specimen failure. In this test
program, crack growth during rising loads was observed in all 2219-T87 base metal
SF specimens. However, there were no indications of transient crack growth for
the WT direction at K levels equal to ninety percent of the fracture toughness.
Previous tests (3) indicated that the K levels above which all four stages of
crack growth could be expected to occur in the WR direction of 2219-T87 aluminum
alloy SF specimens were 90, 81, and 87 percent of the corresponding fracture
toughness in ambient air, LN_2 and LH_2, respectively. In this program, com-
parable ratios were found to be greater than 90 and 93 percent in ambient air
and LH_2, respectively.

2.4   Observations and Conclusions

This experimental program was undertaken to evaluate the combined effects of
load and environment on the stress corrosion cracking (SCC) susceptibility of
2219-T87 aluminum and 5Al-2.5 Sn (ELI) titanium alloy plate and welds. The
following observations were made during the course of the program.

Observations For 5Al-2.5 Sn (ELI) Titanium Alloy

1. The Ti-5Al-2.5 Sn (ELI) plate and welds were susceptible to SCC in the environments of methanol, methanol plus 2 percent (by volume) distilled water, dye penetrant (ZL-2A), 3 1/2 percent sodium chloride solution, eth·nol plus two percent (by volume) distilled water, and distilled water. The base metal was susceptible to crack propagation in hydrogen gas at ambient temperature. The weld metal was prone to SCC in methyl ethyl ketone and ethanol. No SCC was observed in either base or weld metal in the 72F (295K) environments of argon, air, acetone and helium, or in the cryogenic environments of liquid nitrogen and liquid hydrogen.

2. Susceptibility to SCC of 5Al-2.5 Sn (ELI) titanium alloy plate was dependent on crack propagation direction with the WR direction more susceptible than RW direction.

3. There was not a great deal of difference between the SCC susceptibility of base and weld metal. In general, SCC velocities in weld metal tended to be less than in base metal specimens and there were two environments (ethanol and methyl ethyl ketone) in which SCC was observed in the weld metal but not in the base metal.

4. Specimens that were loaded in air prior to being subjected to the test environment were much less susceptible to SCC than were specimens that were loaded in the test environment.

5. There did seem to be a tendency for SCC to be more pronounced in surface-flawed than in double cantilever beam specimens. The test data did not permit a good evaluation of the effect of specimen type on SCC susceptibility.

6. Tests of Ti-5Al-2.5 Sn (ELI) base metal surface-flawed specimens in methanol where specimen thickness was varied from 0.35 to 0.05 inch (0.89 to 0.13 cm) revealed no trend of decreasing SCC susceptibility with decreasing specimen thickness.

Observations For 2219-T87 Aluminum Alloy

1. Indications of SCC was observed in three of the environments tested in this program. Both 2219-T87 plate (WR direction) and 2219 as-welded weld metal underwent what appeared to be SCC in salt water at 72F (295K). Traces of apparent SCC were noted in the plate material in trichloroethylene and dye penetrant (type ZL-4B). Test durations were not sufficiently long to allow strong indications of either the presence or absence of SCC to develop. No evidence of SCC was detected in any of the other test environments including, argon, air, distilled water, hydrogen, oxygen, fluorine, fluorine-oxygen mixture, and oxygen difluoride.

2. Stable crack growth was observed during rising loads in both base metal and weld metal surface flawed specimens.

The following conclusions were drawn on the basis of results obtained both from this program and from the literature:

1. Titanium alloy 5Al-2.5 Sn (ELI) plate and welds can be very susceptible to SCC in a number of environments. Accordingly, fabrication and operating environments should be closely controlled for successful use of this alloy.

2. Aluminum alloy 2219-T87 plate and as-welded welds are very resistant to SCC.

3. For thin materials, surface flawed specimen tests may indicate that a material is more susceptible to SCC than would tests of through the thickness cracked specimen types. Hence, results of SCC tests from through-cracked specimens should be checked using surface flawed specimens prior to use of a specific material/environment combination in engineering structures.

4. SCC tests should be conducted for a period of time sufficient to establish that crack growth rates have decreased to negligibly small values, or longer than the intended life of the structure for which the material/environment combination is under consideration, whichever is the shorter; SCC velocities ranging from 5×10^4 to 10^{-5} in/hr (35 to 7×10^{-9} cm/sec) have been observed in aluminum alloys. Aqueous environments usually promote SCC velocities ranging from about 10^{-2} to 10^{-5} in/hr (7×10^{-6} to 7×10^{-9} cm/sec).

32

3.0   COMPATIBILITY STUDY OF MATERIAL/ENVIRONMENT COMBINATIONS PERTINENT TO HIGH ENERGY UPPER STAGE PROPULSION SYSTEMS

Tests were undertaken to study the compatibility of material/environment combinations suitable for fuel and oxidizer tanks in high energy upper stage propulsion systems. Material/environment combinations tested included: 2219-T87 aluminum alloy in fluorine, fluorine-oxygen mixture, and methane; 2219-T6E46 aluminum alloy in fluorine and fluorine/oxygen mixture; and titanium alloys 5Al-2.5 Sn (ELI), 6Al-4V (ELI) and 6Al-4V (ELI) STA in methane. Tests were conducted in both gas and liquid phases at temperatures slightly above and slightly below the 20 psig boiling temperature of the test media.

The test program is summarized in Table 3-1. All tests were conducted using surface flawed specimens having thicknesses representative of minimum gage tanks, namely, 0.04 inch (1.02 mm) for the aluminum alloys and 0.032 inch (0.81 mm) for the titanium alloys. The longitudinal axis of the specimens coincided with the transverse direction of the parent plate. One flaw depth-to-length ratio of 0.10 was used and specimens were fabricated with the maximum flaw depth that could survive a proof overload at -320F (78K) to 100 percent and 90 percent of the guaranteed minimum yield stress for the aluminum and titanium alloys, respectively. That flaw depth was experimentally evaluated prior to the sustained load tests. The test sequence included a -320F (78K) proof overload followed by sustained load tests ranging in duration from 10 to 500 hours. Two tests were conducted at different stress levels for each combination of variables. Aluminum alloys were tested at $\sigma_y/1.1$ and $\sigma_y/1.2$ where σ_y is the guaranteed minimum -225F (131K) yield stress of the alloy (56 ksi (386 MN/m^2) for the T87 condition and 43 ksi (296 MN/m^2) for the T6E46 condition). Titanium alloys were tested at $\sigma_u/1.4$ and 0.85 ($\sigma_u/1.4$) where σ_u is the guaranteed minimum -225F (131K) ultimate tensile stress of the alloys (210 ksi (1448 MN/m^2), 173 ksi (1193 MN/m^2) and 133 ksi (917 MN/m^2) for the 6Al-4V STA, 6Al-4V annealed, and 5Al-2.5 Sn (ELI) alloys, respectively).

3.1   Materials

The 2219 alloy was tested in both the T87 and T6E46 conditions. All specimens were taken from a single 0.125 by 36.0 by 84.0 inches (0.32 by 91.4 by 213.4 cm) plate purchased in the T87 condition per Boeing Material Specification BMS 7-105C

(equivalent to MIL-A-8920 (ASG) specification). Part of the plate was brought to the T6E46 condition (a Boeing Company heat treatment) by successively solution treating at 995 $\pm$ 10F (808 $\pm$ 6K) for four hours, water quenching, natural aging for four days, artificial aging at 350 $\pm$ 10F (450 $\pm$ 6K) for twelve hours, and air cooling to room temperature. Specification limits on chemical content and mechanical properties measured by The Boeing Company are included in Tables 2-5 and 2-6, respectively. Mechanical properties are plotted as a function of temperature in Figure 3-1.

The 5A1-2.5 Sn (ELI) titanium alloy was tested in the mill annealed (MA) condition. All specimens were taken from a single 0.04 by 24.0 by 72.0 inches (0.10 by 61.0 by 182.9 cm) plate purchased in the MA condition per MIL-T-9046E, Type II, Composition B. Certified chemical content provided by the vendor and mechanical properties measured by The Boeing Company are included in Tables 2-5 and 2-6, respectively. Mechanical properties are plotted as a function of temperature in Figure 3-1.

The 6A1-4V (ELI) titanium alloy was tested in both the mill annealed (MA) and solution treated and aged (STA) conditions. All specimens were taken from a single 0.375 by 24.0 by 72.0 inches (0.95 by 61.0 by 182.9 cm) plate purchased in the MA condition per AMS 4911A, except that the interstitial content was specified not to exceed the following limits in percent by weight: $C = 0.08$, $Fe = 0.25$, $O_2 = 0.13$, $N_2 = 0.05$, $H_2 = 0.0125$. Part of the plate was brought to the STA condition by successively solution treating at 1730F (1217K) for ten minutes, water quenching, and aging at 1000F (811K) for four hours. Certified chemical composition provided by the vendor and mechanical properties measured by The Boeing Company are included in Tables 2-5 and 2-6, respectively. Mechanical properties are plotted as a function of temperature in Figure 3-1.

3.2   Procedures

3.2.1   Specimen Preparation

Configurations for surface flawed and mechanical property specimens used in these tests are detailed in Figures C10, C11 and C12 in Appendix C. Surface flaws were prepared by growing fatigue cracks from starter slots. Slots were produced using an electrical discharge machine (EDM) and 0.06 inch (0.15 cm) thick circular electrodes with tips machined to a radius of 0.003 inch (7.6 mm) and an included

34

angle of 20 degrees. Fatigue cracks were grown to a depth of from three to five
mils (0.08 to 0.10 mm) from the EDM slot using fatigue cycles having an R value
of 0.06, frequency of 1800 cpm (30 Hz), and peak stresses of 12 and 25 ksi (82.7
and 172.4 MN/m^2) for the aluminum and titanium specimens, respectively.

The gage area of all specimens was cleaned with naphtha then blown dry with
compressed air. Aluminum alloy specimens tested in fluorine and FLOX were
cleaned immediately prior to testing using the procedure detailed in Appendix E.

3.2.2   Testing

Proof Overload Test Procedures – All proof overload testing was accomplished at
-320F (78K) with the specimen completely submerged in liquid nitrogen. Each
specimen was instrumented to detect the load at which the surface crack penetrated
the parent specimen thickness. Instrumentation consisted of sealed pressurized
chambers attached to the specimen as shown in Figure 3-2. The chamber on the
flawed surface was pressurized with helium gas to 3-10 psig (34 to 69 MN/m^2 gage
pressure) before load application. The chamber on the back specimen face was left
unpressurized. Test records of pressure in both cups versus applied load were
obtained using an X-Y recorder. A typical test record is included in Figure 3-3
where it can be seen that an abrupt change in pressure occurred in both cups at a
well defined load. The pressure changes were due to penetration of the specimen
thickness by the flaw.

For specimens tested to determine the maximum flaw depth that could survive a
-320F (78K) proof overload without penetrating the specimen thickness, the
following loading sequence was used: (1) specimens were loaded at a uniform rate
to targeted peak stress levels of 182, 160, 128, 59, and 46 ksi (1254.9, 1103.2,
882.6, 40.7 and 31.7 MN/m^2) for the 6Al-4V(ELI)STA, 6Al-4V(ELI), 5Al-2.5Sn(ELI),
2219-T87, and 2219-T6E46 alloys, respectively. The loading rate was such that
the peak stress level was reached one minute after initiation of loading; (2) if
the flaw penetrated the specimen thickness prior to the attainment of the targeted
proof stress, the loading was continued until the specimen failed; (3) if the
flaw had not penetrated the specimen thickness prior to the attainment of the
targeted stress, the load was held constant at the proof stress for two minutes
and was then increased until the specimen failed.

In order to prepare specimens for subsequent sustained load testing, each specimen was proof loaded at -320F (78K) using the procedures described in the preceding paragraph. If the crack had not penetrated the specimen thickness at the peak proof stress level, each specimen was immediately unloaded and used for sustained load testing.

Sustained Load Test Procedures - Four specimens were simultaneously tested in a single tensile test machine by loading the specimens in series as shown in Figure 3-4. The test media were contained in small pressure cups clamped to the faces of the specimen. The cups were similar to those shown in Figure 3-1 except that cups and clamping plates were integral. Virgin teflon seals were used in all tests. The specimen train and pressure cups were surrounded by a cryostat as shown in the left hand machine in Figure 3-4. The cryostat was filled with either liquid nitrogen or a mixture of gaseous and liquid nitrogen to cool the specimens to the test temperatures. A thermocouple was used to monitor the temperature and control a valve which mixed the liquid and gaseous nitrogen in the needed proportions. For tests at temperatures other than at -320F (78K), cool down time averaged about 2.5 hours after which the desired test temperature was controlled within ± 5F (± 3K). Pressurized bottles were used as the source of both test media and pressure. Schematic drawings of the test systems for test in methane and fluorine or FLOX are shown in Figures 3-5 and 3-6.

The initiation sequence for fluorine tests was different from that for methane tests. For tests in environments containing fluorine, the following sequence was used: (1) passivate system with test media at ambient temperature; (2) purge system with helium gas; (3) bring system to test temperature; (4) load specimens; and (5) introduce the test media. For tests in methane, steps 4 and 5 were reversed so that the specimens were loaded in the test environments rather than in helium gas.

At the completion of the sustained load tests, all specimens were loaded while instrumented with pressure cups to determine if the surface crack had grown through the specimen thickness during the sustained load test. Procedures were the same as those used in the proof overload tests.

36

<u>Mechanical Property Test Procedures</u> - Tests were conducted at a strain rate of 0.005/minute until yield strength had been exceeded. The strain rate was then increased to 0.02/minute until failure. Stress-strain curves were obtained using a 2.0 inch (5.08 cm) gage length extensometer.

3.3   Results and Discussion

Results of the proof overload and sustained load tests are separately discussed in the following two subsections.

3.3.1   Proof Overload Tests

Details and results for the proof overload tests are included in Tables 3-2 and 3-3. Specimen dimensions, initial flaw dimensions, targeted proof stress levels, and stress levels at which either crack growth penetrated the specimen thickness or failure of the specimen occurred are summarized. Stress levels at both break-through and failure conditions are plotted against initial crack dimensions in Figure 3-7.

For the 2219-T87 aluminum alloy, two specimens (A-5 and A-7) containing cracks having initial depths of 0.028 and 0.029 inch (0.071 and 0.074 cm) failed before the targeted proof stress of 59 ksi (406.8 MN/m^2) was reached. A third specimen (A-4) containing a 0.026 inch (0.066 cm) deep crack withstood the 59 ksi (406.8 MN/m^2) proof stress without undergoing flaw growth through the specimen thickness. A fourth specimen (A-8) containing a 0.024 inch (0.061 cm) deep crack was loaded to the proof stress level; the proof stress was sustained for 40 seconds at which time the flaw penetrated the specimen thickness; the stress was then increased until the specimen failed at 63 ksi (434.4 MN/m^2). The foregoing results led to the selection of the following surface flaw dimensions for subsequent sustained load tests: a = 0.022 inch (0.56 mm) and 2c = 0.220 inch (5.59 mm).

The 2219-T6E46 alloy was very resistant to flaw growth during the proof load cycle. The maximum flaw depth tested (85 percent of the specimen thickness or 0.035 inch

(0.089 cm) in specimen AL-6 did not grow through the specimen thickness during the 46 ksi (317.2 MN/m^2) proof load. Since the distance between the flaw tip and back specimen face was only 0.006 inch (0.15 mm) in specimen AL-6, it was decided that further refinement of the maximum flaw dimension that could withstand the proof cycle was not practical. Accordingly, the following surface flaw dimensions were chosen for subsequent sustained load tests: a = 0.035 inch (0.89 mm) and 2c = 0.350 inch (8.89 mm).

Flaw growth through the specimen thickness was not observed in any Ti-5Al-2.5Sn(ELI) specimens. It was apparent that the maximum initial flaw dimensions that could withstand the proof test were somewhat greater than the 0.022 by 0.240 inch (0.56 by 6.10 mm) flaw dimensions in specimen 5T-5. Hence, the following surface flaw dimensions were chosen for the sustained load tests: a = 0.025 inch (0.64 mm) and 2c = 0.250 inch (6.35 mm).

For the 6Al-4V(ELI) titanium alloy, test results similar to those for the other alloys led to the selection of the following surface flaw dimensions for the sustained load tests: for the annealed condition, a = 0.020 inch (0.51 mm) and 2c = 0.200 inch (5.08 mm); and for the STA condition, a = 0.013 (0.33 mm) and 2c = 0.130 inch (3.30 mm).

3.3.2   Sustained Load Tests

Results of the longest duration tests in each environment are summarized in Table 3-4. The surface cracks did not grow through the specimen thickness during any of the sustained load tests summarized in Table 3-4. A visual examination of all fracture surfaces through a 30X microscope did not reveal any visible signs of Stress Corrosion Cracking (SCC).

The maximum possible SCC velocity (specimen thickness less initial crack depth divided by specimen duration) for any of the 500 hour duration tests was about 10^{-5} inches/hour (7 x 10^{-8} cm/sec). This velocity appears to be about an order of magnitude lower than any previously reported (12) SCC velocities for titanium alloys. Hence, it appears that SCC did not occur during any of the titanium alloy tests. For aluminum alloys, SCC velocities as low as 10^{-5} inches/hour (7 x 10^{-8}

38

cm/sec) have been reported (16) and it appears that SCC could progress at even slower velocities. Hence, the absence of SCC in the aluminum alloy tests cannot be inferred from maximum possible rate calculations.

After the 500 hour duration sustained load tests, aluminum alloy specimens that had been loaded to the higher stress level in the gas phase were subjected to fatigue loadings in room air to delineate the crack front. Visual observation of the fracture faces of these specimens revealed no evidence of flaw growth between the initial fatigue crack front and the fatigue crack growth induced at the end of the sustained load test. Other aluminum alloy specimens that had been tested for 500 hours were loaded to failure at -320F (78K). The failure loads for the 2219-T87 specimens were as high as those obtained from proof overload specimens that were loaded directly to failure. Hence, the failure data yielded no indications of SCC. A visual observation of the fracture faces of both 2219-T87 and -T6E46 specimens revealed no indications of SCC. Hence, the evidence strongly supports the conclusion that no SCC occurred during the sustained load aluminum alloy tests.

3.4   Conclusion

Minimum gage pressure vessels involving the material/environment combinations listed in Table 3-1 should not be prone to SCC problems after a proof test. The proof test cycle used in these tests consisted of a -320F (78K) load-unload cycle having a peak stress equal to 100 and 90 percent of the design yield strength for the aluminum and titanium alloys, respectively. The results obtained herein cannot be used to predict SCC behavior for other gages and proof test procedures using linear elastic fracture mechanics parameters since the plastic zones in the test specimen were not small relative to important specimen dimensions. However, moderate variations to the test details used in this program would not be expected to significantly increase SCC susceptibility of the material/environment combinations tested.

LIST OF REFERENCES

1. C.F. Tiffany, *"Fracture Control of Metallic Pressure Vessels"*, NASA Space Vehicle Design Criteria (Structures) NASA SP-8040, May 1970.

2. C.F. Tiffany, P.M. Lorenz, and L.R. Hall, *"Investigation of Plane Strain Flaw Growth in Thick-Walled Tanks"*, NASA CR-54837, February 1966.

3. C.F. Tiffany, P.M. Lorenz, and R.C. Shah, *"Extended Loading of Cryogenic Tanks"*, NASA CR-72252, July 1967.

4. L.R. Hall, *"Plane-Strain Cyclic Flaw Growth in 2014-T62 Aluminum and 6Al-4 V(ELI) Titanium"*, NASA CR-72396, November 1968.

5. L.R. Hall and R.W. Finger, *"Investigation of Flaw Geometry and Loading Effects on Plane Strain Fracture in Metallic Structures"*, NASA CR-72659 August 1971.

6. ASTM Committee E-24, *"Proposed Method of Test for Plane Strain Fracture Toughness of Metallic Materials"*, ASTM Standards Part 31, May 1969, pps. 1099-1114 (to be approved).

7. S. Mostovoy, P.B. Crosley, and E.J. Ripling, *"Use of Crack-Line-Loaded Specimens for Measuring Plane Strain Fracture Toughness"*, Journal of Materials, Vol. 2, No. 3, September 1967.

8. G.R. Irwin, *"Crack Extension Force for a Part-Through Crack in a Plate"*, Journal of Applied Mechanics, Vol. 29, Trans. ASME, Vol. 84, Series E, December 1962.

9. J.N. Masters, W.P. Haese, and R.W. Finger, *"Investigation of Deep Flaws in Thin Walled Tanks"*, NASA CR-72606, December 1968.

LIST OF REFERENCES (Con't.)

10. E.G. Haney, and W.R. Wearmouth, *"Effect of "Pure" Methanol on the Cracking of Titanium"*, Corrosion, Vol. 22, No. 2, 1959 p. 87.

11. D.P. Williams and H.G. Nelson, *"Gaseous - Hydrogen - Induced Crack Propagation in Ti-5Al-2.5 SN"*, NASA Ames Research Center, (to be published).

12. M.J. Blackburn, J.A. Feeney, and T.R. Beck, *"Stress Corrosion Cracking of Titanium Alloys"*, Boeing Scientific Research Laboratories, Document D1-82-1054, June 1970 (to be published by Plenum Press in Advances in Corrosion Science and Technology, edited by M.G. Fontana and R.W. Staehle).

13. H.P. Leckie, *"Stress Corrosion Characteristics of a Ti-7Al-2Cb-1Ta Alloy"*, Corrosion, Vol. 23, 1967.

14. M.H. Peterson, B.F. Brown, R.L. Newberger, and R.E. Grooves, *"Stress Corrosion Cracking of High Strength Steel and Titanium Alloys at Ambient Temperature"*, Corrosion, Vol. 23, 1967.

15. D.E. Piper, S.H. Smith, and R.V. Carter, *"Corrosion Fatigue and Stress Corrosion Cracking in Aqueous Environments"*, ASM Metals Engineering Quarterly, Vol. 8, 1968.

16. M.V. Hyatt and M.O. Speidel, *"Stress Corrosion Cracking of High Strength Aluminum Alloys"*, The Boeing Company Document D6-24840, June 1970.

17. R.L. Horst, Jr., E.H. Hollingsworth, and W. King, *"A New Solution Potential Measurement for Predicting Stress-Corrosion Performance of 2219 Aluminum Alloy Products"*, Corrosion, Vol. 25, No. 5, May 1969.

APPENDIX A---TEST DATA

This appendix contains raw test data for all stress corrosion cracking tests conducted during the investigation of stress corrosion cracking in 2219-T87 aluminum and 5Al-2.5 Sn(ELI) titanium alloys. The aluminum alloy data are listed in Tables A1 through A6. The titanium alloy data are listed in Tables A7 through A12.

APPENDIX B---DCB SPECIMEN STUDIES

INTRODUCTION

This appendix describes tests undertaken to explore crack growth behavior and compliance of side-grooved double cantilever beam (DCB) specimens. In DCB specimens, propagating cracks have a strong tendency to rotate from the original crack plane. This problem can be alleviated through the use of side grooves to restrict crack growth to the original crack plane. In this investigation, one specimen configuration and two side groove geometries were tested for each of two alloys. Specimen configuration is shown in Figure B1. Both semi-circular and Vee-shaped grooves were tested. Groove depth was set at either ten or fifteen percent of the specimen thickness. Tests were conducted for the WR direction of 1.0 inch (2.5 cm) thick 2219-T87 aluminum alloy plate, and 0.38 inch (0.97 cm) or 0.35 inch (0.90 cm) thick 5Al-2.5 Sn(ELI) titanium alloy plates.

BACKGROUND

Approximate compliance (C) values and opening mode stress intensity factors (K_1) for DCB specimens can be obtained from the literature (1). Compliance can be expressed by the equation.

$$C = \frac{2}{3EI} [(a + a_o)^3 + h^2 a]$$ (B1)

where E is Young's Modulus, 1 is the moment of intertia of one specimen arm, 'a' is crack length, a_o is an experimentally determined crack length increment to force agreement between experimentally measured compliance and Equation B1, and 2h is specimen height. Stress intensity factors for side grooved specimens are calculated from the expression

$$K_1 = \frac{2P}{b} \cdot \left(\frac{b}{b_n}\right)^{1/2} \left[\frac{3(a + a_o)^2 + h^2}{(1 - \mu^2) h^3}\right]^{\frac{1}{2}}$$ (B2)

where P is applied load, b is specimen width, b_n is crack width, and μ is Poisson's ratio.

PRECEDING PAGE BLANK NOT FILMED

45

PROCEDURES

Specimens were pin loaded in tensile test machines and clip gages were used to measure crack displacement. Load cell and clip gage output were connected to an X-Y recorder to obtain the load-displacement records from which compliance was determined.

Clip gages were spring loaded against integrally machined knife edges located at the end of the specimen rather than at the load line. Gage and load line locations are illustrated in Figure B1. For the specimen configuration tested, the major portion of compliance is due to rotation of the specimen arms at the vertical line passing through the crack tip, and from shear forces in the specimen arms. Since these two deflections vary linearly with distance from the crack tip, it was concluded that it would be sufficiently accurate to calculate deflections at the load line by multiplying deflections measured at the end of the specimen by the ratio of distance from crack tip to load line to distance from crack tip to clip gage location. Calculations based on simple beam theory showed that this procedure results in a maximum error of about two percent in calculated stress intensity. To substantiate this approach, two specimens were pin loaded in a test machine and deflection measurements were made across the specimen width using a micrometer. The resulting deflections are plotted as a function of distance from the end of the specimen in Figure 32. Over a major portion of the crack length, the deflections increase linearly in the manner assumed in the foregoing approach.

Calculated load-line compliance values were substituted into Equation B1 to evaluuate values of a_o. A beam height (h) of 1.5 inches (3.81 cm) was used in the calculations rather than the net beam height of 1.45 inches (3.68 cm). This procedure results in negligible error in calculated stress intensity factors as long as both a_o and stress intensity factors are calculated using the same beam height. The value of a_o does, however, vary significantly with the value of beam height used in the calculations.

46

RESULTS AND DISCUSSION

Eight initial tests were conducted to determine the effect of side groove geometry and depth on the shape of propagating crack fronts, and on the direction of propagations for rapidly propagating cracks. Four 2219-T87 aluminum and four 5Al-2.5 Sn(ELI) titanium specimens were tested. Aluminum alloy specimens fabricated with either Vee or semicircular grooves having depths equal to ten and twenty percent of the specimen thickness were tested in laboratory air. Titanium alloy specimens fabricated with both Vee and semicircular grooves having depths equal to ten percent of the specimen thickness were tested at 72F (295K) and -320F (78K). Testing consisted of subjecting specimens to zero to tension loading profiles using peak cyclic loads of 1500 and 3000 pounds (6672 and 13,344 N), followed by a static loading to failure. The fracture surfaces showed that the fatigue crack fronts in all specimens with semicircular grooves were straight and uniform across the specimen width. In specimens having vee-shaped grooves, crack growth was accentuated in the vicinity of the junction of crack front and side grooves. This result is illustrated by full scale drawings of the aluminum alloy fracture faces in Figure B3. These results were interpreted to mean that variables affecting crack propagation were more uniform across the specimen width for semicircular grooves than for Vee grooves. When pulled to failure, the crack propagated along the grooves in all but one specimen, namely, the titanium specimen with semicircular grooves that was tested at room temperature.

Compliance tests were conducted to determine values of a_o for use in the stress intensity factor Equation B2. Results of aluminum alloy compliance tests are summarized in Table B1. Specimens for which one compliance value is reported were pulled to failure and the slope of the straight line portion of the load deflection curve was used to compute compliance. Specimens for which multiple compliance values are reported were alternately subjected to fatigue and static loadings so that compliance values were obtained for several crack lengths. It is evident that values of a_o were quite insensitive to all test variables. There was a tendency for a_o to increase slightly with increased crack length. A value of a_o = 0.90 inch (2.29 cm) was selected for use in calculating stress

47

intensity values for all aluminum alloy DCB specimen tests discussed in the main body of this report. It is of interest to note that the ratio of a_o/h was 0.60 which is the same value previously reported (1) for 7075-T6 aluminum alloy DCB specimens having thicknesses ranging from 0.25 inch (0.64 cm) to 1.00 inch (2.54 cm), and groove depths ranging from five to thirty-five percent of the specimen thickness.

Fracture toughness values were computed using Equation B1, the appropriate a_o value from Table B1, and loads corresponding to the intersection of test records and a five percent offset slope through the origin of the test record. The values are in reasonable agreement with previously reported (2) plane strain fracture toughness values of 29 and 35 ksi $\sqrt{\text{in}}$ (32 and 38 $MN/m^{3/2}$) for the WR direction of 1.0 inch (2.54 cm) thick 2219-T87 aluminum alloy plate at 72F (295K) and -320F (78K), respectively.

Results of the titanium alloy compliance tests are included in Tables B2 and B3. The data in Table B2 were obtained from tests of 0.38 inch (0.97 cm) inch thick specimens. Values of a_o appeared to be dependent on groove shape and test temperature. For example, Vee shaped grooves seemed to yield lower a_o values at 72F (295K) than did semicircular grooves. In addition, a_o values appeared to be more temperature sensitive for semicircular grooves than for Vee grooves. The data in Table B3 were obtained from tests of 0.35 inch (0.89 cm) thick specimens taken from the same plate stock as used for all titanium DCB tests reported in the main body of this report. The a_o values are quite insensitive to temperature and are the same for both parent and weld metal. An a_o value of 0.78 inch (1.98 cm) was used to calculate stress intensity factors for all titanium alloy DCB specimen tests described in the main body of this report.

Fracture toughness values for the titanium alloy were computed using Equation B2, a_o values from Table B3, and five percent offset loads obtained from the test records. One room temperature base metal base metal specimen (T-1) underwent a rather abrupt onset of crack instability. The test record was valid by ASTM E399-70T standards and yielded a fracture toughness value of

48

115 ksi $\sqrt{in}$ (126 MN/m$^{3/2}$). This value is in good agreement with other reported values of ambient temperature plane strain fracture toughness for the 5Al-2.5 Sn(ELI) titanium alloy ranging between 100 and 120 ksi $\sqrt{in}$ (110 and 132 MN/m$^{3/2}$). All other 72F (295K) base and weld metal tests yielded rounded load-displacement curves that showed no evidence of an abrupt crack size instability. Average plane strain fracture toughness values reported in (3) for the RW direction of a 0.25 inch (0.64 cm) thick rolled 5Al-2.5 Sn(ELI) plate were 49 ksi $\sqrt{in}$ (54 MN/m$^{3/2}$) at -423F (20K) and 56 ksi $\sqrt{in}$ (62 MN/m$^{3/2}$) at -320F (78K). Hence, the fracture toughness values obtained from the -320F (78K) and -423F (20K) DCB tests in this program are equivalent to plane strain fracture toughness values.

Comparisons made between crack opening displacements measured using both clip gage and micrometer are included in Table B4. Micrometer measurements were made between points A as shown in Figure B1 and clip gage measurements were made as previously described. Comparisons are shown for aluminum base metal DCB specimens both pin loaded in a test machine and wedge loaded in a vise. For the pin loaded test, the micrometer readings are consistently less than the clip gage readings with a maximum discrepancy of 0.0011 inch (0.028 mm). For the wedge loaded test, the micrometer measurements were again less than the clip gage measurements with a maximum difference of 0.0015 inch (0.038 cm). In view of the good agreement between the two different readings, it was concluded that micrometer measurements provided a sufficiently accurate method of controlling stress intensity factor during the wedge loading of DCB specimens.

LIST OF REFERENCES FOR
APPENDIX B

1. S. Mostovoy, P.B. Crosley, and E.J. Ripling, *"Use of Crack Line Loaded Specimens for Measuring Plane Strain Fracture Toughness"*, Journal of Materials, Vol. 2, No. 3, September 1967.

2. C.M. Carman, J.W. Forney, and J.M. Katlin, *"Plane Strain Fracture Toughness of 2219-T87 Aluminum Alloy at Room and Cryogenic Temperatures"*, NASA CR-54297, August 1966.

3. R. Pyle, D.E. Schillinger, and C.M. Carman, *"Plane Strain Fracture Toughness and Mechanical Properties of 2219-T87 Aluminum and 5Al-2.5 Sn(ELI) Titanium Alloy Weldments and One Inch Thick 5Al-2.5 Sn(ELI) Titanium Alloy Plate"*, NASA CR-72154, Semptember 1968.

APPENDIX C---TEST SPECIMENS

This appendix contains detailed drawings of all test specimens used in this investigation. Table C1 relates the specimen configurations to the particular series of tests for which they were used. Figures C1 through C12 contain detailed drawings of each specimen configuration.

APPENDIX D---WELDING PARAMETERS

Welding Parameters: 1.00 inch -- 2219-T87 Aluminum

Surface Flawed Specimens:

First Side - First Pass

Current - 200 amps

Voltage - 12.5 volts

Travel - 15 ipm (6.3 mm/sec)

Wire - None

First Side - Second Pass*

Current - 400 amps

Voltage - 12.0 volts

Travel - 3 ipm (1.27 mm/sec)

Wire - None

   *Panel was turned over and the joint completed in one pass with these settings.

DCB Specimens:

First Side - First Pass

Current - 200 amps

Voltage - 12.5 volts

Travel - 15 ipm (6.3 mm/sec)

Wire - None

First Side - Second Pass**

Current - 390 amps

Voltage - 12.0 volts

Travel - 3.5 ipm (1.48 mm/sec)

Wire - None

   **Panel was turned over and the joint completed in one pass with these settings.

Both panel series were welded with a Linde HW-27 torch; a 5/32 inch (0.40 cm) diameter, 2% thoriated, tungsten electrode, rounded to 1/8 inch (0.32 cm) diameter ball nose over a 3/8 inch (0.95 cm) taper; and pure helium shielding gas at 110 CFH (3.1 m^3/hr)

Welding Parameters: <u>0.350 inch − 5Al-2.5Sn (ELI) Titanium</u>
<u>Surface Flawed and DCB Specimens.</u>

<u>First Pass</u>   <u>Second Pass</u>

Current − 215 amps   Current − 200 amps

Voltage − 14 volts   Voltage − 14 volts

Travel − 3 ipm (1.27 mm/sec)   Travel − 3 ipm (1.27 mm/sec)

Electrode: 2% thoriated tungsten, 1/8 inch (0.32 cm) diameter, 45° included
            angle to 0.030 inch (0.076 cm) diameter end.

APPENDIX E---CLEANING PROCEDURE FOR FLUORINE ENVIRONMENTS

The cleaning procedure used for all of the specimens and test equipment (valves, tubing, etc.) exposed to fluorine environments (F_2, OF_2 and FLOX) is listed below:

1. Vapor degrease and trichloroethylene flush - 10 minutes

2. Detergent flush - 10-15 minutes

3. Cold water flush - 10 minutes

4. Passivate with 50% nitric acid solution - 5 minutes maximum

5. Flush with De-ionized water - 10 minutes

6. Purge dry with hot nitrogen gas

7. Oven dry - 1-2 Hours

8. Bag and seal in plastic

NOTE: Components with enclosed areas, such as valves, were vacuum baked for 1-2 hours instead of oven dried.

APPENDIX F---CONVERSION OF U.S. CUSTOMARY UNITS TO SI UNITS

In the text of this report, all numerical values are given in U.S. customary units with corresponding SI units in parenthesis. Due to the complexity of the tables of results, only U.S. customary units are used therein. Conversion factors for converting U.S. customary to SI units are given in the following table:

To Convert From (U.S. Customary Unit)	Multiply by	To Obtain (SI Units)
in.	2.54×10^{-2}	meter (m)
lbf	4.448	newton (n)
kip	4.448	kilonewton (kN)
ksi	6.895	meganewton/meter^2 (MN/m^2)
ksi $\sqrt{in}$	1.099	$MN/m^{3/2}$
°F	$5/9 \ (F + 459.67)$	°K

Figure 2-1: MECHANICAL PROPERTIES FOR 2219-T87 ALUMINUM—ONE INCH (2.54 cm) THICK PLATE
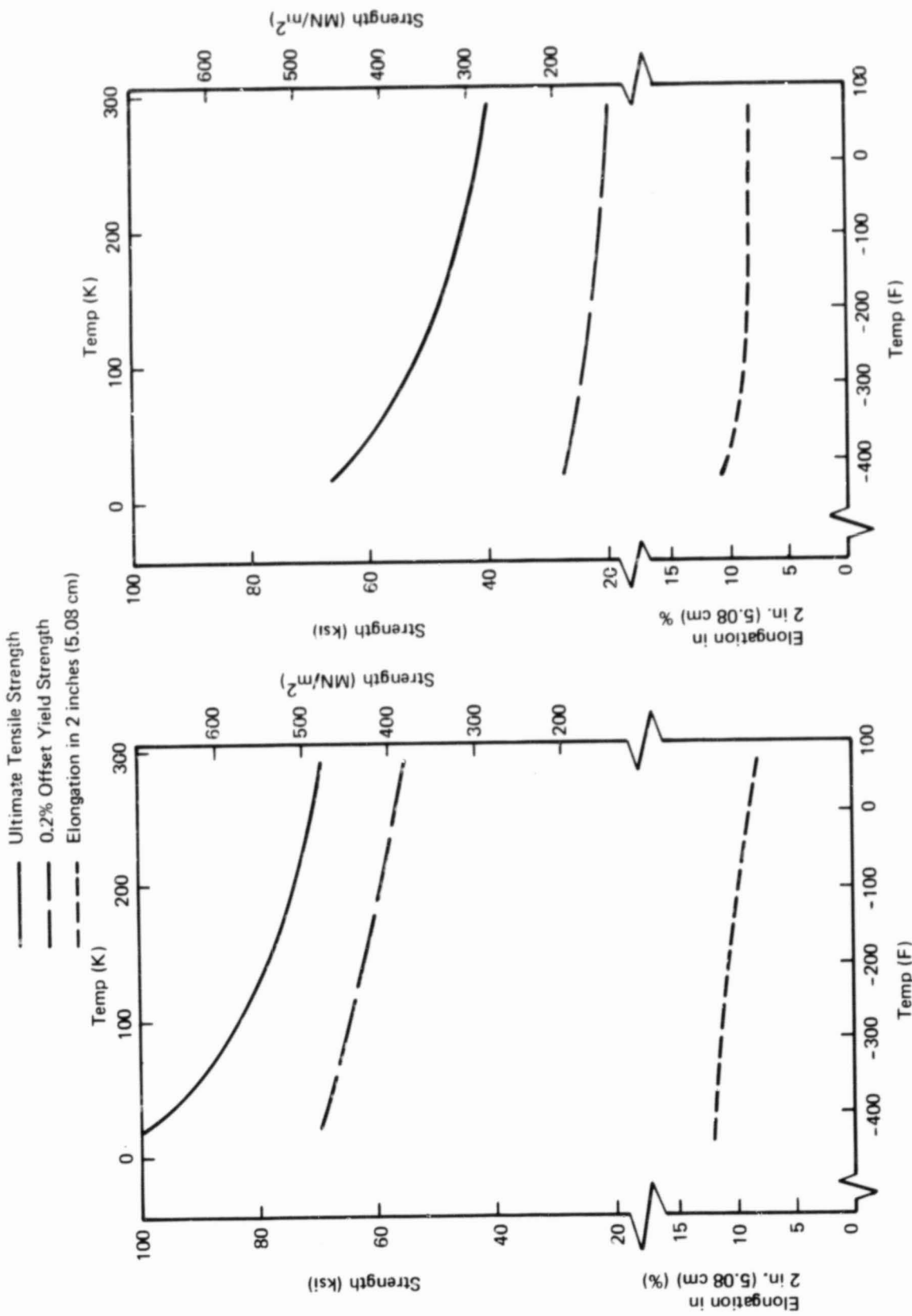
(a) Plate (Transverse Direction)

(b) Weld Metal

Legend:
—— Ultimate Tensile Strength
— — 0.2% Offset Yield Strength
– – – Elongation in 2 inches (5.08 cm)

Figure 2-2: MECHANICAL PROPERTIES FOR 5Al-2.5 Sn (ELI) TITANIUM—0.35 INCH (0.89 cm) THICK PLATE
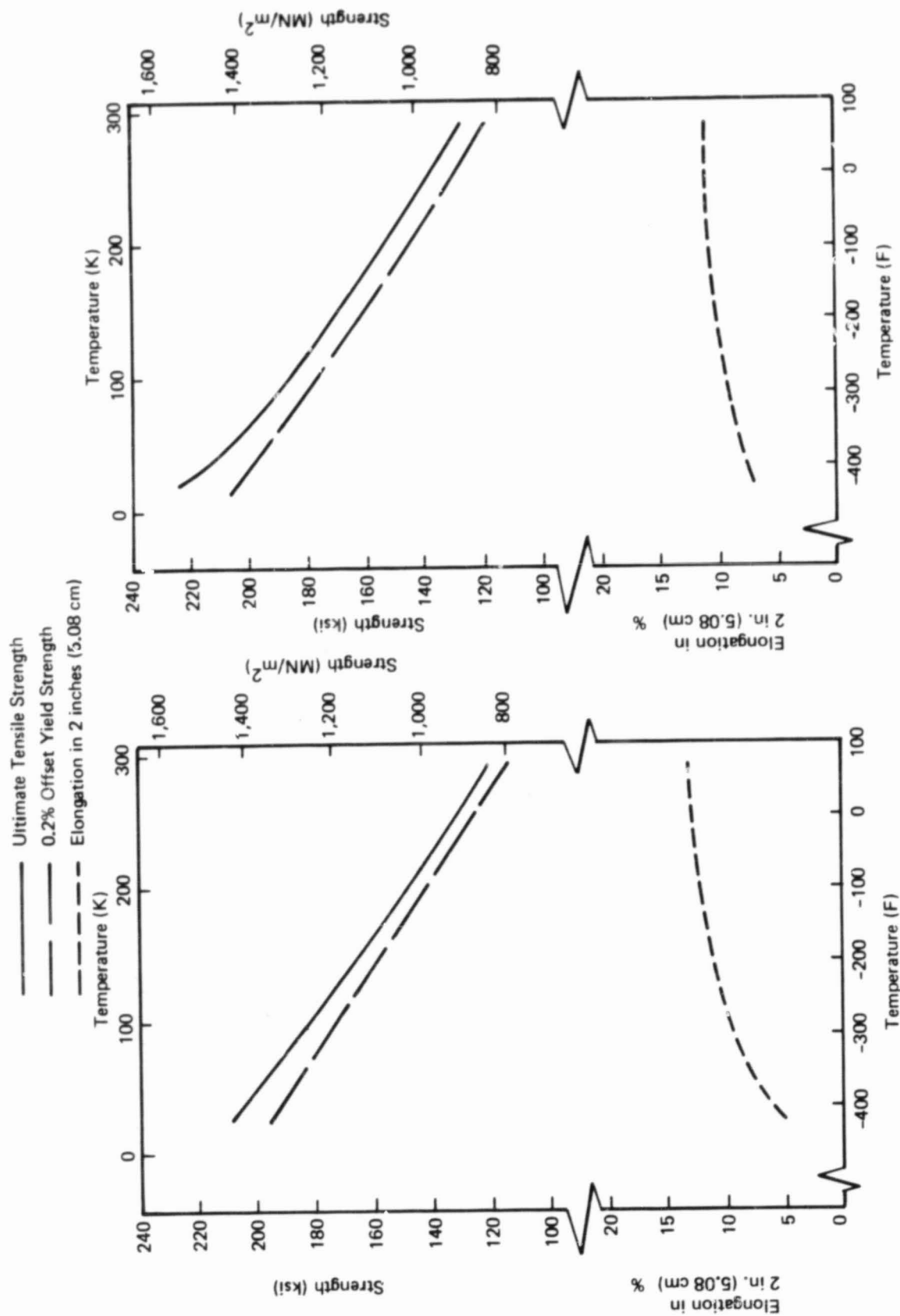
(a) Base Metal (Longitudinal Direction)

(b) Weld Metal

61
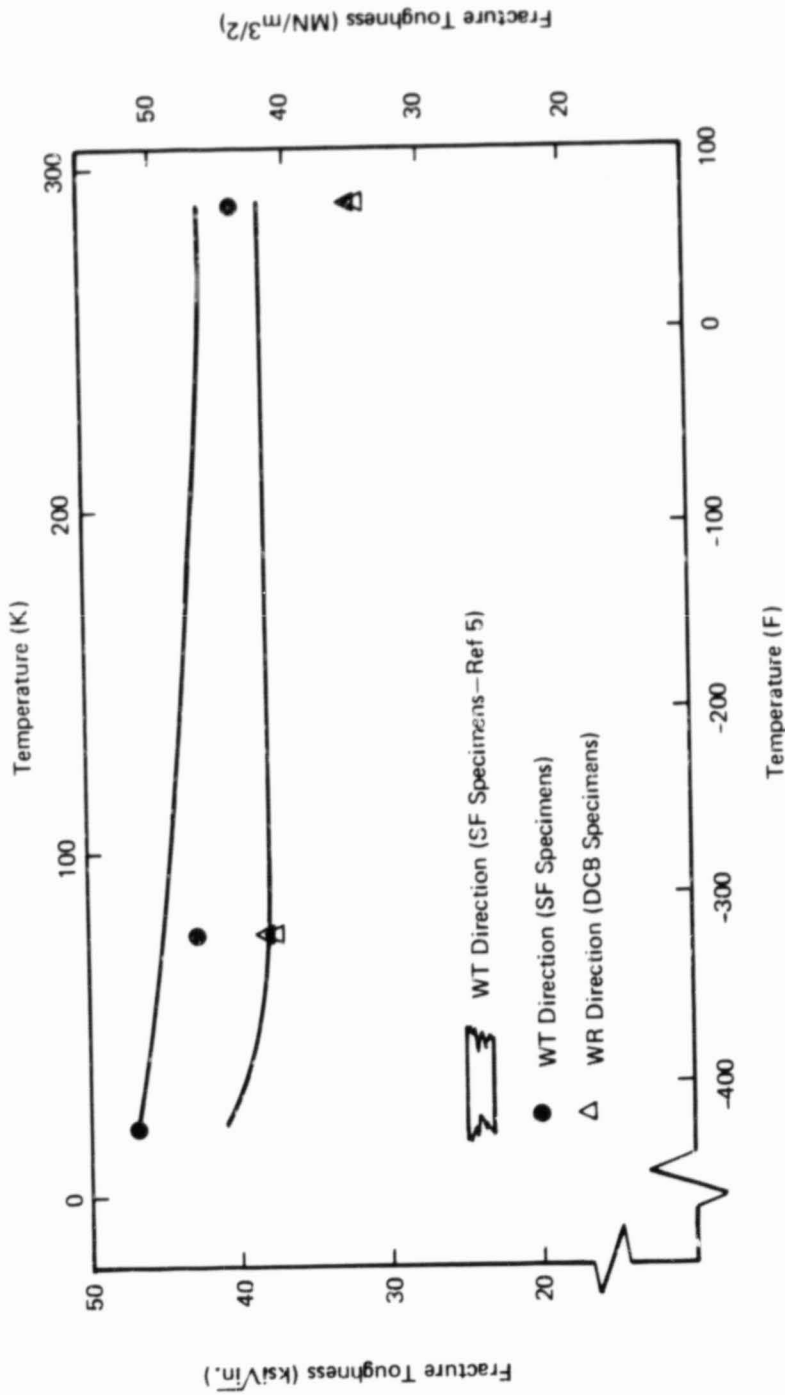
Figure 2-3: FRACTURE TOUGHNESS DATA FOR 1.0 INCH (2.54 cm) THICK 2219-T87 ALUMINUM ALLOY PLATE

62
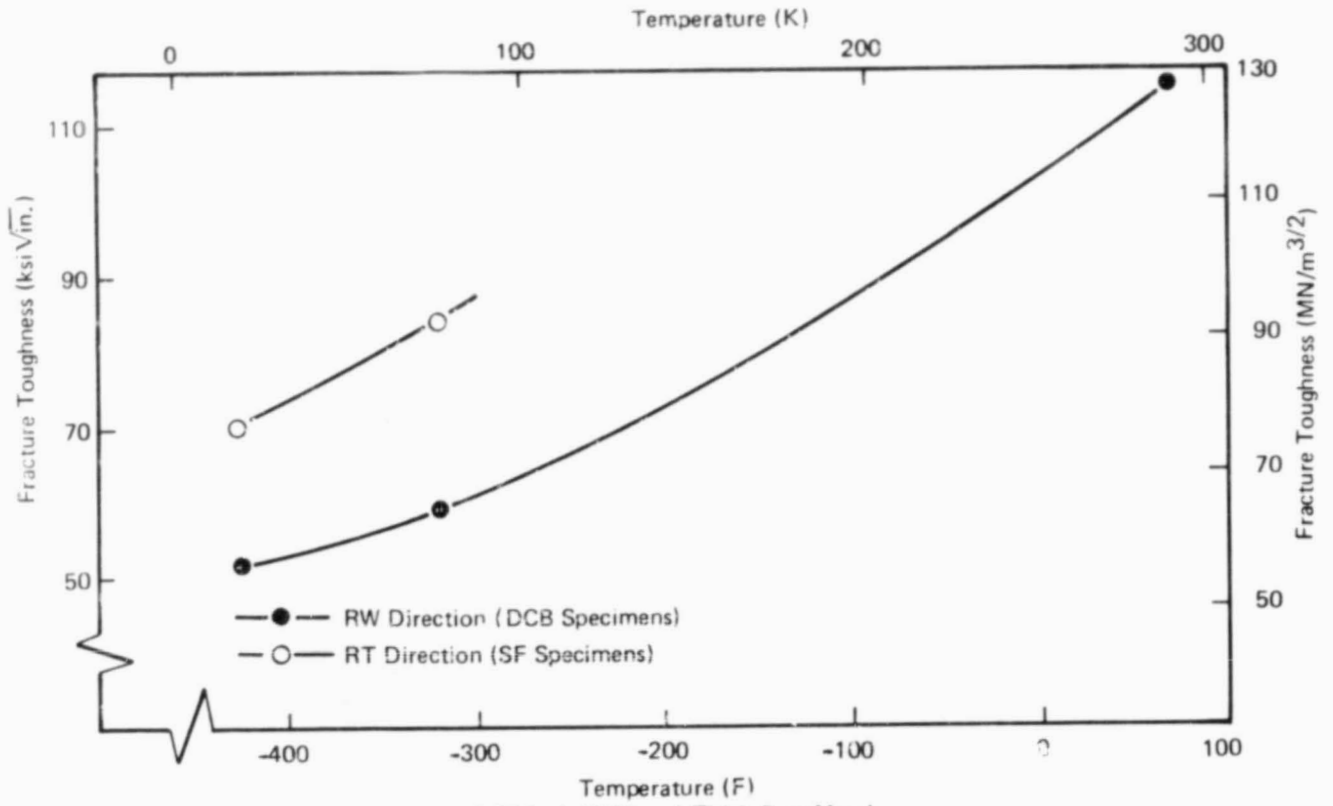
(a) 0.35-Inch (0.89 cm) Thick Base Metal
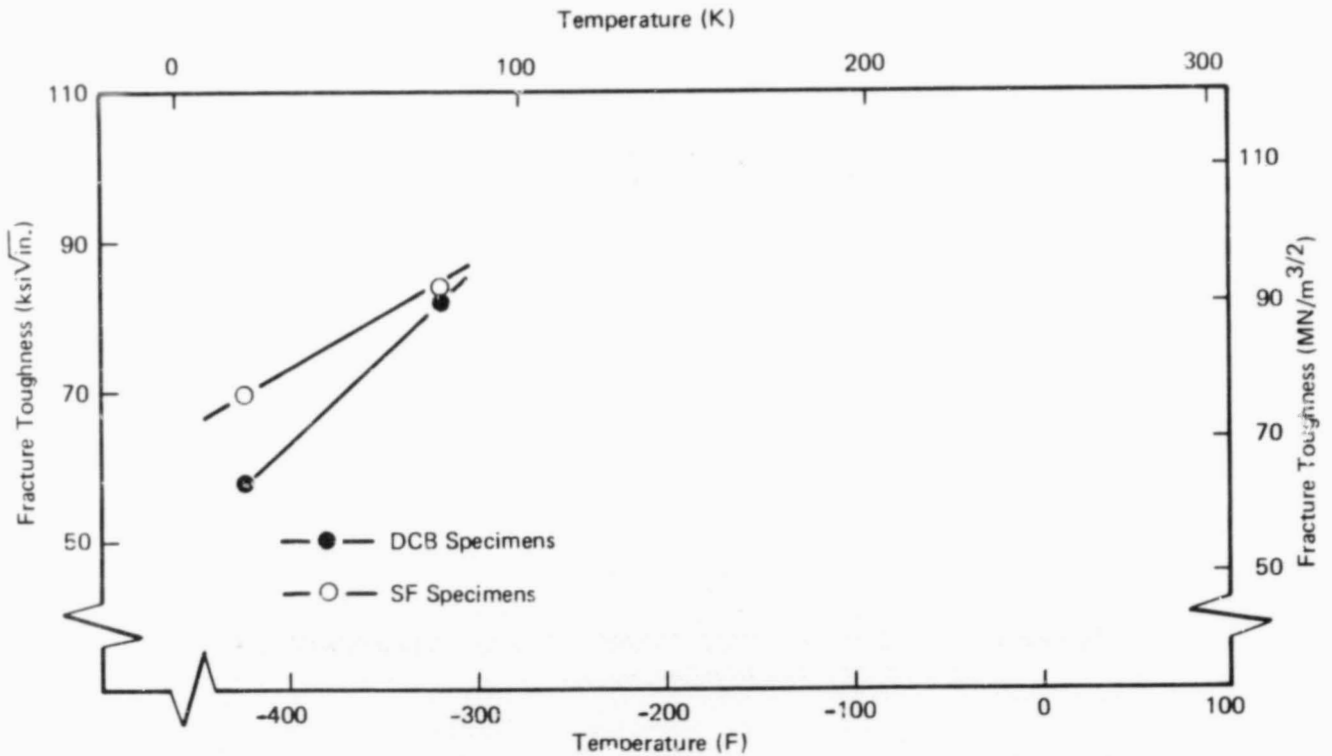
(b) 0.35-Inch (0.89 cm) Thick GTA Weld Centerlines

Figure 2-4: FRACTURE TOUGHNESS DATA FOR ALLOYS USED IN SCC TESTS
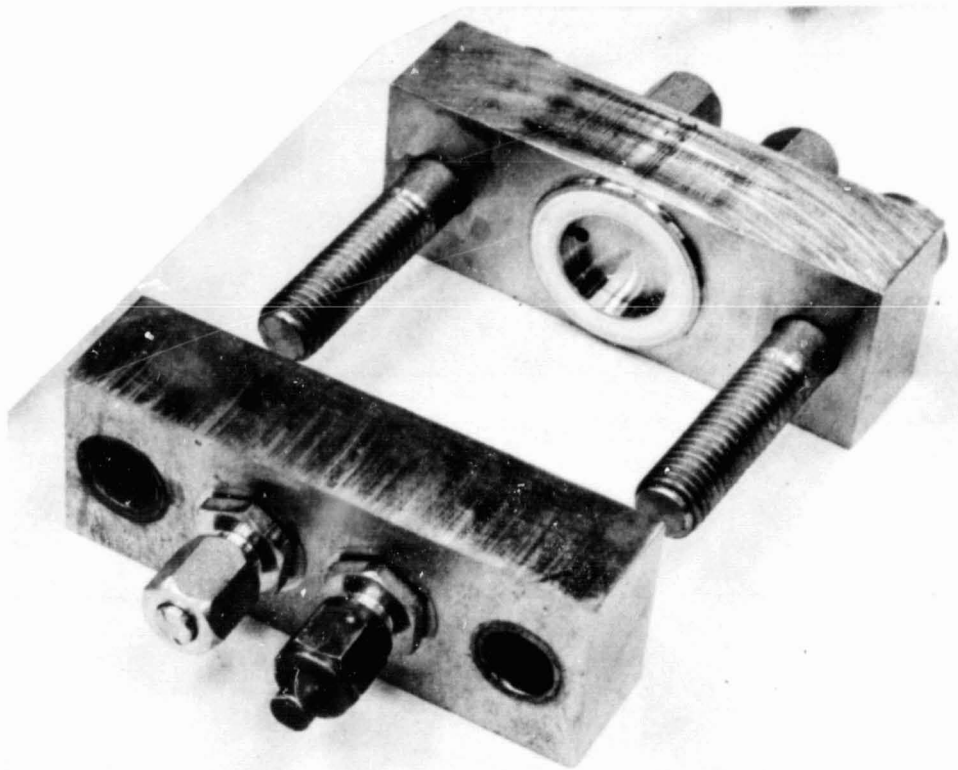
Figure 2-5: *PRESSURE CUPS USED TO DETECT CRACK BREAKTHROUGH IN SURFACE FLAWED SPECIMENS.*

Cap for Titanium Specimens

SECTION A–A
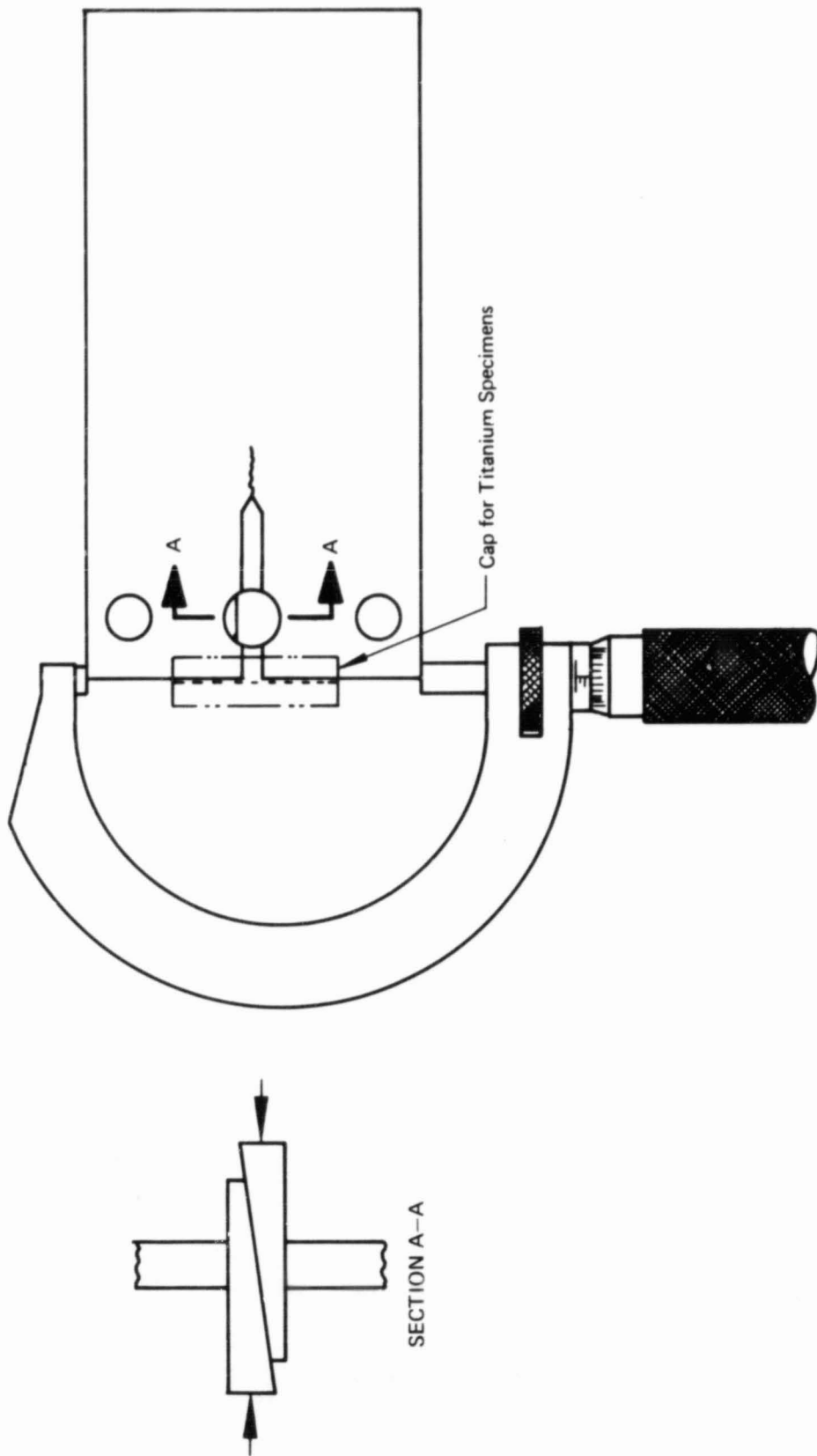
Figure 2-6: METHOD OF LOADING DCB SPECIMENS

65
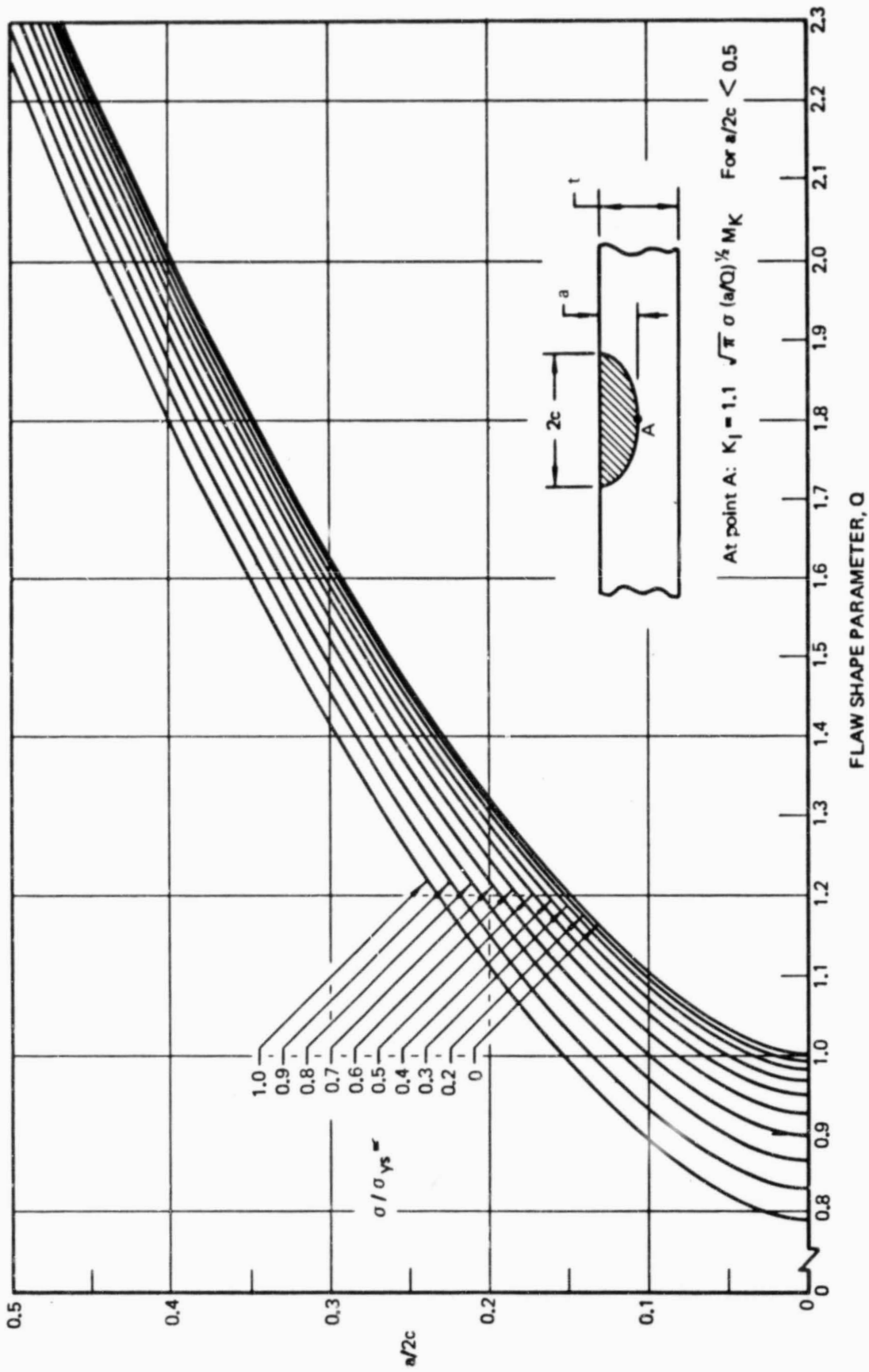
Figure 2-7: SHAPE PARAMETER CURVES FOR SURFACE AND INTERNAL FLAWS

At point A: $K_I = 1.1 \sqrt{\pi} \, \sigma \, (a/Q)^{1/2} \, M_K$ For $a/2c < 0.5$
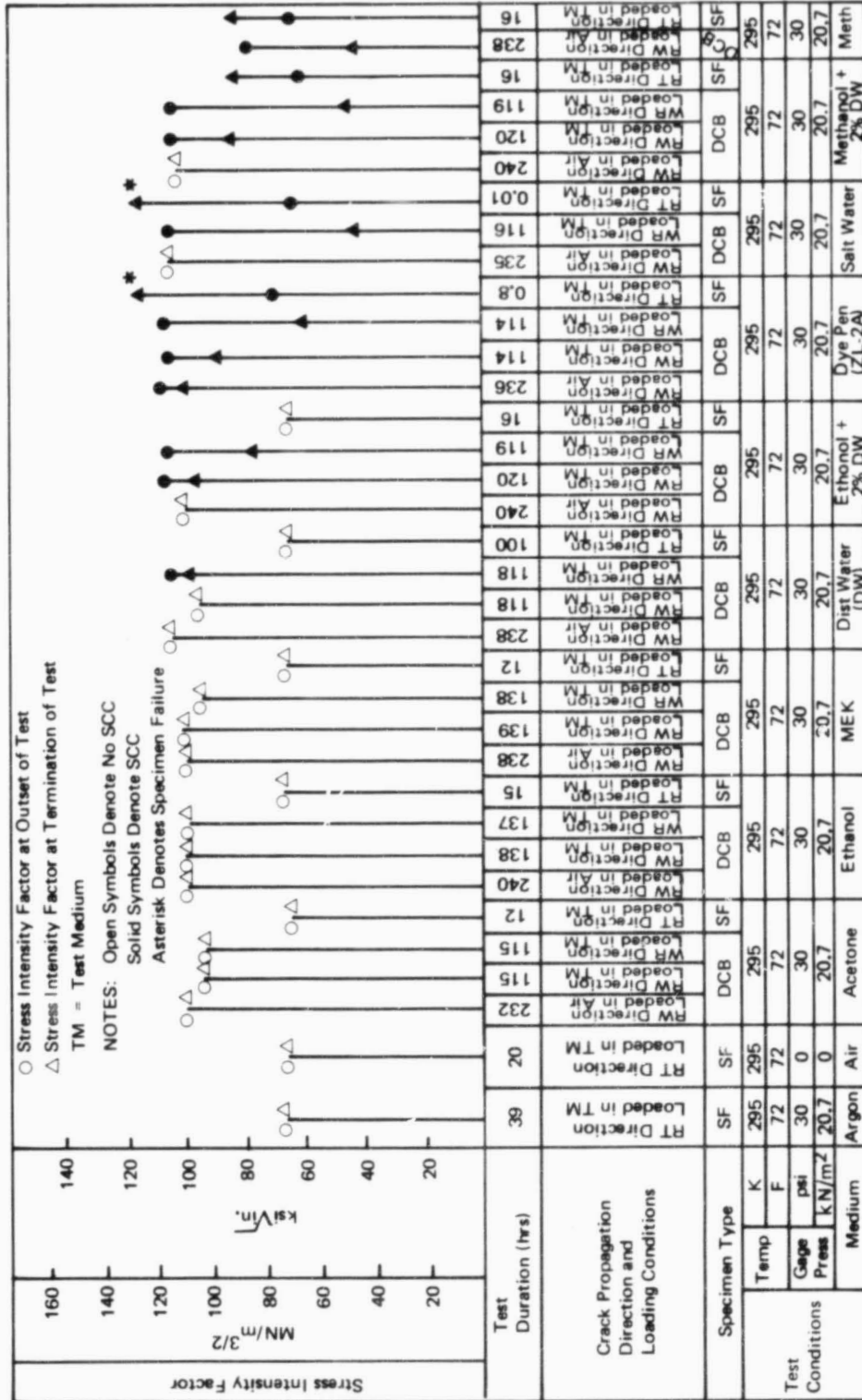
Figure 2-8: RESULTS OF STRESS CORROSION CRACKING TESTS FOR Ti-5Al-2.5 Sn (ELI) 0.35-INCH (0.89 cm) THICK PLATE (Excluding Nitrogen, Helium and Hydrogen Tests)

Figure 2-9: stress corrosion cracking test chart

Legend:
○ Stress Intensity Factor at Outset of Test
△ Stress Intensity Factor at Termination of Test
TM = Test Medium
NOTE: Open Symbols Denote No SCC
Solid Symbols Denote Occurrence of SCC

Vertical axis (upper scale): ksi√in. — 20, 40, 60, 80, 100, 120, 140
Vertical axis (lower scale): MN/m^{3/2} — 20, 40, 60, 80, 100, 120, 140, 160
Axis label: Stress Intensity Factor

Test Duration (hrs)	Crack Propagation Direction and Loading Conditions	Specimen Type	Temp K	Temp F	Gage Press psi	Gage Press KN/m²	Medium
12	RT Direction Loaded in Env.	SF	78	-320	0	0	LN₂
31	RW Direction Loaded in Air	DCB	278-289	40 - 60	30	20.7	GHe
10	RT Direction Loaded in TM	SF	278-289	40 - 60	1,000	690	GHe
12	RT Direction Loaded in TM	SF	278-289	40 - 60	1,000	690	
42	RW Direction Loaded in Air	DCB	20	-423	30	20.7	GHe
10	RT Direction Loaded in TM	SF					
30	RW Direction Loaded in Air	DCB	278-289	40 - 60	30	20.7	
12	RT Direction Loaded in TM	SF	278-289	40 - 60	30	20.7	
24	RW Direction Loaded in Air	DCB	278-289	40 - 60	100	69	
10	RT Direction Loaded in TM	SF					
32	RW Direction Loaded in Air	DCB	78	-320	30	20.7	GH₂
10	RT Direction Loaded in TM	SF					
46	RW Direction Loaded in Air	DCB	~20	~-423	0	0	
10	RT Direction Loaded in TM	SF					
10	RT Direction Loaded in TM	SF	20	-423	0	0	LH₂
20	RT Direction Loaded in TM	SF	20	-423	0	0	LH₂

Test Conditions

Figure 2-9: RESULTS OF STRESS CORROSION CRACKING TESTS FOR 5Al-2.5 Sn (ELI) TITANIUM 0.35 INCH (0.89 cm) THICK PLATE (NITROGEN, HELIUM, HYDROGEN TESTS)
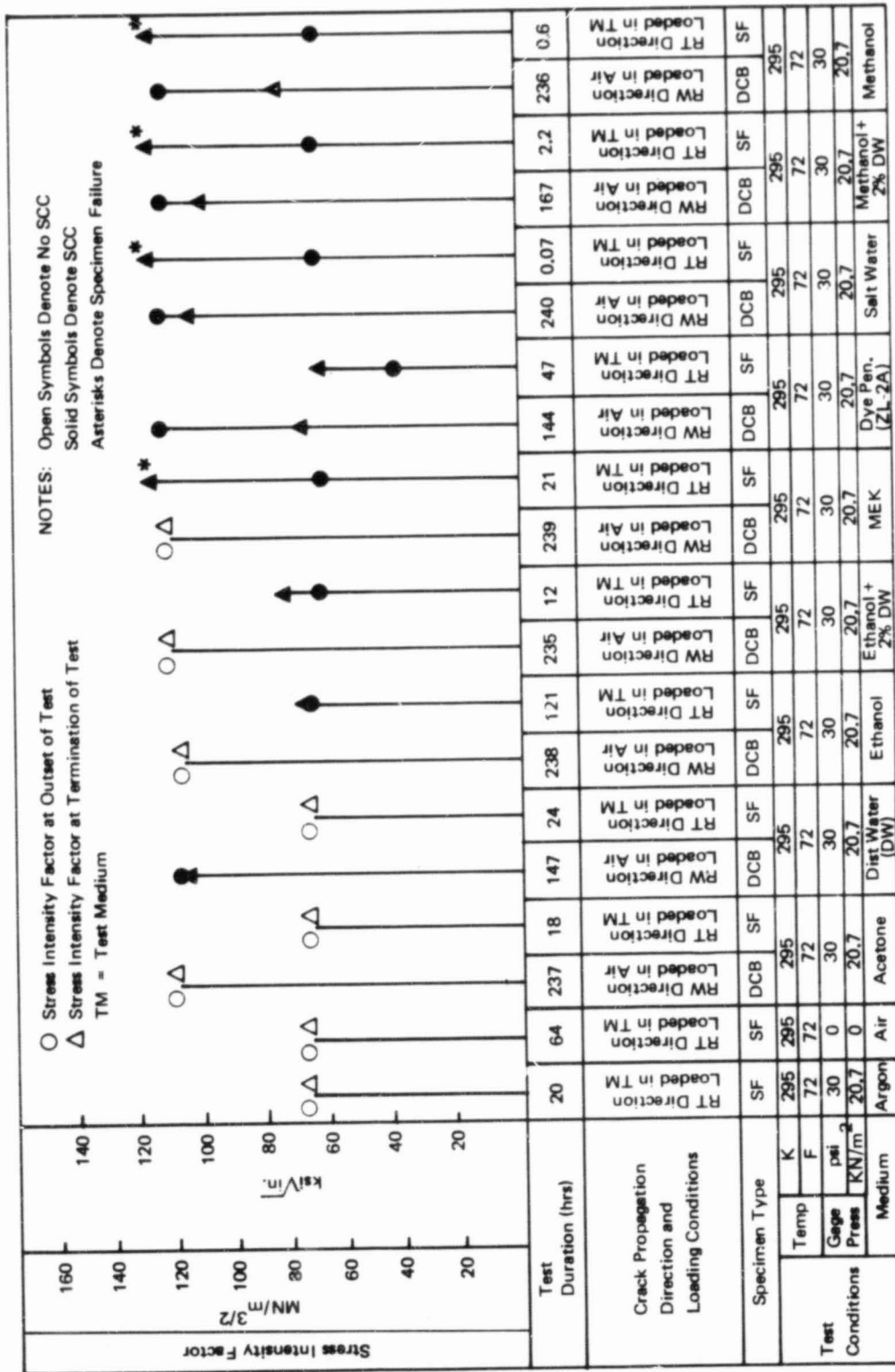
Figure 2-10: RESULTS OF STRESS CORROSION CRACKING TESTS FOR 5Al-2.5Sn (ELI) TITANIUM 0.35 INCH (0.89 cm) THICK GTA WELD CENTERLINES (EXCLUDING HYDROGEN AND HELIUM TESTS)

Stress Intensity Factor

MN/m³/2

ksi√in.

○ Stress Intensity Factor at Outset of Test
△ Stress Intensity Factor at Termination of Test
TM = Test Medium
NOTE: No SCC observed in Tests Summarized Below

Test Duration (hrs)	Crack Propagation Direction and Loading Conditions	Specimen Type	Temp K	Temp F	Gage psi	Press KN/m²	Medium
24	RW Direction Loaded in Air	DCB	278-289	40 - 60	30	20.7	GHe
15	RT Direction Loaded in TM	SF	278-289	40 - 60			GHe
10	RT Direction Loaded in TM	SF	278-289	40 - 60	1,000	690	GHe
42	RW Direction Loaded in Air	DCB	20	-423	30	20.7	GHe
10	RT Direction Loaded in TM	SF					
33	RW Direction Loaded in Air	DCB	278-289	40 - 60	30	20.7	
9	RT Direction Loaded in TM	SF	278-289	40 - 60			
33	RW Direction Loaded in Air	DCB	278-289	40 - 60	100	69	GH₂
9	RT Direction Loaded in TM	SF	278-289	40 - 60			
32	RW Direction Loaded in Air	DCB	78	-320	30	20.7	
12	RT Direction Loaded in TM	SF					
46	RW Direction Loaded in Air	DCB	~	~ -423	0	0	
12	RT Direction Loaded in TM	SF	20	-423	0	0	
9	RT Direction Loaded in TM	SF	20	-423	0	0	LH₂

Figure 2-11: RESULTS OF STRESS CORROSION CRACKING TESTS FOR 5Al-2.5Sn (ELI) TITANIUM 0.35 INCH (0.89 cm) THICK GTA WELD CENTERLINES (HYDROGEN AND HELIUM TESTS)

70

Figure 2-12: RESULTS OF STRESS CORROSION CRACKING TESTS FOR 2219-T87 ALUMINUM ONE INCH (2.54 cm) THICK PLATE (EXCLUDING HAZARDOUS ENVIRONMENT TESTS)

71

Figure 2-13: RESULTS OF STRESS CORROSION CRACKING TESTS FOR 2219-T87 ALUMINUM ONE INCH (2.54 cm) THICK PLATE (HAZARDOUS ENVIRONMENT TESTS)
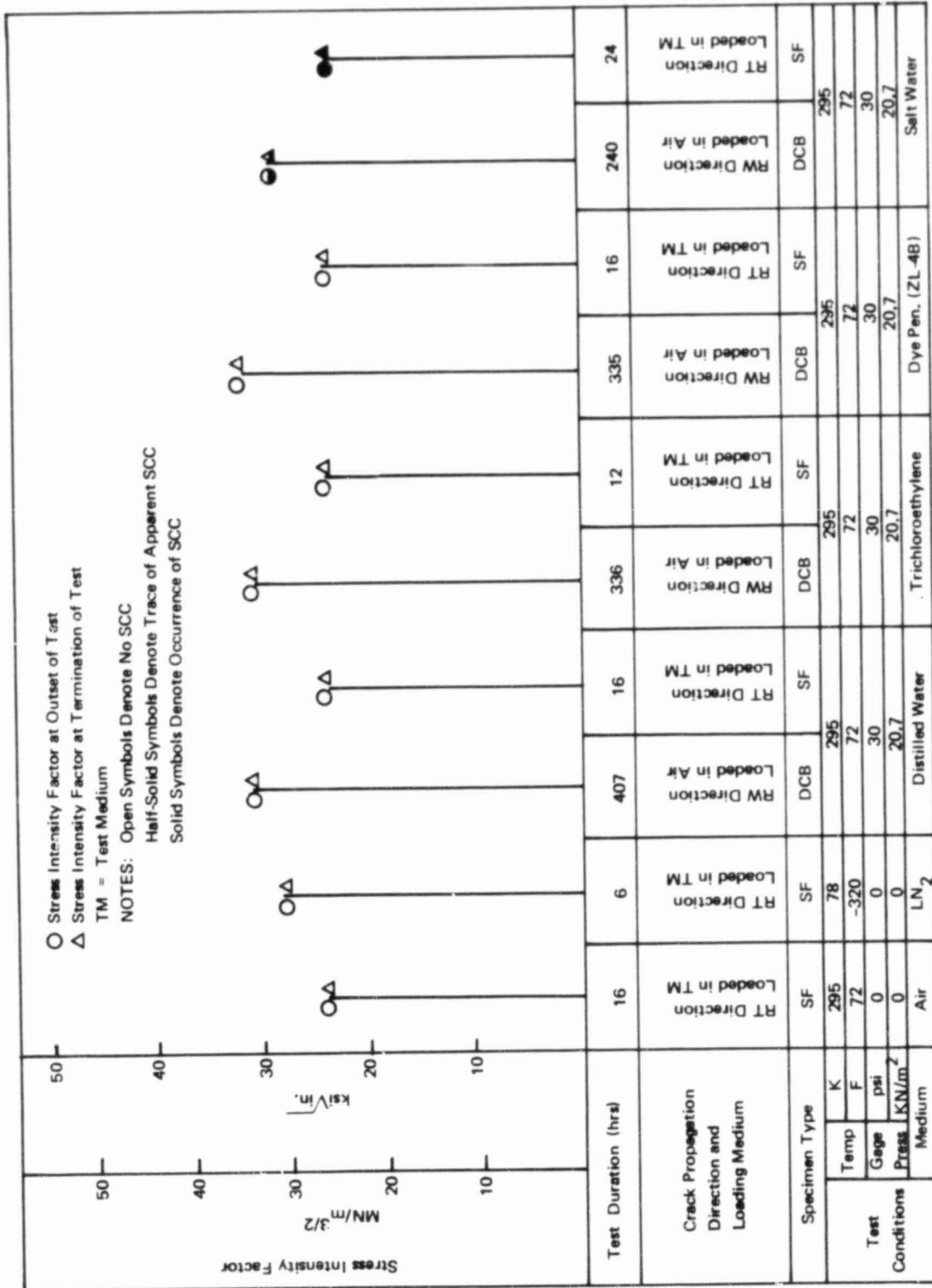
Figure 2-14: RESULTS OF STRESS CORROSION CRACKING TESTS FOR 2219 ALUMINUM AS-WELDED GTA ONE INCH (2.54 cm) THICK WELD CENTERLINES (EXCLUDING HAZARDOUS ENVIRONMENT TESTS)

Figure 2-15: RESULTS OF STRESS CORROSION CRACKING TESTS FOR 2219 ALUMINUM AS-WELDED GTA ONE INCH (2.54 cm) THICK WELD CENTERLINES (HAZARDOUS ENVIRONMENT TESTS)
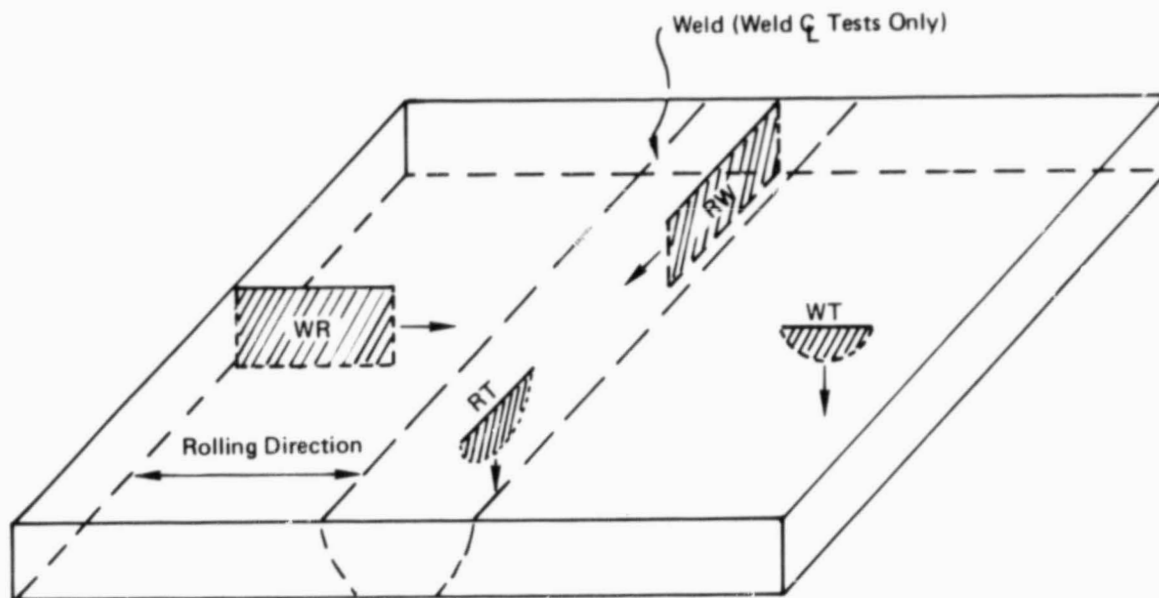
Figure 2-16: NOMENCLATURE FOR DENOTING CRACK PROPAGATION DIRECTIONS IN PLATE MATERIAL AND WELD CENTERLINES

Figure 2-17: SUMMARY OF SCC CRACK GROWTH OBSERVED IN TESTS OF 0.35 INCH (0.89 cm) THICK 5Al-2.5 Sn (ELI) TITANIUM PLATE MATERIAL AND GTA WELD CENTERLINES

SPECIMEN NUMBER	TEST MEDIUM
TDL-1	Dye Penetrant
TH-5	Hydrogen Gas
TEDL-1	Dilute Ethanol
TM-2	Methanol
TWD-3	Dye Penetrant
TWM-2	Methanol
TWMD-1	Dilute Methanol
TWME-3	Methyl Ethyl Ketone
TM-1	Methanol
TWM-1	Methanol
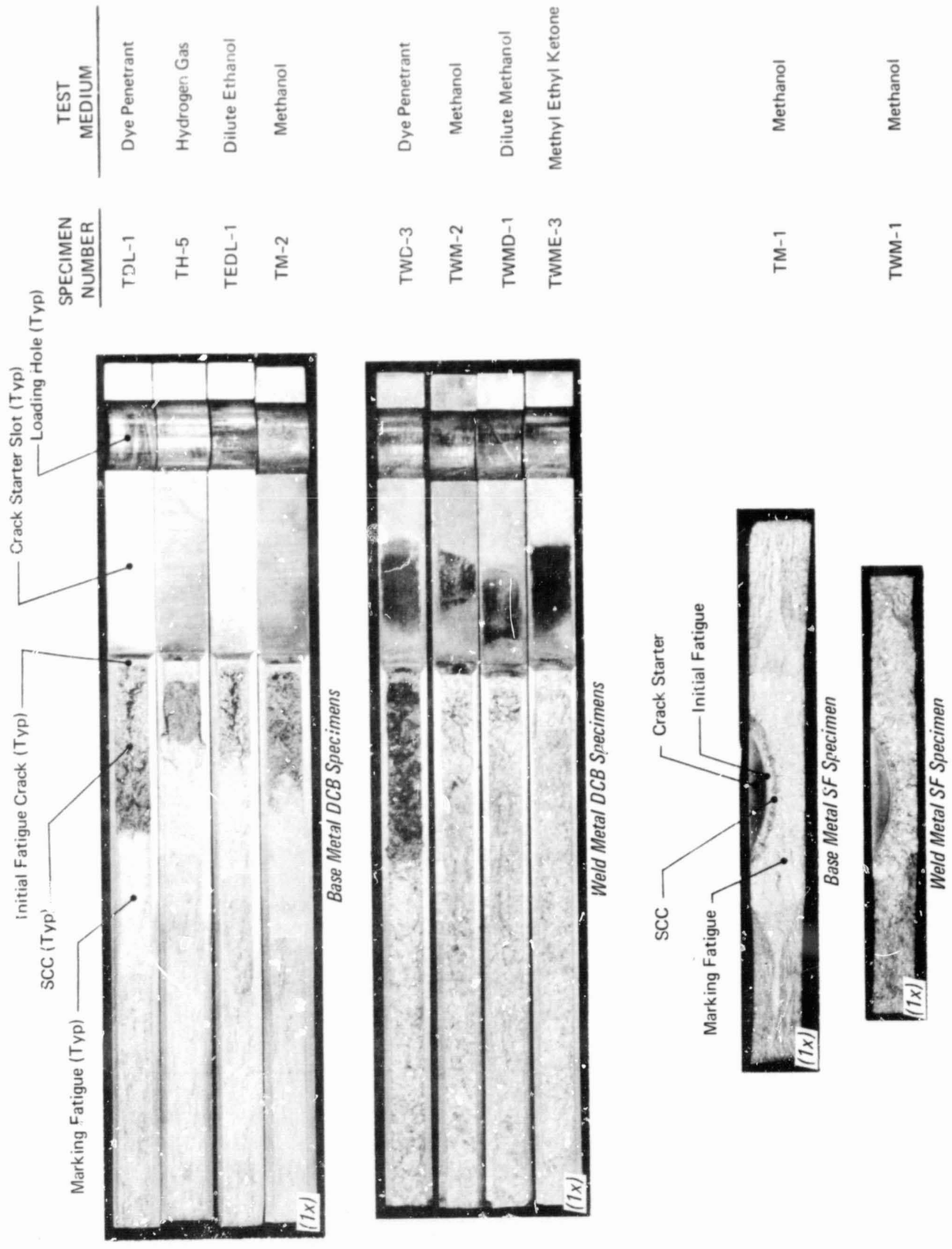
Figure 2-18: FRACTURE SURFACES OF 5Al-2.5Sn (ELI) TITANIUM ALLOY SPECIMENS

77
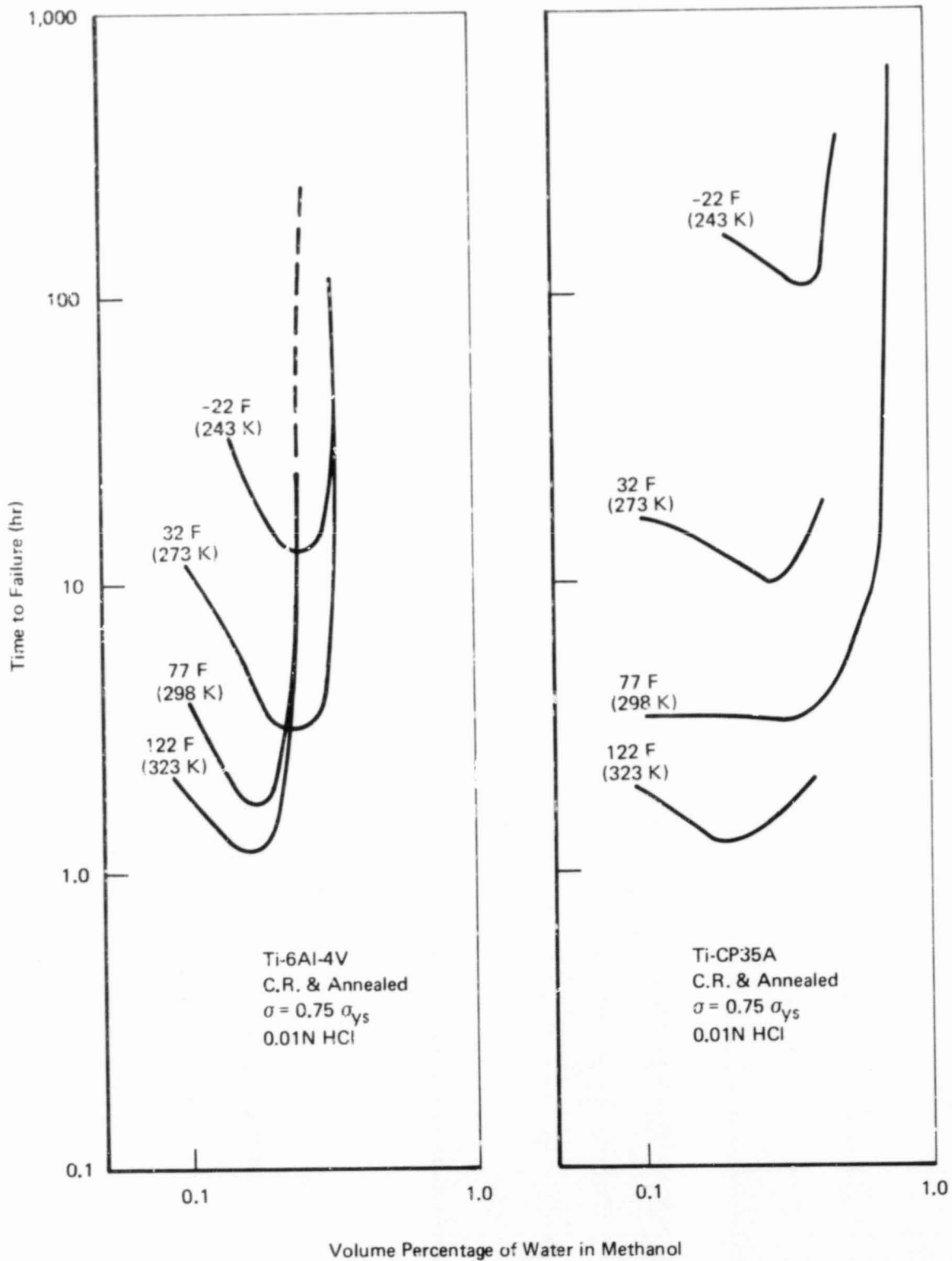
Figure 2-19: EFFECT OF TEMPERATURE AND VOLUME PERCENTAGE OF WATER ON TIME TO FAILURE FOR SMOOTH TITANIUM FOIL SPECIMENS (REF. 10)
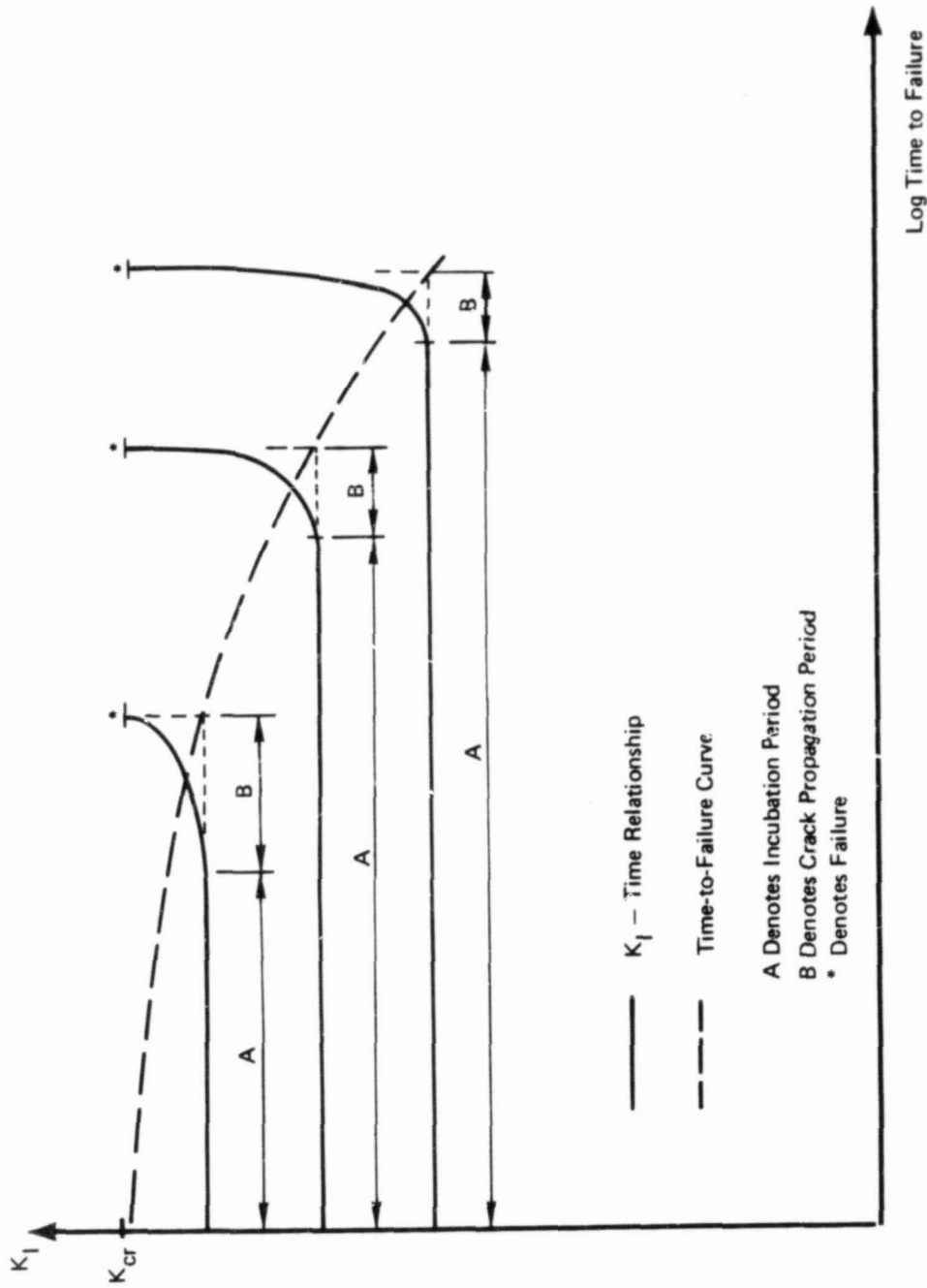
Figure 2-20:   SCHEMATIC REPRESENTATION OF THE RELATIONSHIP BETWEEN INCUBATION PERIOD, CRACK GROWTH, AND TIME TO FAILURE FOR ENVIRONMENTALLY INDUCED CRACK GROWTH

79
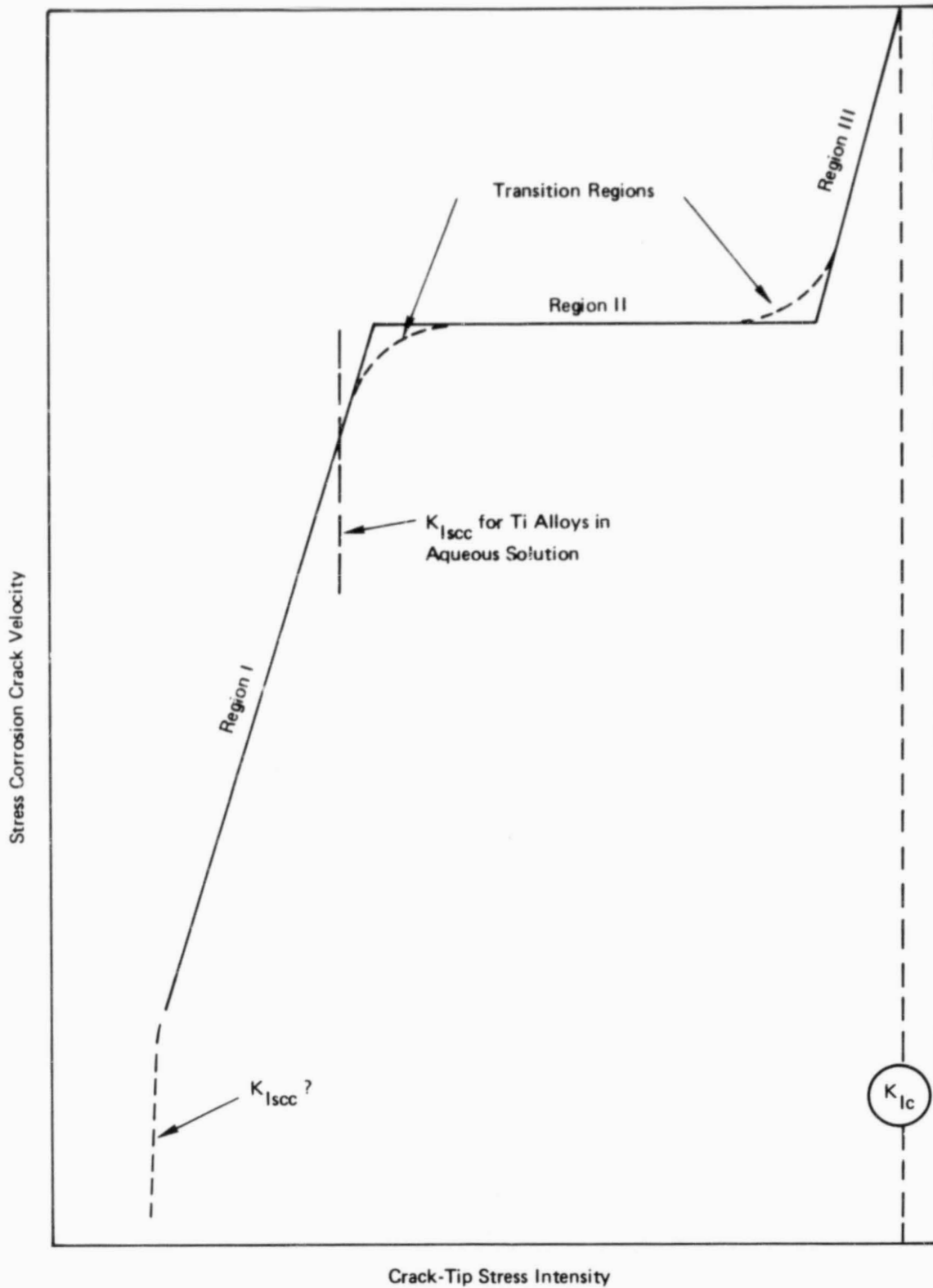
Figure 2-21: *GENERALIZED VELOCITY VERSUS STRESS INTENSITY RELATIONSHIP FOR STRESS CORROSION CRACKING*
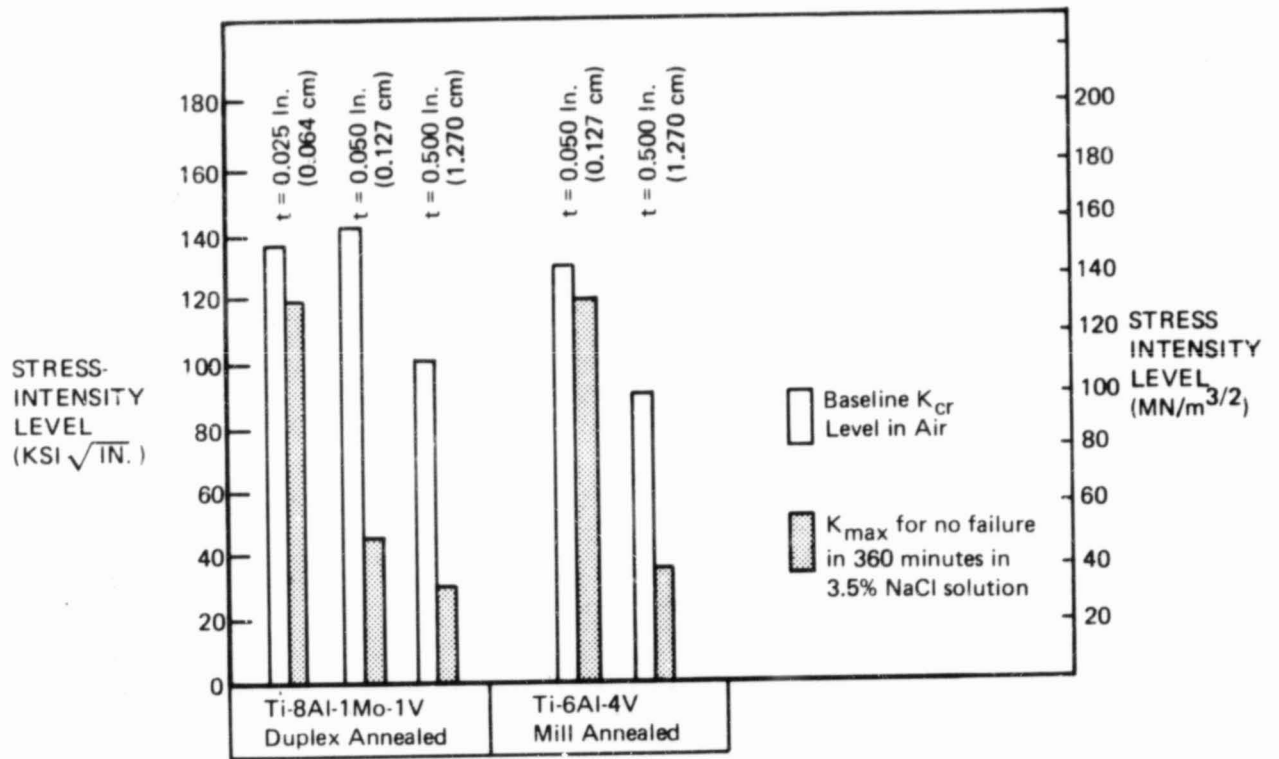
Figure 2-22: EFFECT OF SPECIMEN THICKNESS ON SCC SUSCEPTIBILITY OF Ti-8Al-1 Mo-1V (DA) and Ti-6Al-4V (MA) IN 3.5% NaCl SOLUTION (REF 15)
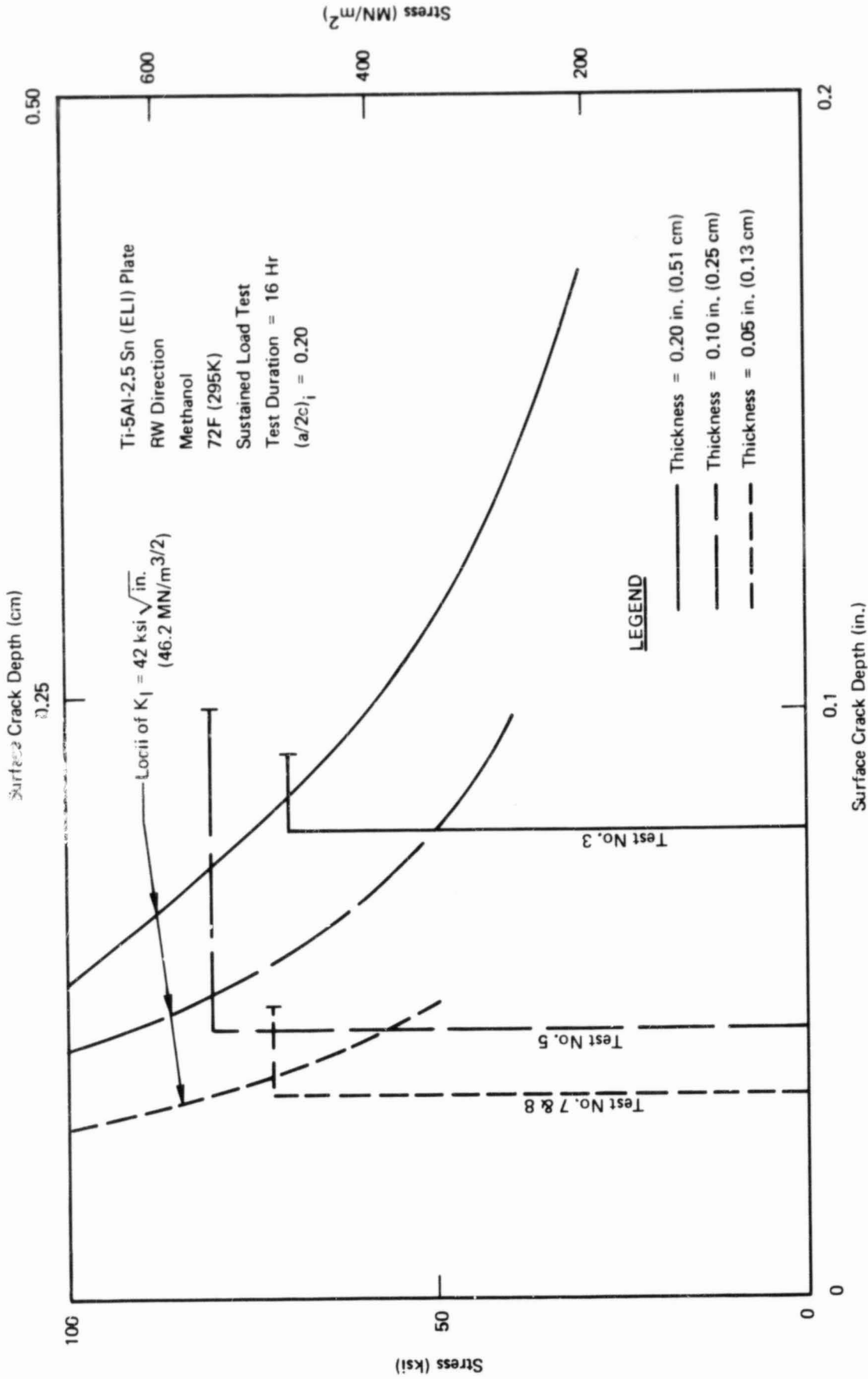
Figure 2-23: RESULTS OF SF SPECIMEN THICKNESS EFFECT TESTS

82
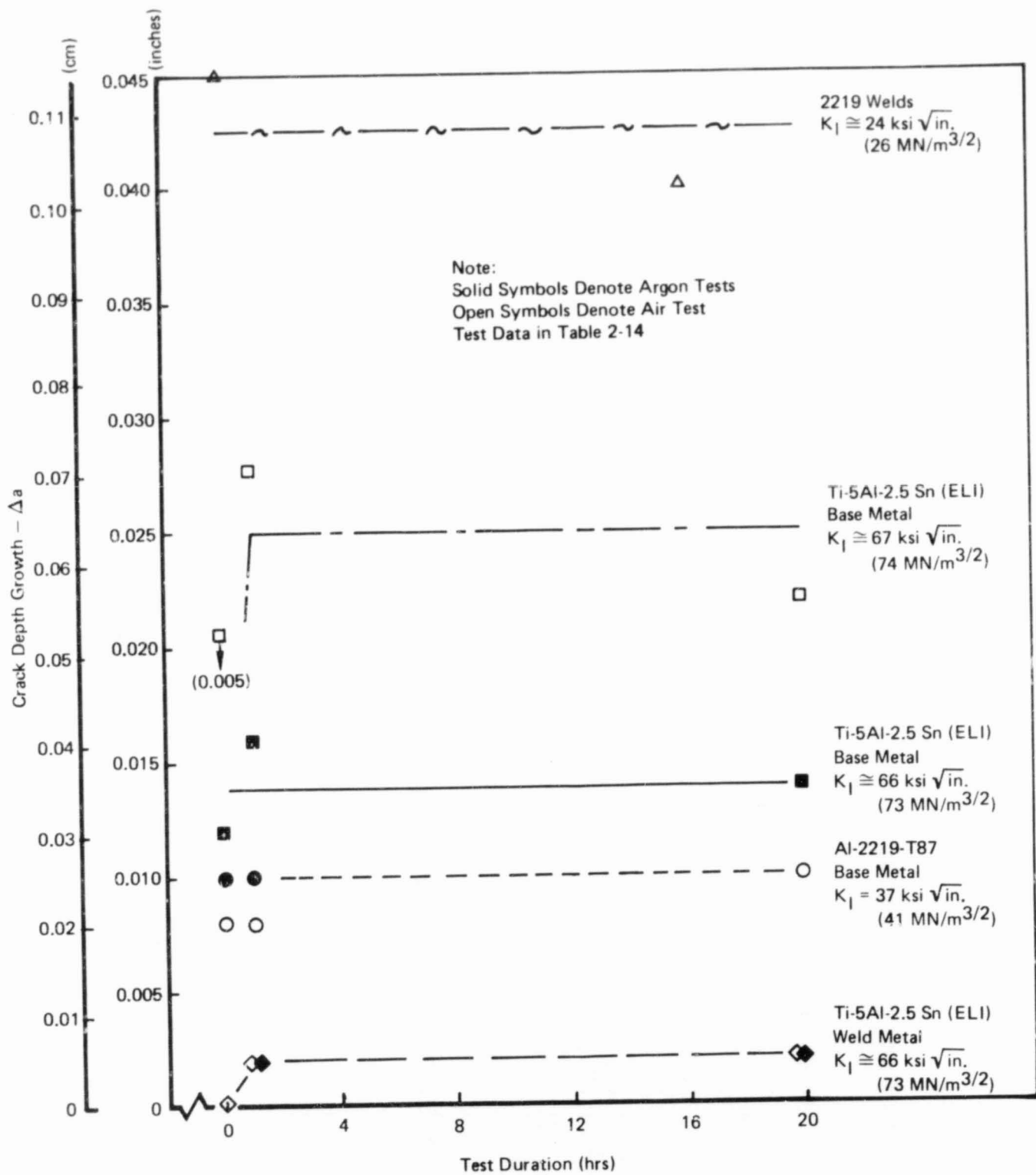
Figure 2-24: *SURFACE CRACK DEPTH GROWTH DURING LOAD—UNLOAD AND SUSTAINED LOAD TESTS IN AIR AND ARGON*

83

SPECIMEN NUMBER	TEST DURATION (Hours)
S-4	262
S-2	50
55	0 (Load-Unload)
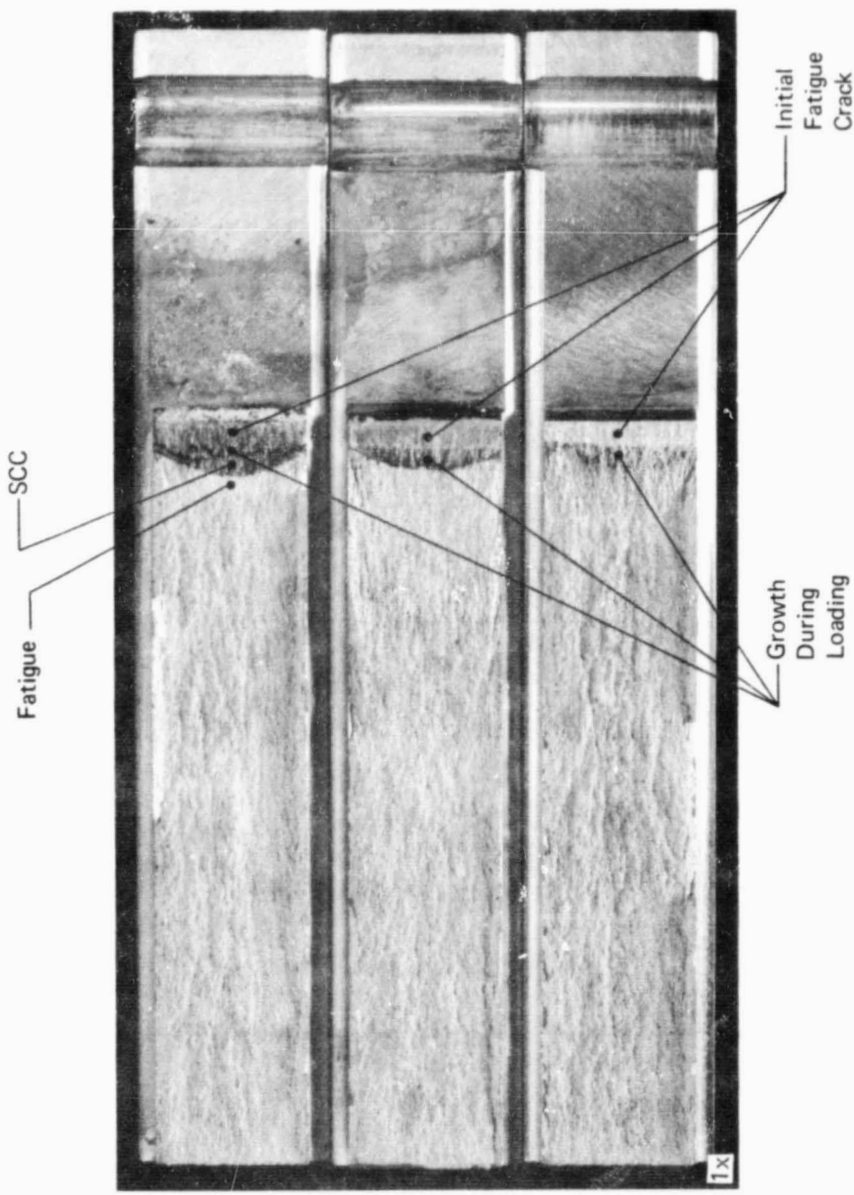
Figure 2-25: FRACTURE SURFACES OF 2219-T87 ALUMINUM ALLOY DCB SPECIMENS. SPECIMENS S-2 AND S-4 WERE TESTED IN SALT WATER. SPECIMEN 55 WAS LOADED THEN IMMEDIATELY UNLOADED IN AIR.

SPECIMEN NUMBER	INITIAL K	TEST DURATION (Hours)
WS-3	31 ksi $\sqrt{in}$, 34 MN/m$^{3/2}$	410
WS-2	30 ksi $\sqrt{in}$, 33 mn/m$^{3/2}$	240

Initial Fatigue Crack

Apparent SCC

Apparent SCC

Marking Fatigue
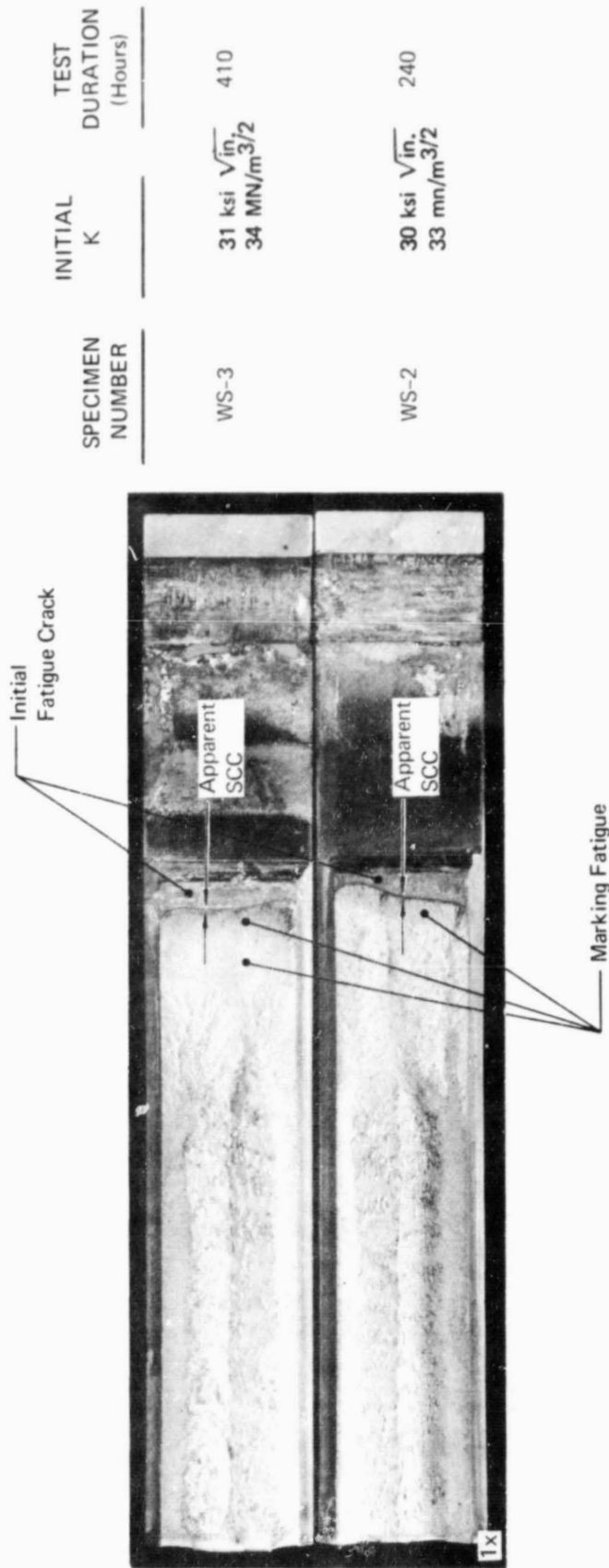
Figure 2-26: FRACTURE SURFACES OF 2219 ALUMINUM ALLOY WELD METAL DCB SPECIMENS TESTED IN SALT WATER SHOWING TYPICAL NONUNIFORM INITIAL FATIGUE CRACKS AND TRACES OF APPARENT SCC.

85

Sustained Load Tests at $\sigma = 22$ ksi (151.7 MN/m^2)
All Environments Except Salt Water

Sustained Load Tests at $\sigma = 25$ ksi (172.4 MN/m^2)
All Cryogenic Environments

△ Sustained Load Test at $\sigma = 22$ ksi (151.7 MN/m^2)
in Salt Water

○ Load–Unload Tests at $\sigma = 22$ ksi (151.7 MN/m^2)

● Load–Unload Tests at $\sigma = 25$ ksi (172.4 MN/m^2)

Temperature (K)

Temperature (F)

Crack Depth Growth, Δa (in.)

Crack Depth Growth, Δa, (cm)
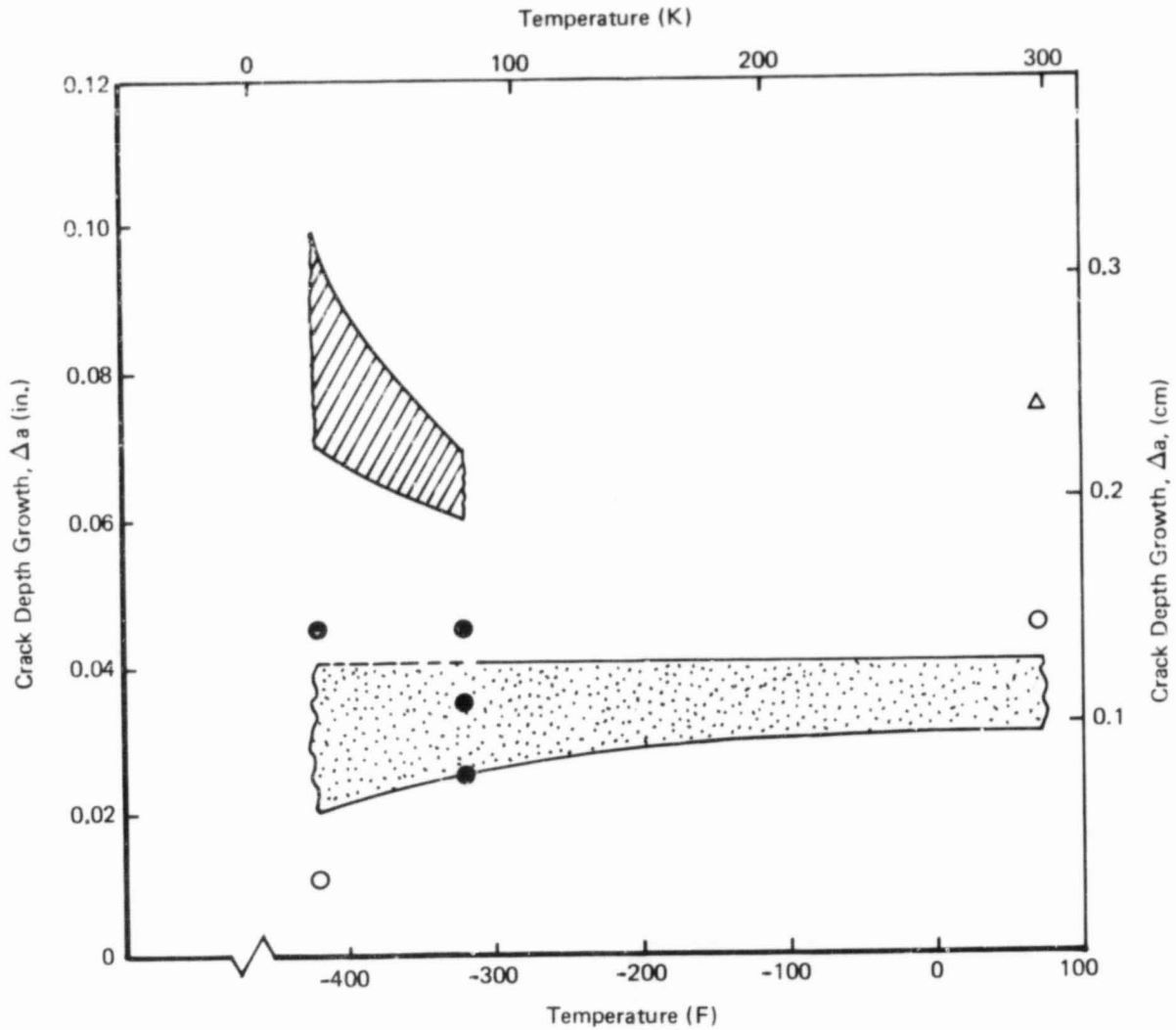
Figure 2-27: SURFACE FLAW DEPTH GROWTH OBSERVED DURING TESTS OF ONE INCH
(2.54 cm) THICK 2219 GTA WELD CENTERLINES

86

Marking Fatigue

SCC

Starter Slot

Initial Fatigue
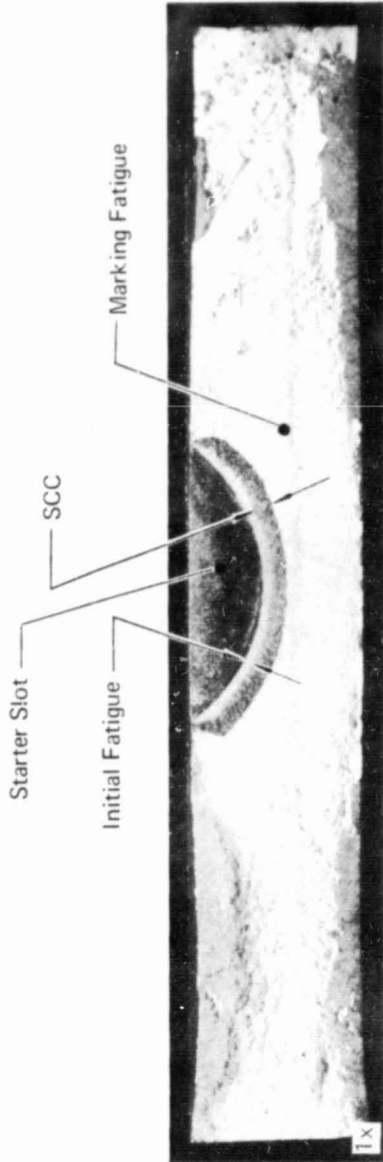
Sustained Load Specimen WS-1 (Tested in Salt Water)

Medium: Salt Water

K_{Ii}: 24 Ksi $\sqrt{\text{In.}}$ $(26 \text{MN/m}^{3/2})$

Test Duration: 24 hrs.

Marking Fatigue

Growth During Loading
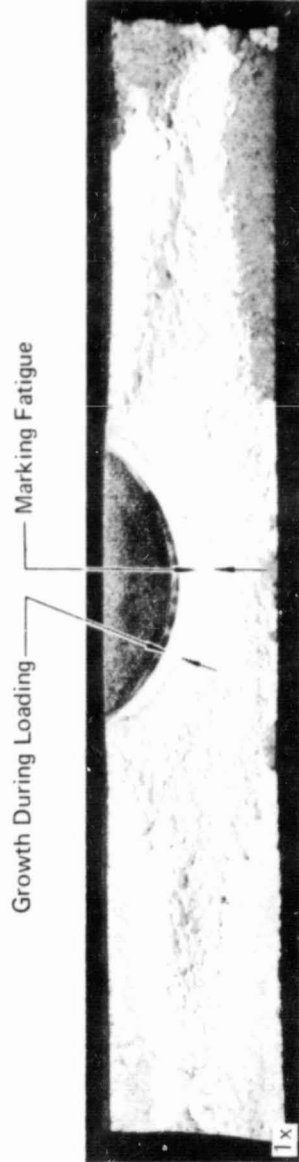
Load-Unload Specimen WDP-1A (Tested in Air)

Test Medium: Air

K_{Ii}: 24 Ksi $\sqrt{\text{In.}}$ $(26 \text{ MN/m}^{3/2})$

Figure 2-28: FRACTURE SURFACES OF 2219 ALUMINUM AS-WELDED SF SPECIMENS ILLUSTRATING CRACK GROWTH DUE TO LOAD-UNLOAD PROFILE IN AIR AND SUSTAINED LOAD PROFILE IN SALT WATER.

Initial Fatigue Crack

Apparent SCC

Marking Fatigue
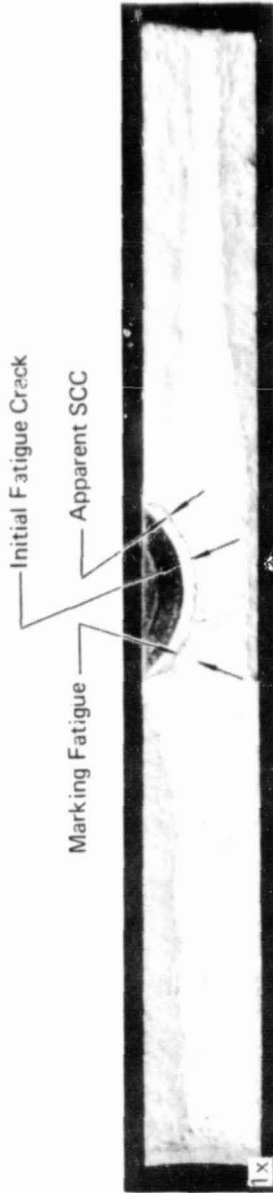
Sustained Load Specimen AD-1
Test Medium: Dye Penetrant
K_{Ii}: 37 Ksi $\sqrt{\text{In.}}$ (41 MN/m$^{3/2}$)
Test Duration: 15 hrs.

WR

WT
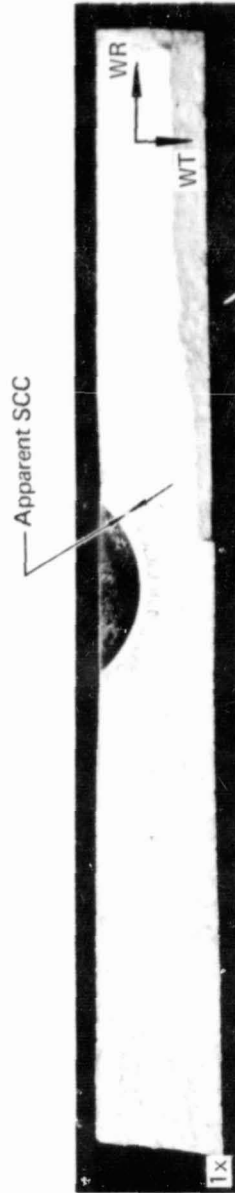
Apparent SCC

Sustained Load Specimen AT-1
Test Medium: Trichloroethylene
K_{Ii}: 37 Ksi $\sqrt{\text{In.}}$ (41 MN/m$^{3/2}$)
Test Duration: 16.2 hrs.

Figure 2-29: FRACTURE SURFACES OF 2219-T87 ALUMINUM ALLOY BASE METAL SURFACE. FLAWED SPECIMENS SHOWING TRACES OF APPARENT SCC.
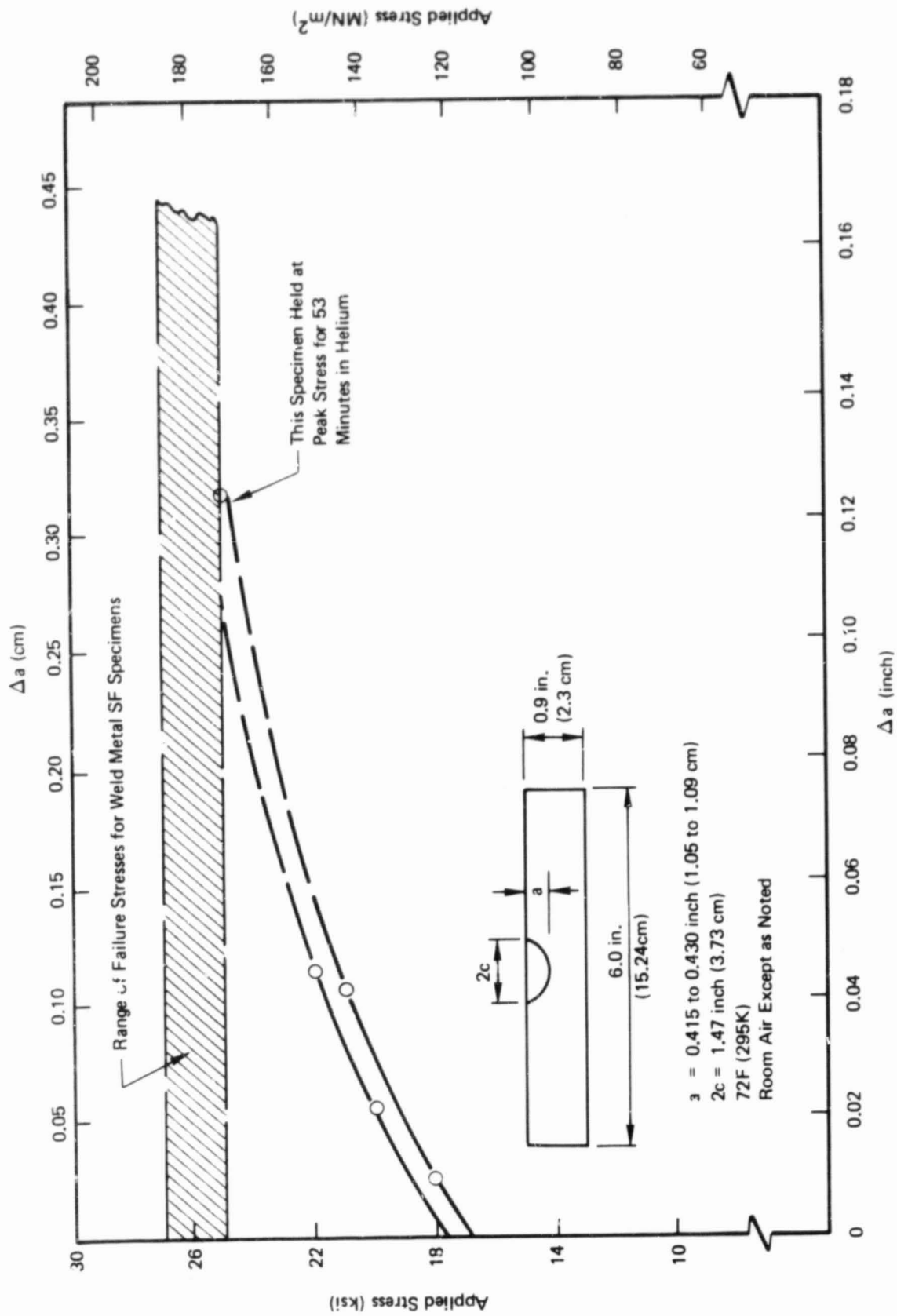
Figure 2-30: CRACK GROWTH DURING RISING LOADS FOR 2219 AS WELDED GTA WELD CENTERLINE
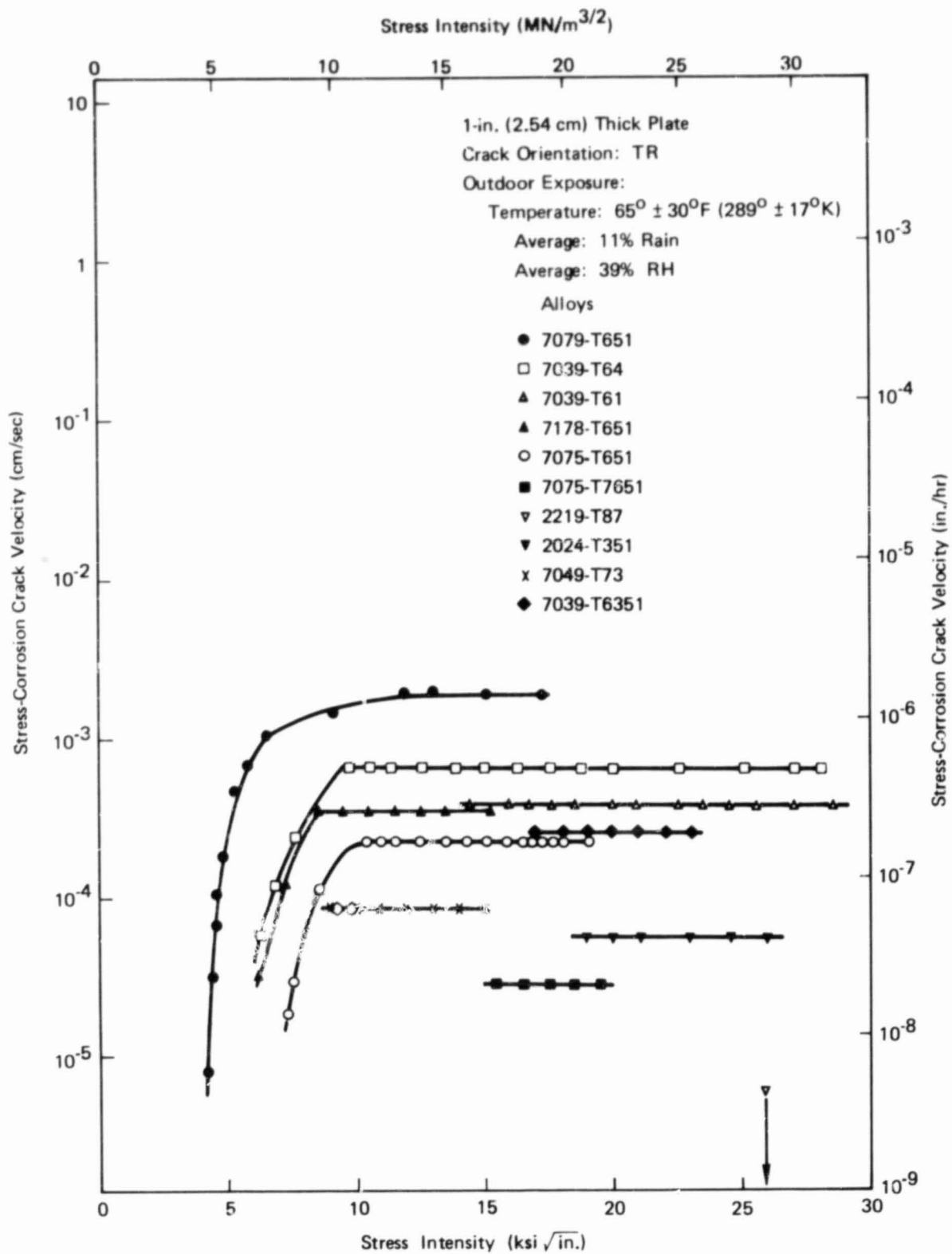
Figure 2-31: EFFECT OF OUTDOOR EXPOSURE AND STRESS INTENSITY ON STRESS-CORROSION
CRACK VELOCITY OF SEVERAL HIGH-STRENGTH ALUMINUM ALLOYS (REF. 16)
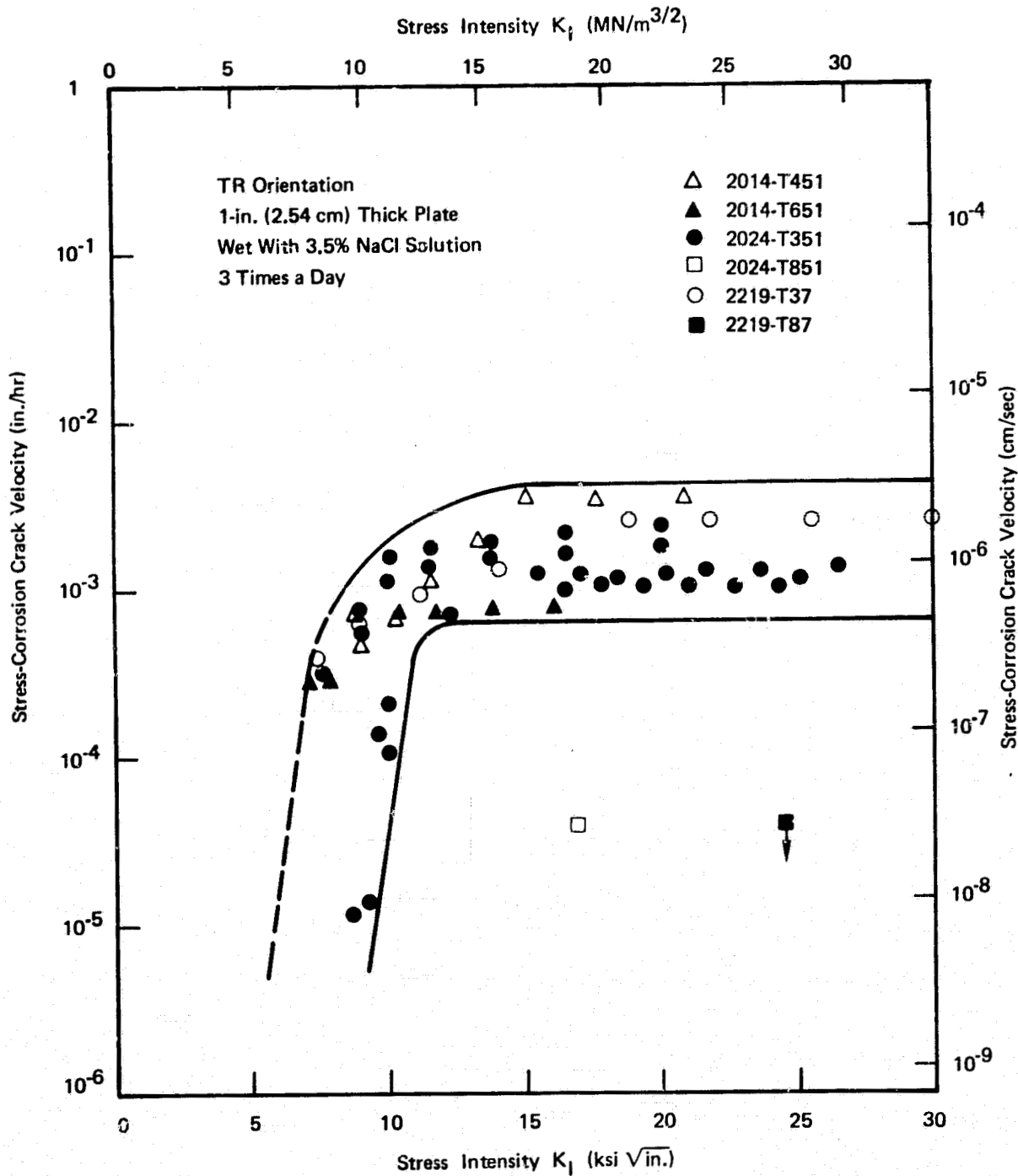
Figure 2-32: TYPICAL V-K CURVES FOR SOME 2000-SERIES ALLOYS OBTAINED USING TR DCB
STRESS-CORROSION SPECIMENS (REF. 16)

91
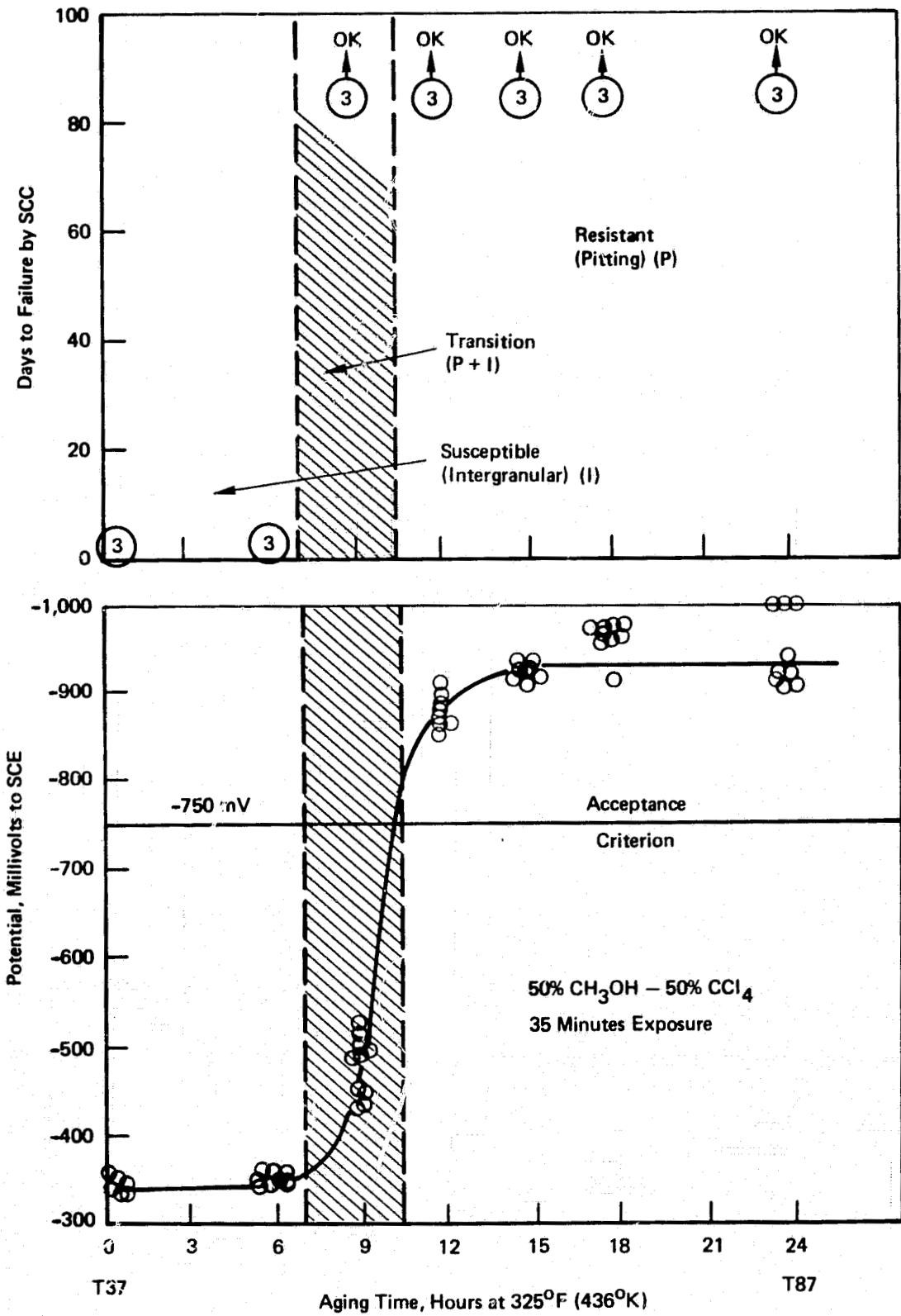
Figure 2-33: *CORRELATION OF SOLUTION POTENTIAL WITH STRESS-CORROSION PERFORMANCE OF 2219-T87 ALLOY PLATE. IN THE UPPER PLOT, THE SMALL NUMBERS INSIDE CIRCLES INDICATE THE NUMBER OF SPECIMENS TESTED (REF. 17)*
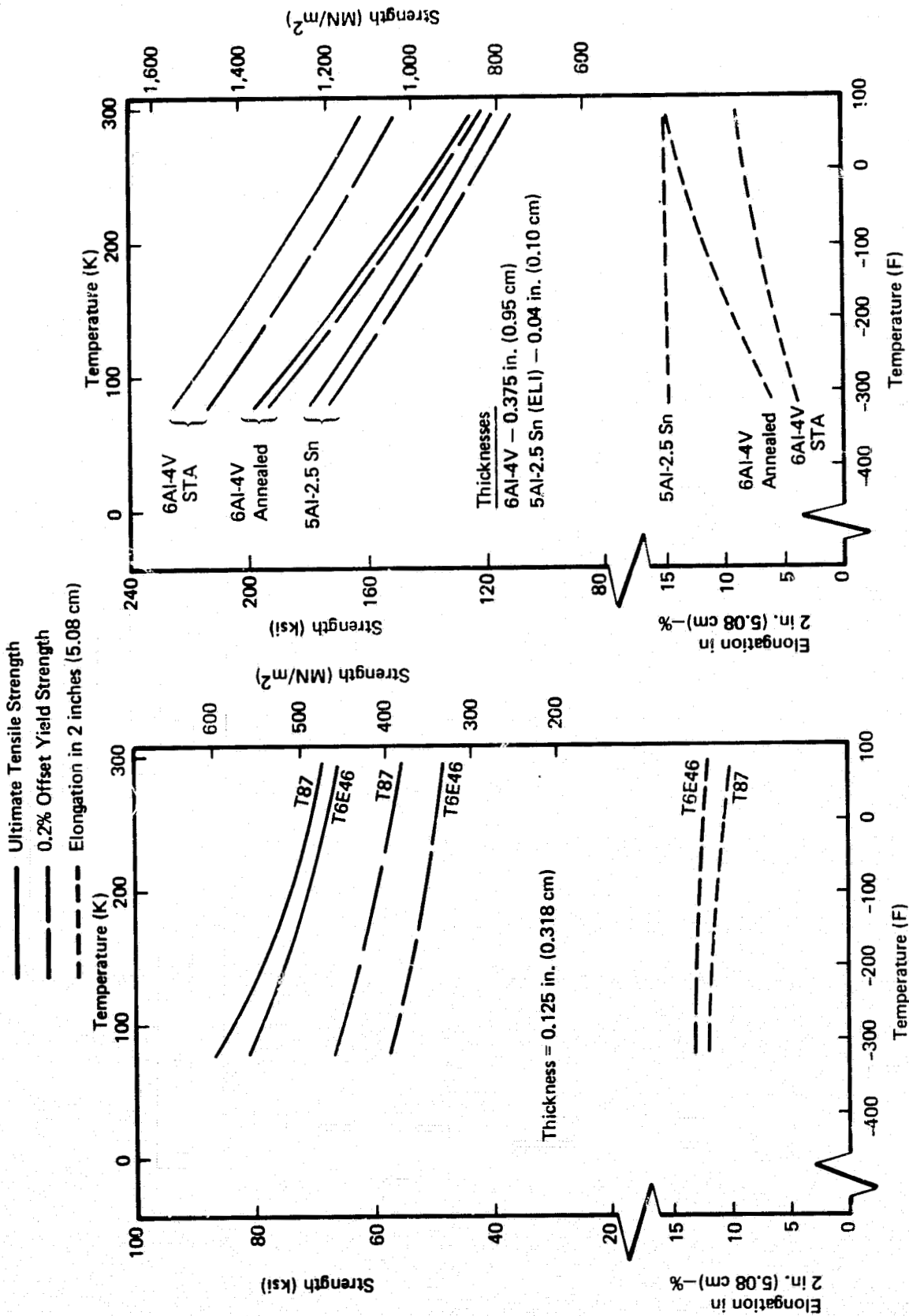
Figure 3-1: MECHANICAL PROPERTIES FOR MATERIALS USED IN COMPATIBILITY STUDIES PERTINENT TO HIGH ENERGY UPPER STAGE PROPULSION SYSTEMS

Clamping Plate

Pressure

Cup

Teflon Seal

Pressure Transducer

SECTION A–A

Flaw

Specimen

6.00 (15.3)

2.00 (5.08)

P

P

A

A
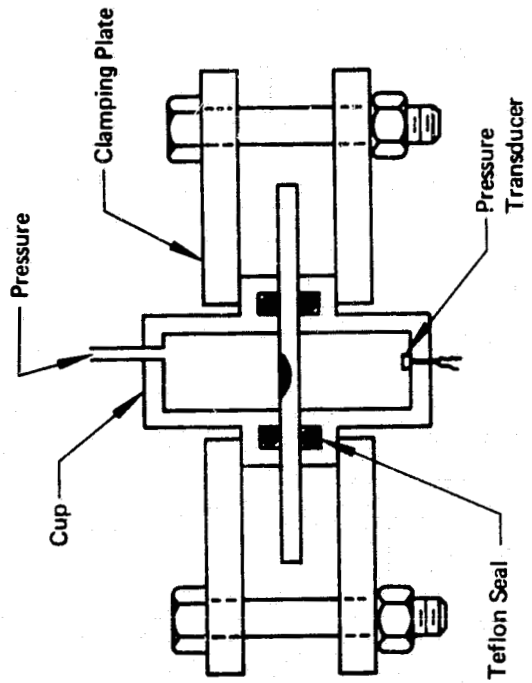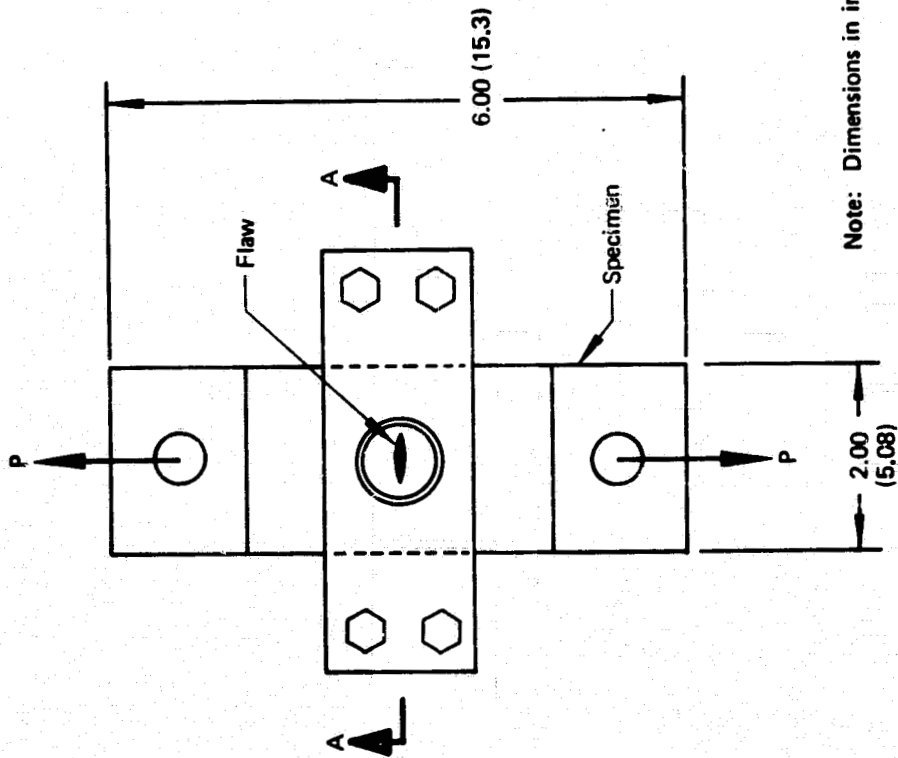
Note: Dimensions in inches (cm)

Figure 3-2: PRESSURE CUP INSTRUMENTATION USED FOR DETECTING SURFACE CRACK PENETRATION OF SPECIMEN THICKNESS
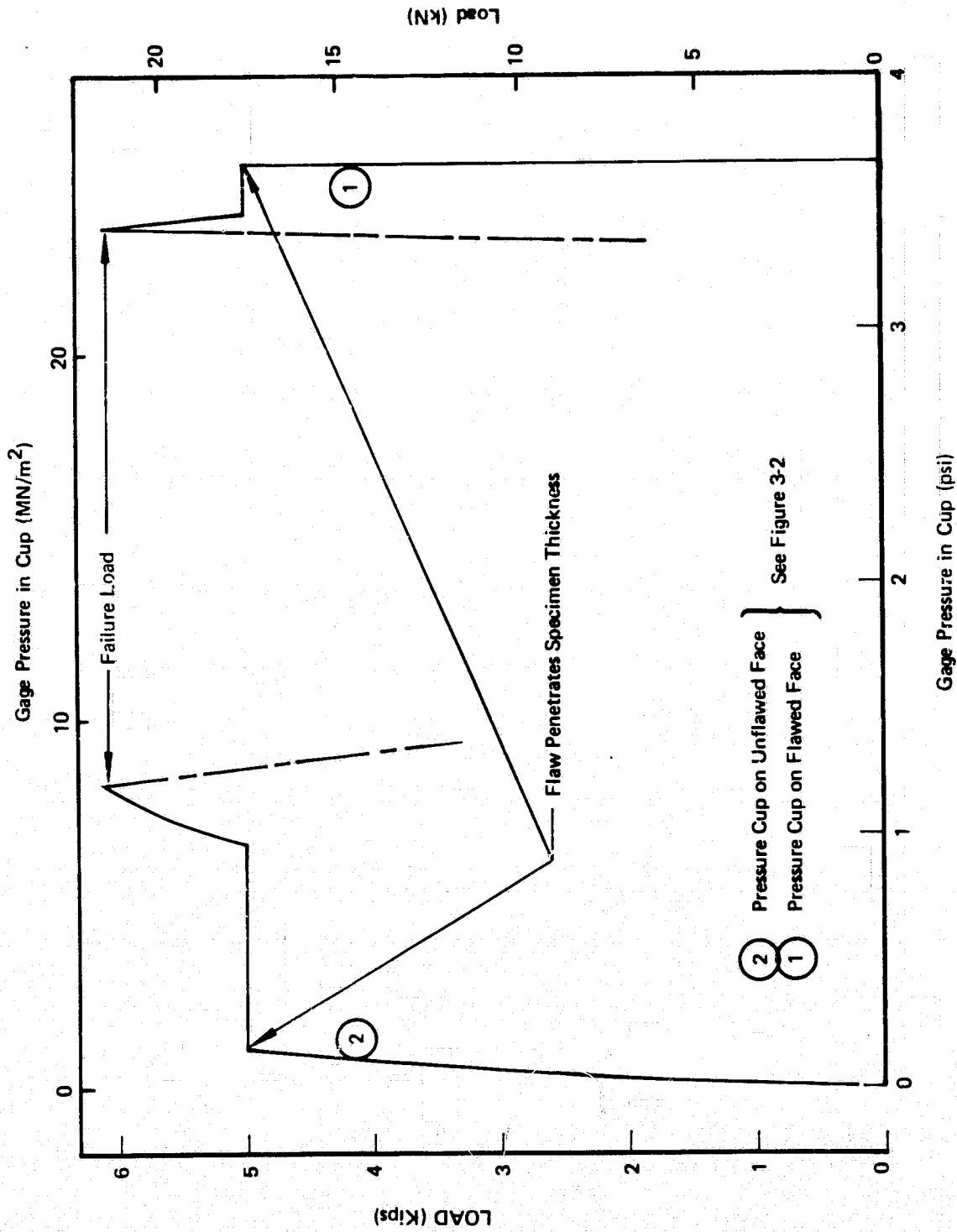
Figure 3-3: *EXAMPLE OF TEST RECORD OBTAINED FROM INSTRUMENTATION SHOWN IN FIGURE 3-2 DURING STATIC FRACTURE TEST OF SURFACE FLAWED SPECIMEN*

95
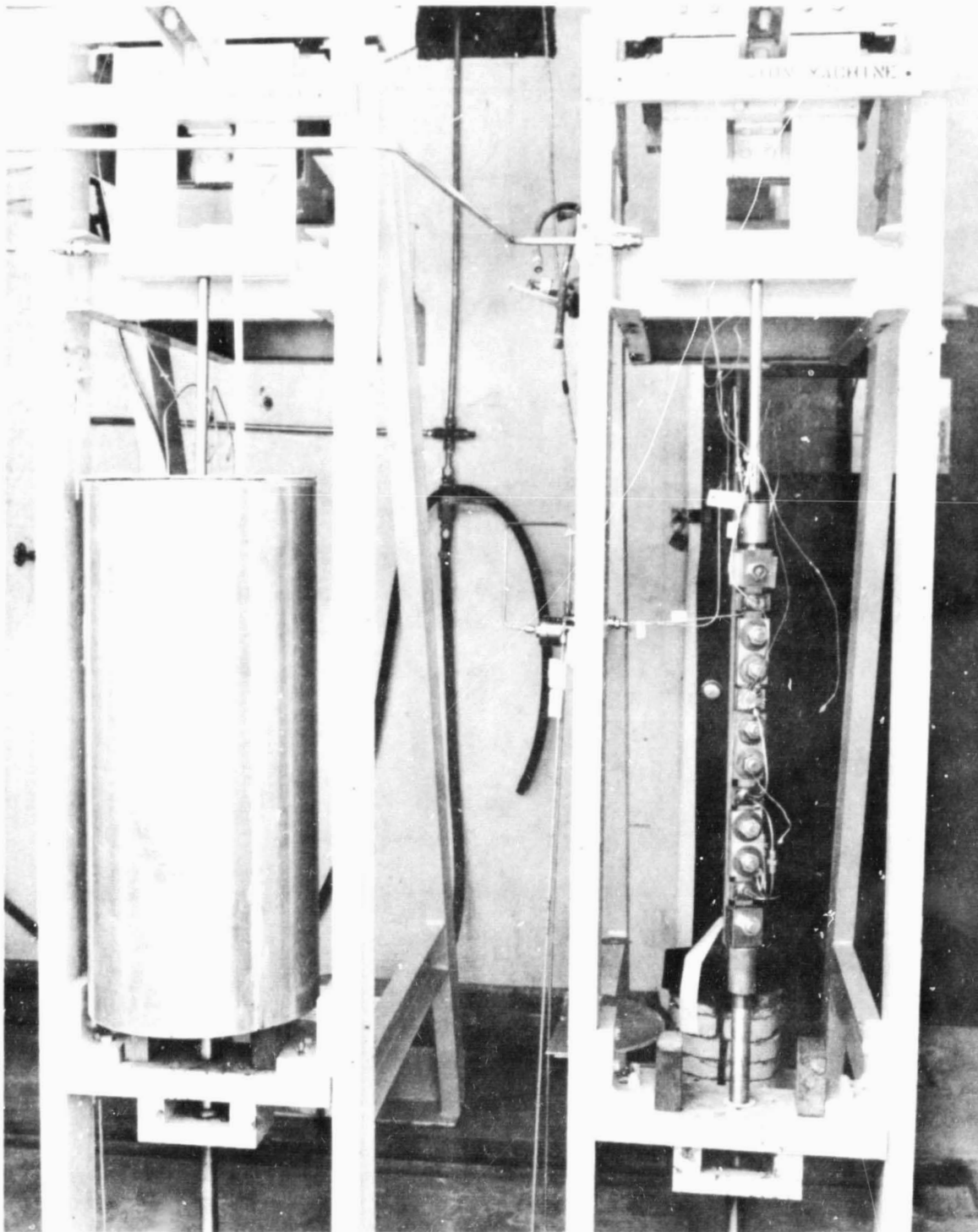
Figure 3-4: LOADING TRAIN AND CRYOSTAT FOR UPPER STAGE MATERIAL/ENVIRONMENT COMBINATION TESTS.
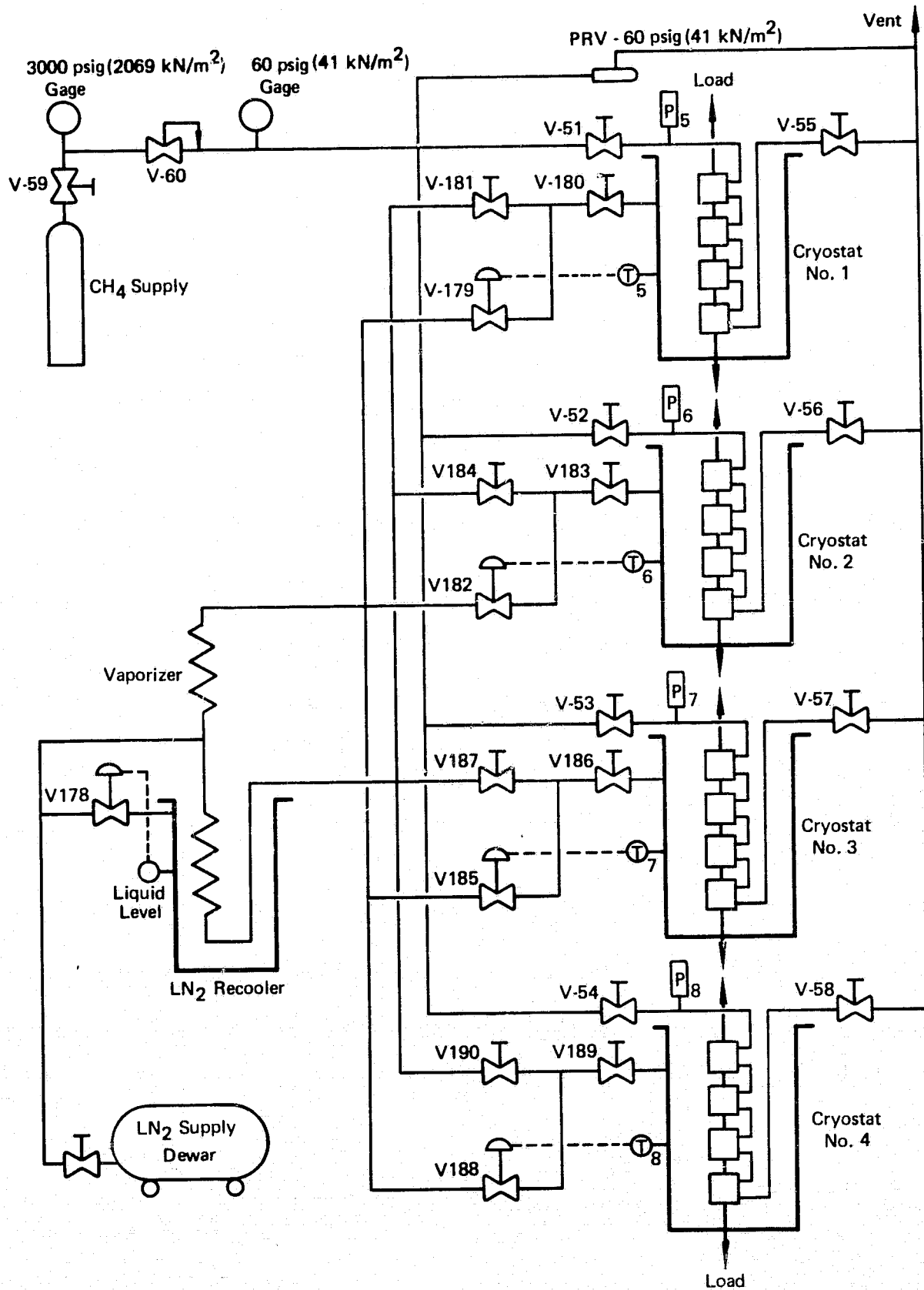
Figure 3-5: *SYSTEM USED FOR TESTING UPPER STAGE MATERIAL/ ENVIRONMENT COMBINATIONS IN METHANE*
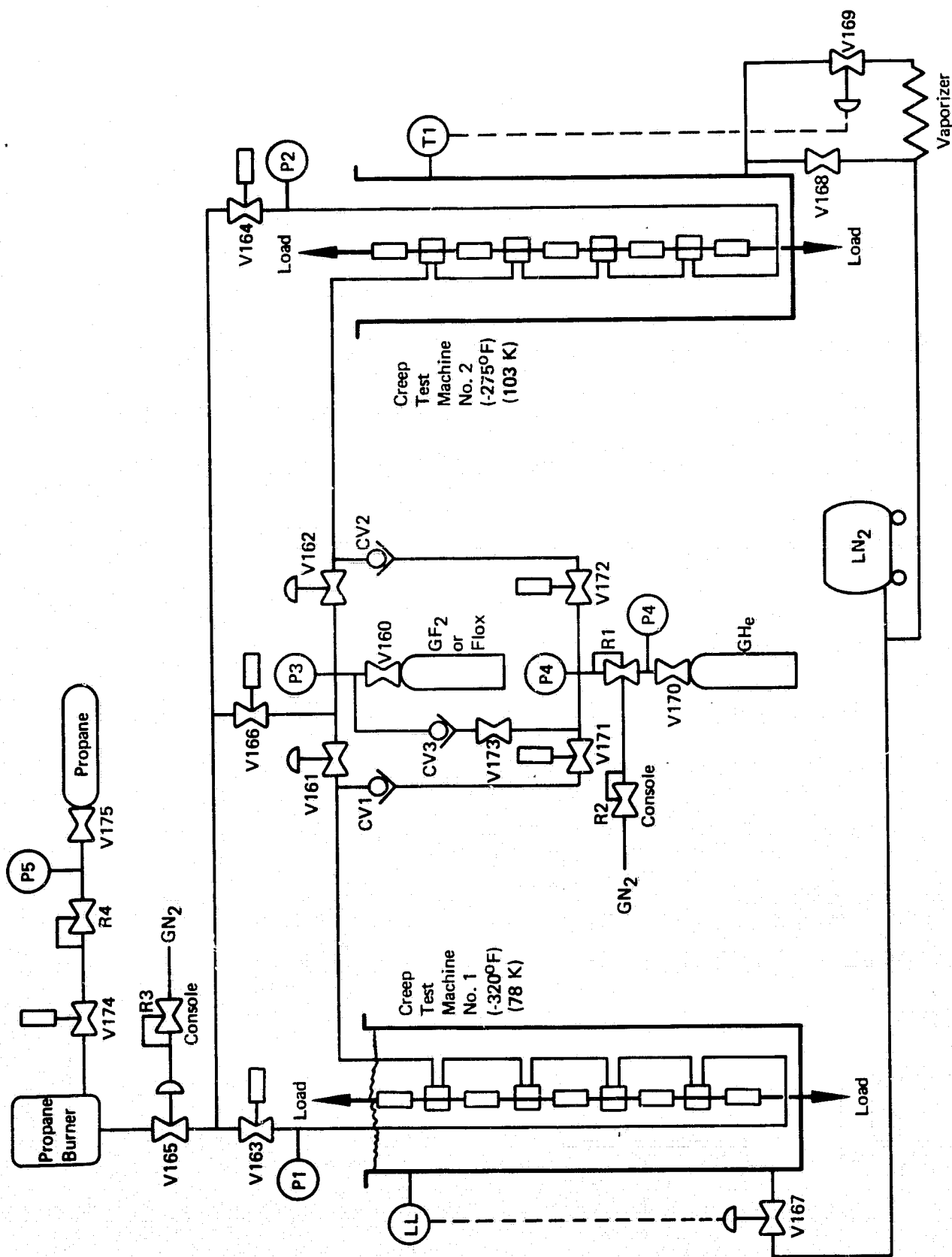
Figure 3-6: SYSTEM USED FOR TESTING UPPER STAGE MATERIAL/ ENVIRONMENT COMBINATIONS IN FLUORINE AND FLOX
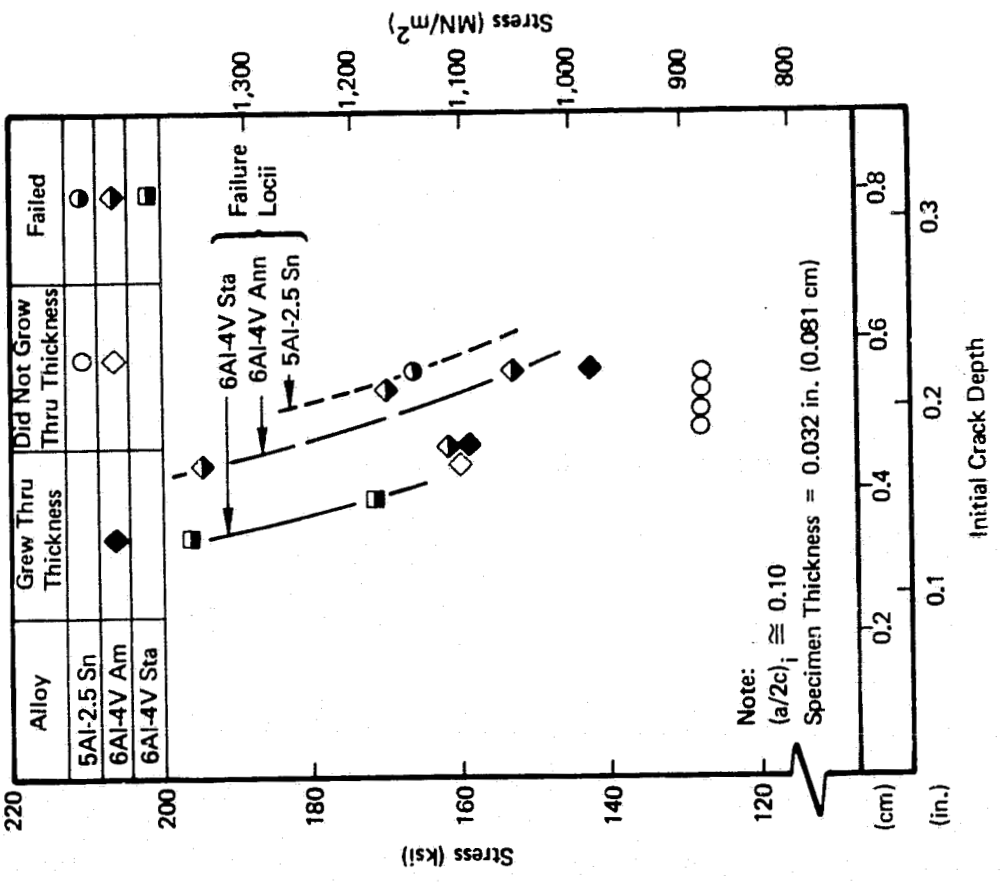
(b) Titanium Alloy Specimens

(a) Aluminum Alloy Specimens

Figure 3-7: RESULTS OF −320F (78K) PROOF OVERLOAD TESTS FOR ALUMINUM AND TITANIUM ALLOY SF SPECIMENS

99
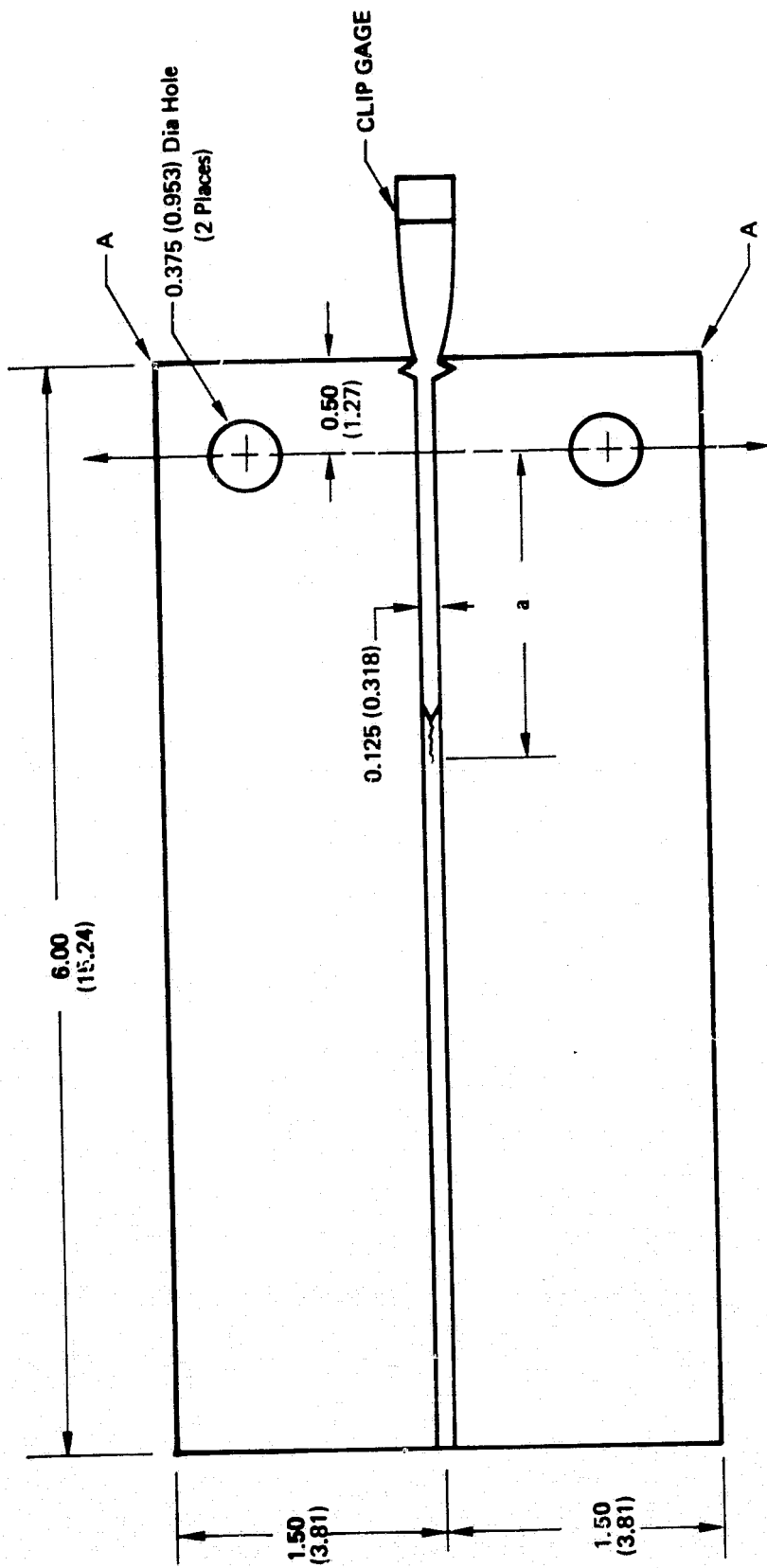
NOTE: MICROMETER MEASUREMENTS MADE BETWEEN POINTS A

ALL DIMENSIONS IN INCHES (CENTIMETERS)

Figure B1: DCB SPECIMEN AND INSTRUMENTATION FOR COMPLIANCE TESTS

100
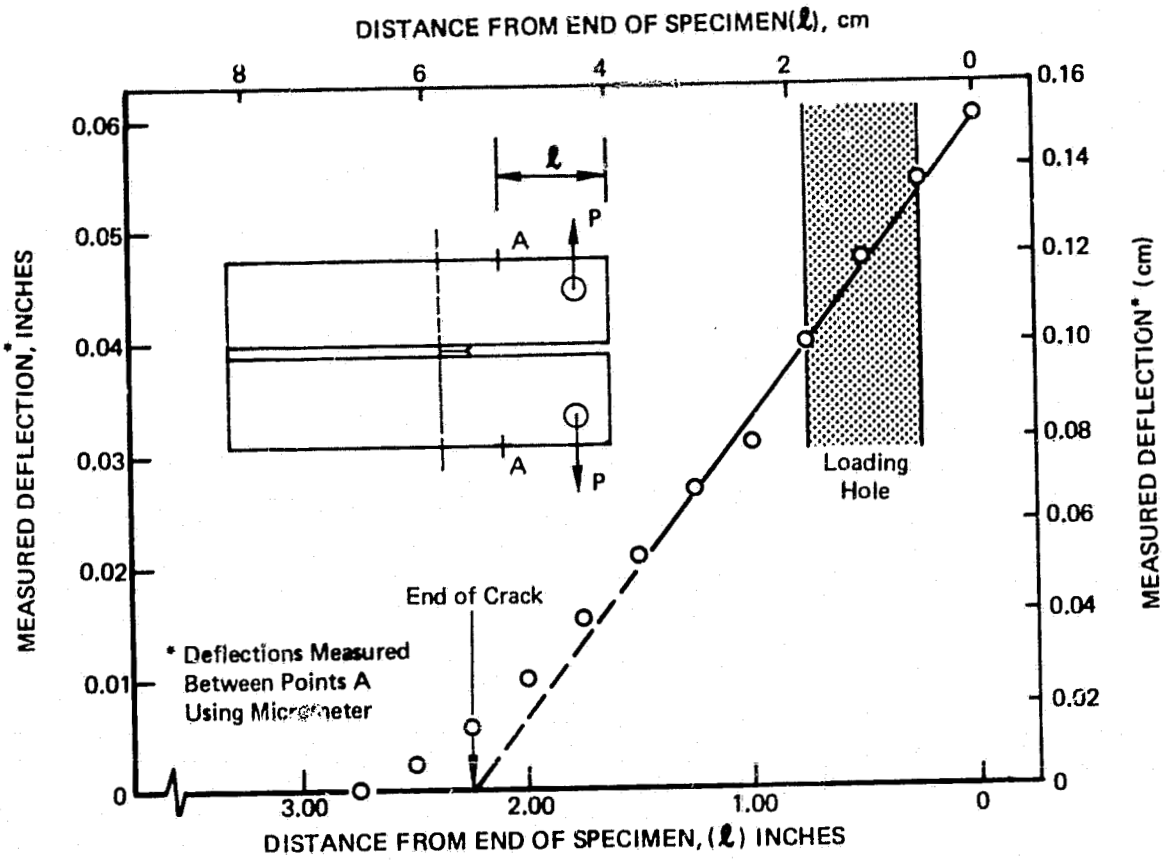
(b): *TITANIUM WELD METAL SPECIMENS*
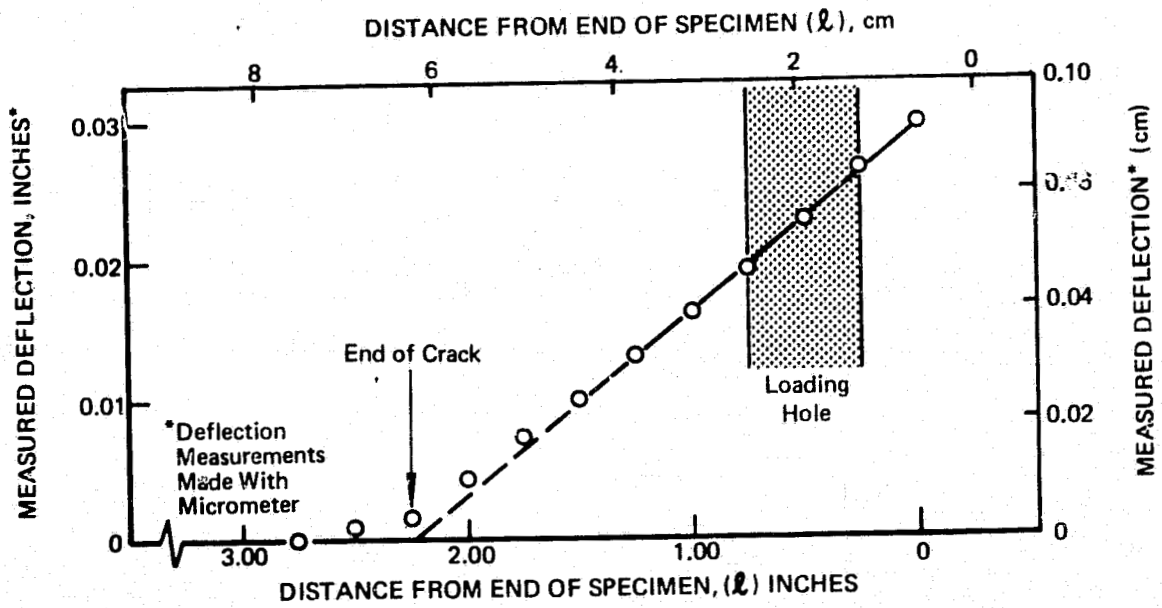
(a): *ALUMINUM BASE METAL SPECIMENS*

Figure B2: *DEFLECTION MEASUREMENTS BETWEEN OUTER SURFACES OF DCB SPECIMEN ARMS*
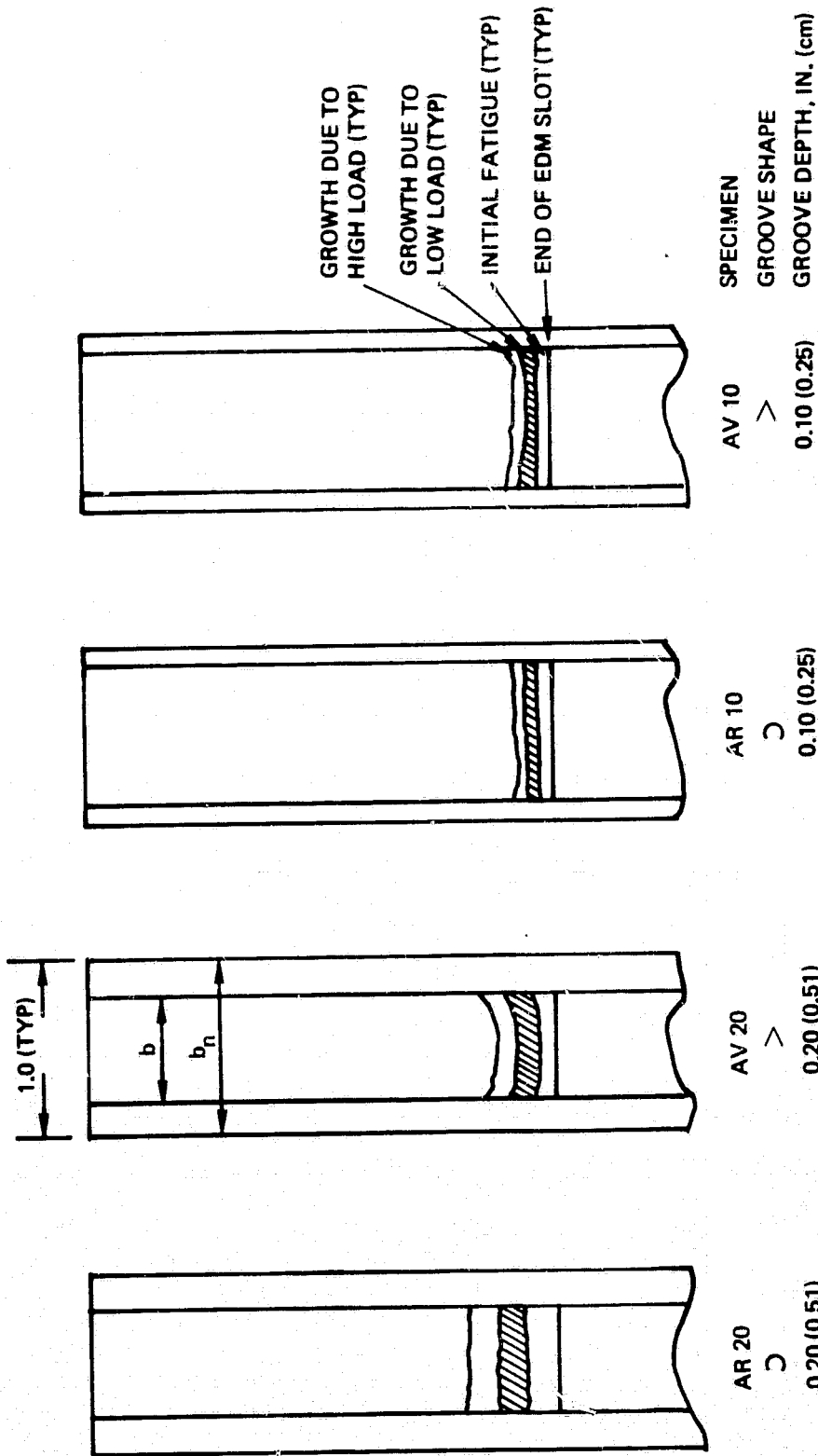
Figure B3: FRACTURE SURFACES FOR 2219-T87 ALUMINUM DCB SPECIMENS USED TO EVALUATE
EFFECT OF GROOVE SHAPE ON CURVATURE OF FATIGUE CRACK FRONT
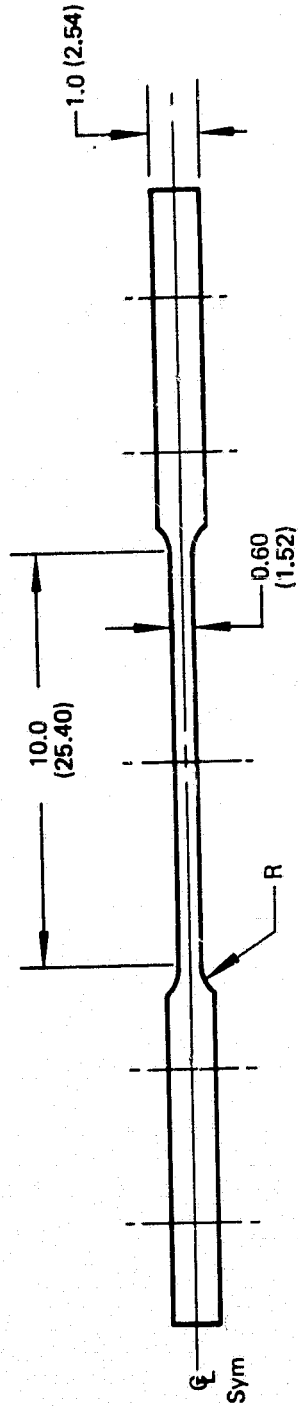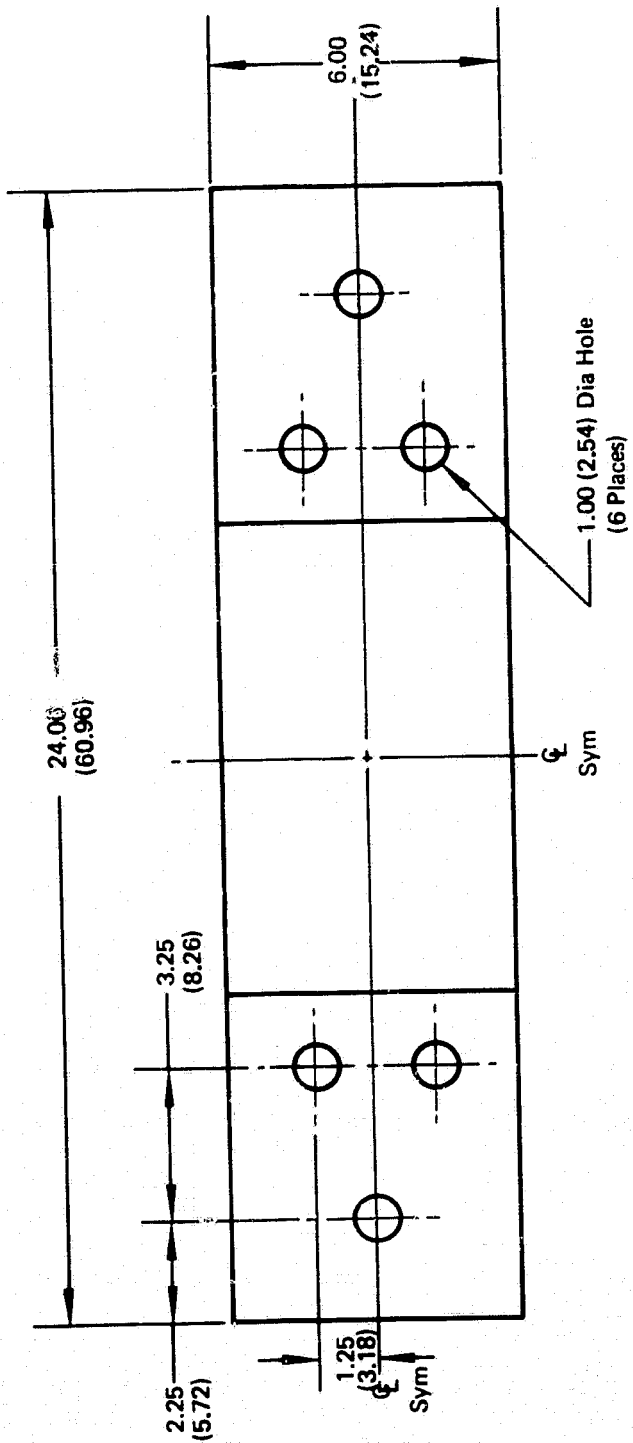
Figure C1: SURFACE FLAWED SPECIMEN FOR ALUMINUM BASE METAL

NOTE: All Dimensions In Inches (cm)

103
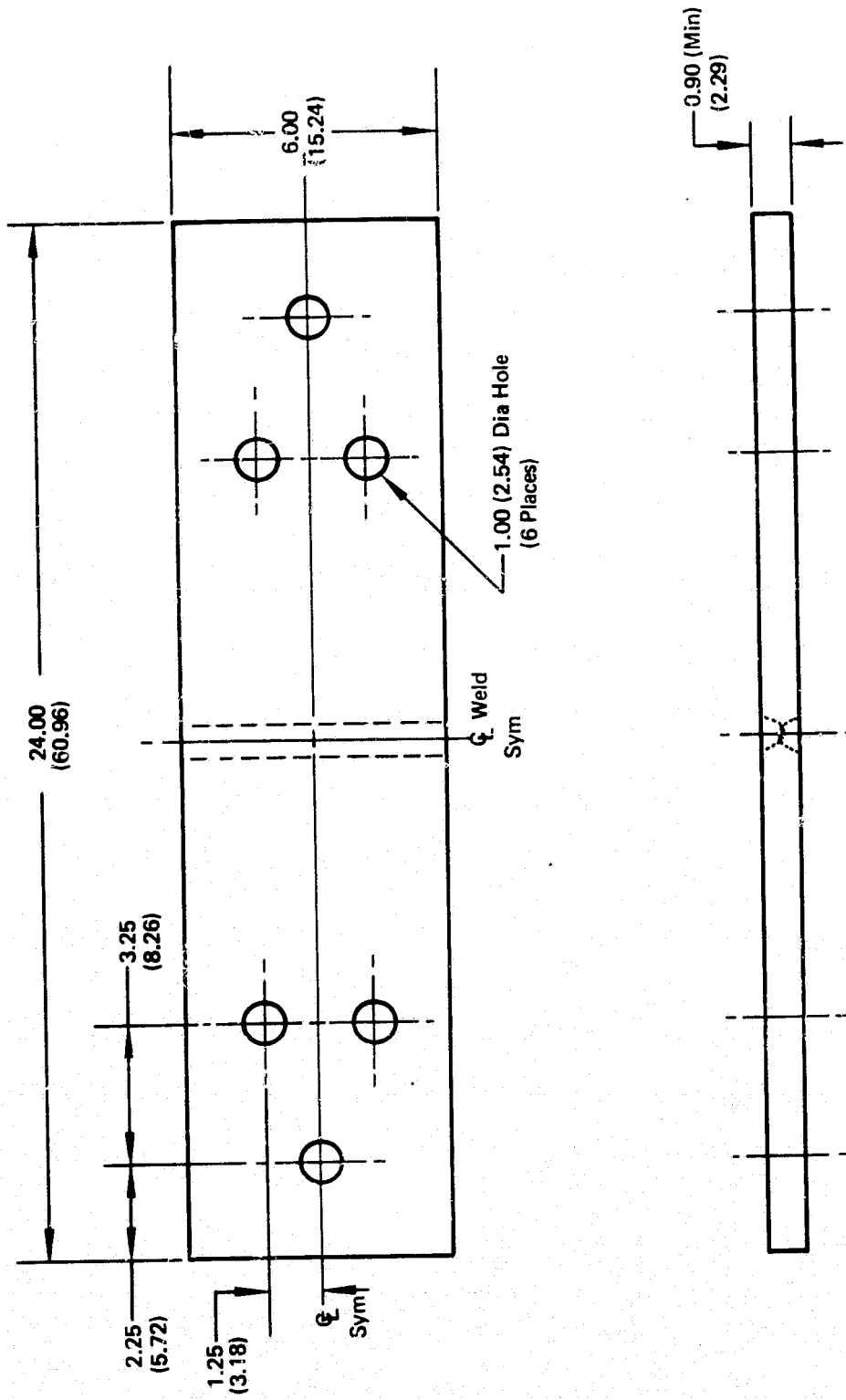
Figure C2: SURFACE FLAWED SPECIMEN FOR ALUMINUM WELD METAL

NOTE: All Dimensions In Inches (cm)
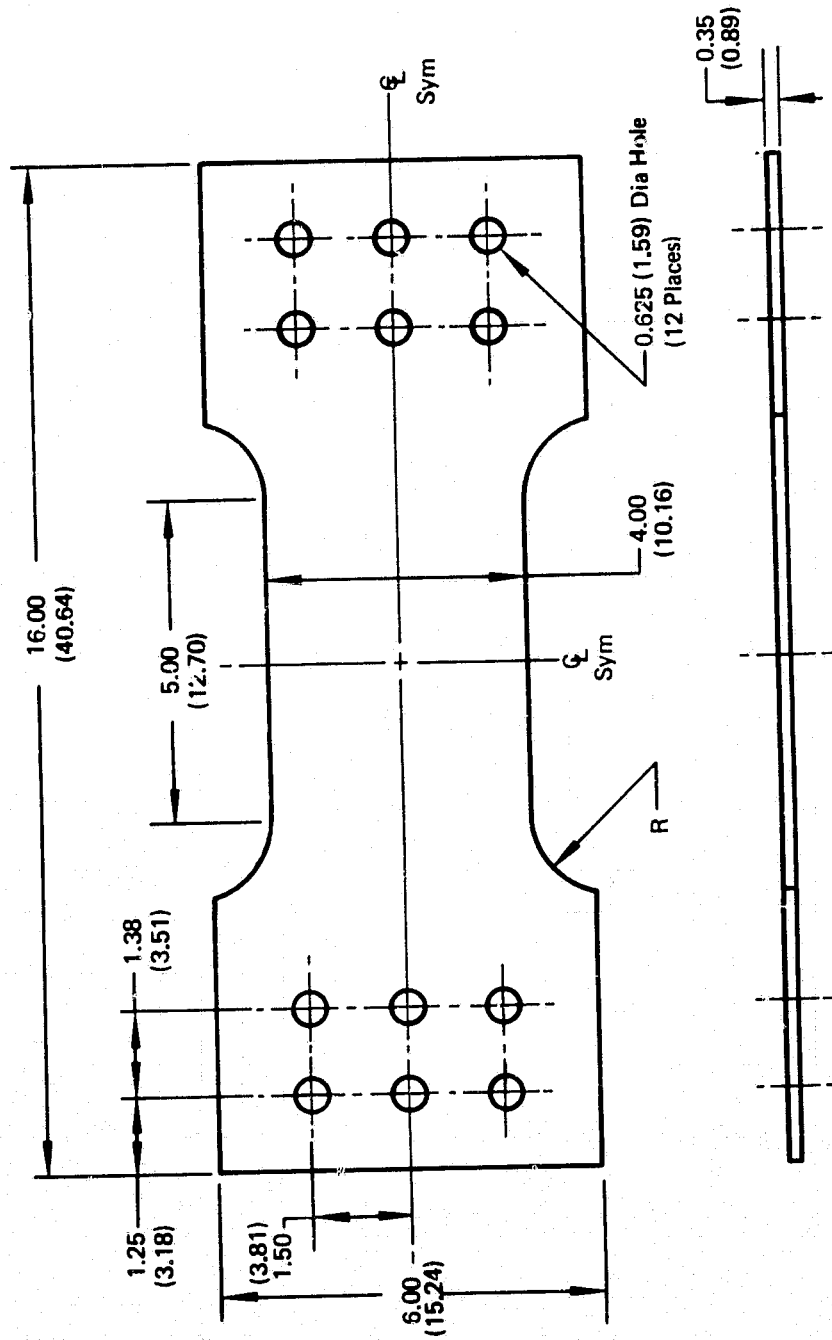
NOTE: All Dimensions In Inches (Cm)

Figure C3: *SURFACE FLAWED SPECIMEN FOR TITANIUM BASE METAL @ ROOM TEMPERATURE*
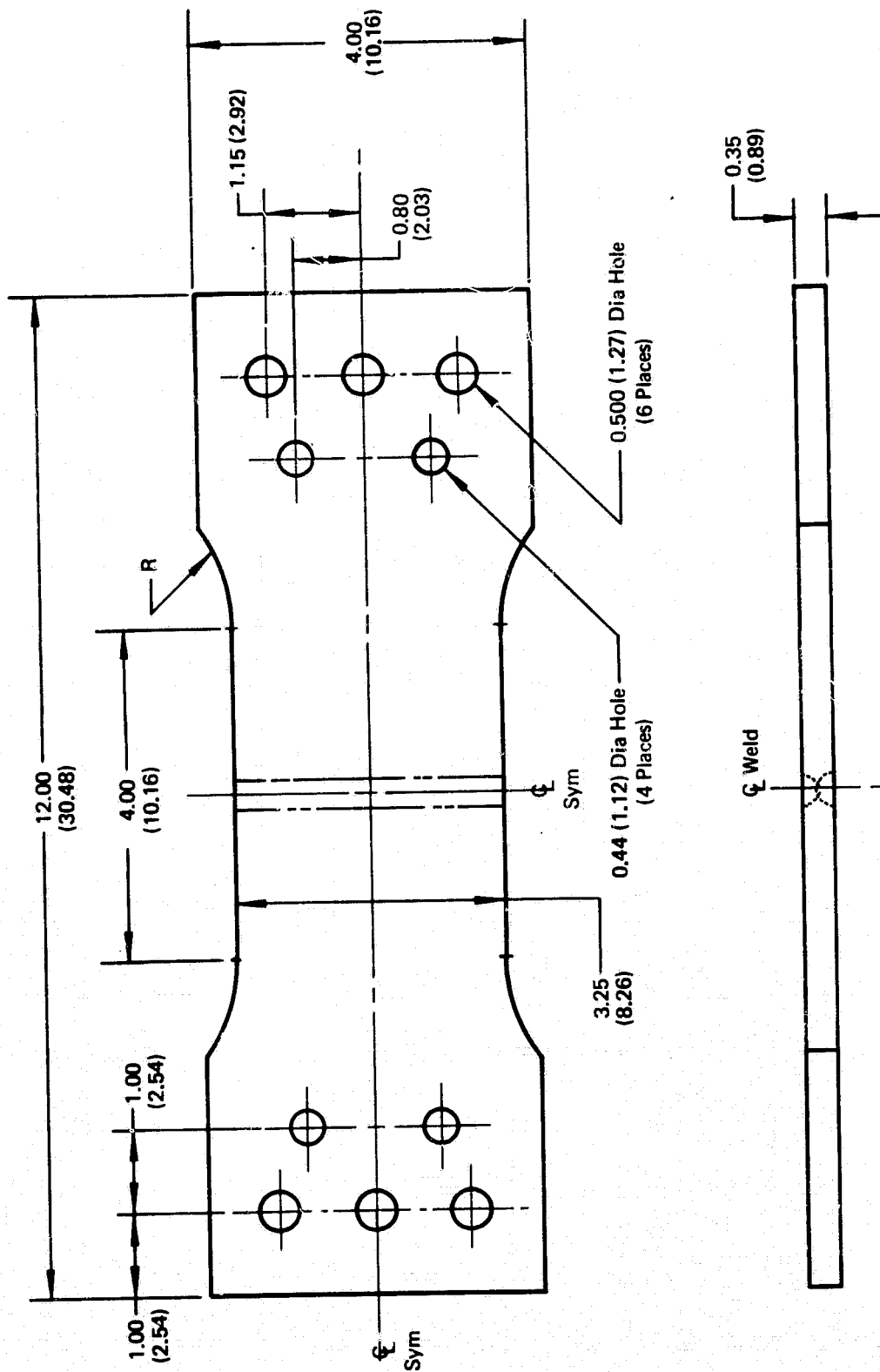
Figure C4: SURFACE FLAWED SPECIMENS FOR TITANIUM WELD METAL @ ROOM TEMPERATURE

NOTE: All Dimensions In Inches (Cm)

NOTE: All Dimensions In Inches (Cm)

Figure C5: SURFACE FLAWED SPECIMEN FOR TITANIUM BASE METAL & WELD METAL @ -320°F (78K)

107
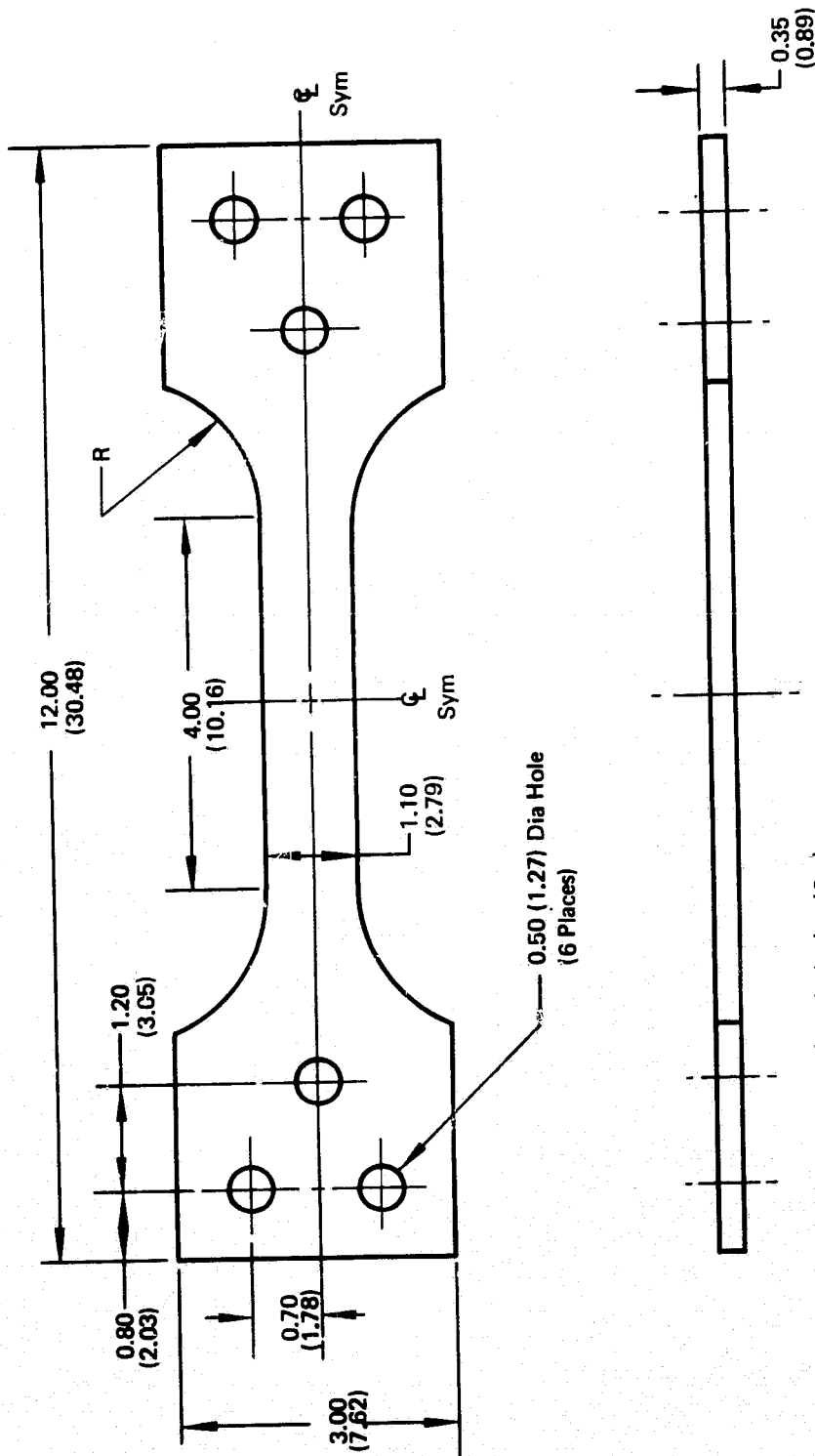
NOTE: All Dimensions In Inches (Cm)

Figure C6: *SURFACE FLAWED SPECIMEN FOR TITANIUM BASE METAL & WELD METAL @ -423°F (20°K)*

108
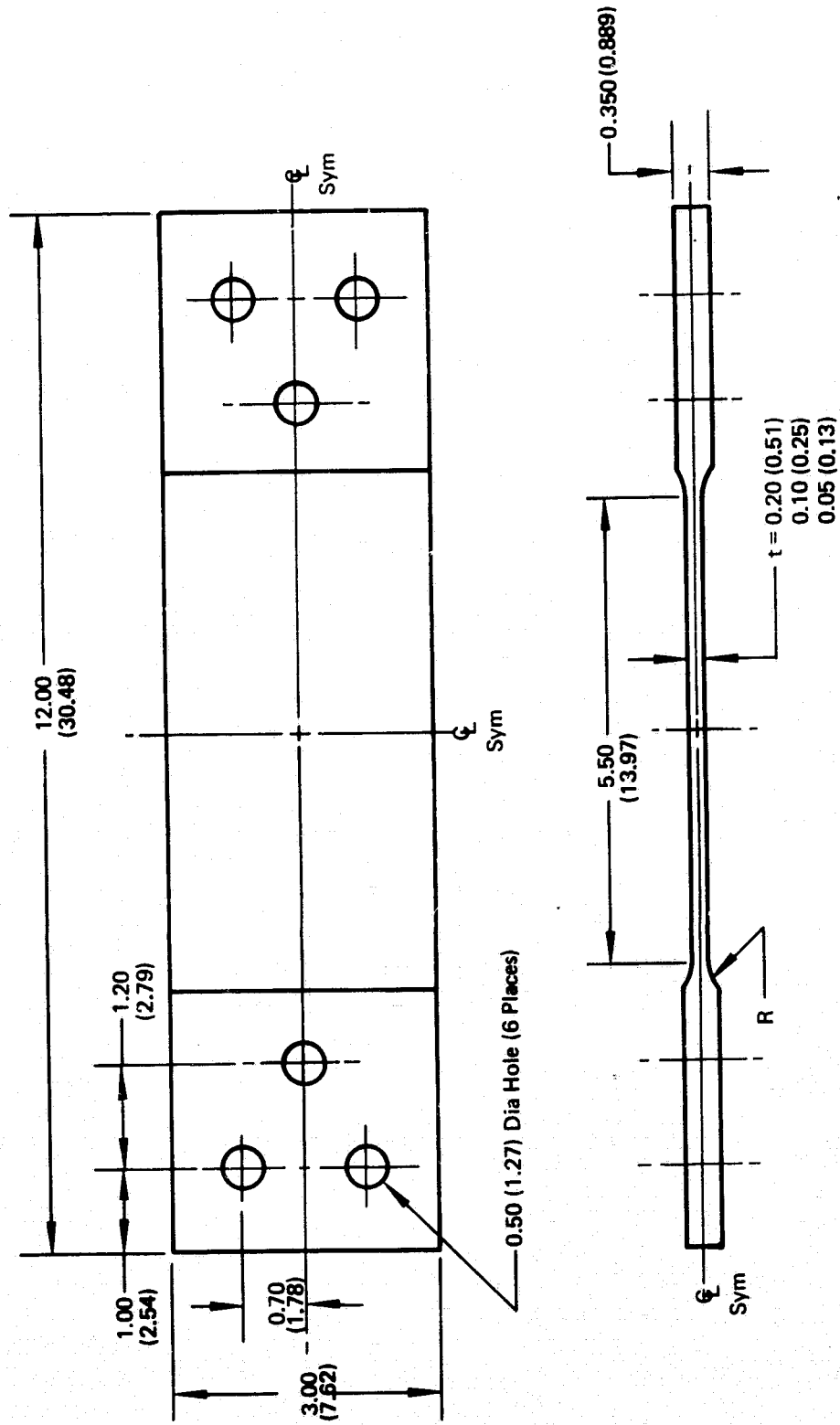
NOTE: All Dimensions in Inches (Cm)

Figure C7: TITANIUM BASE METAL VARIABLE THICKNESS TEST SPECIMENS

109
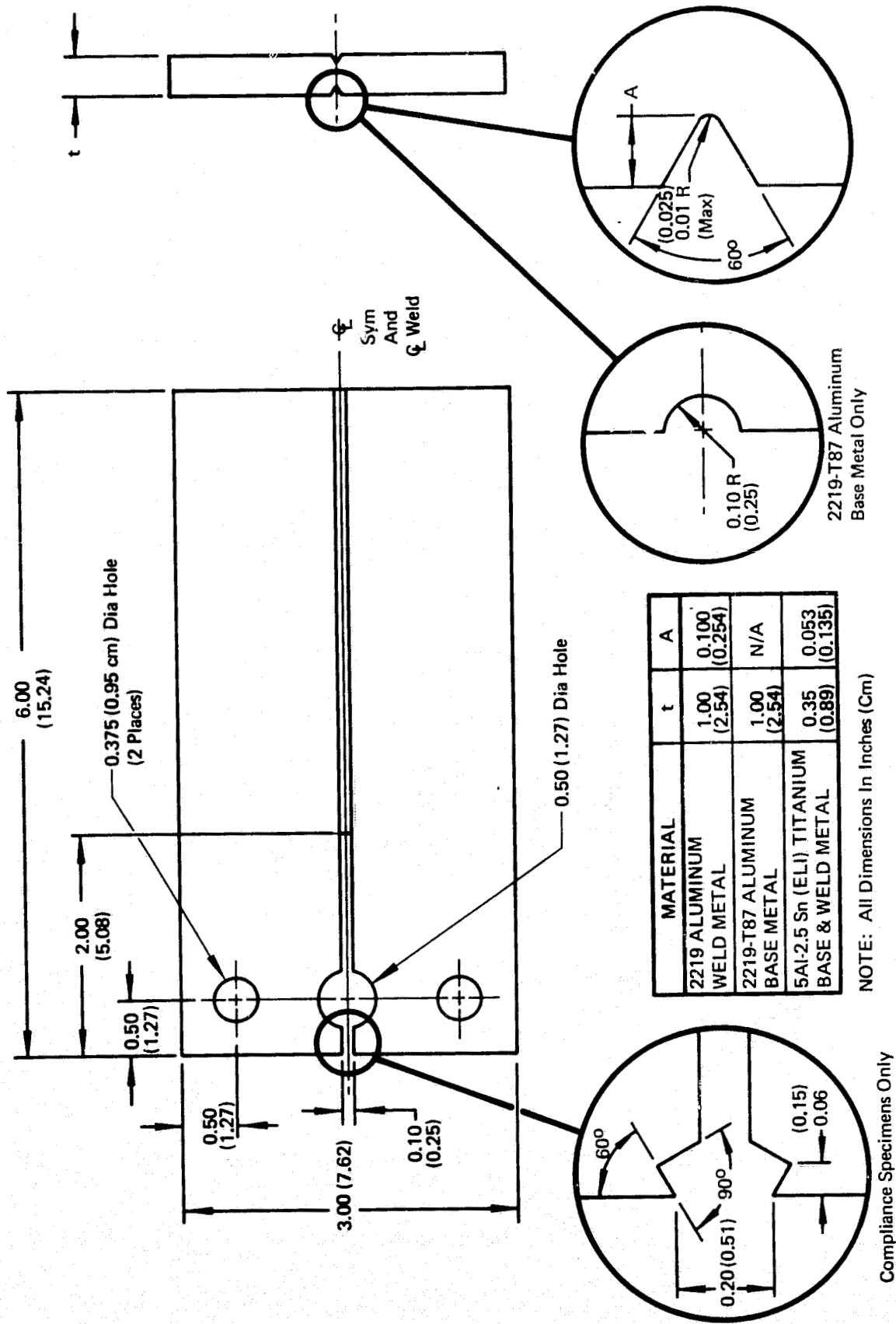
Figure C8: DCB SPECIMEN CONFIGURATIONS

MATERIAL	t	A
2219 ALUMINUM WELD METAL	1.00 (2.54)	0.100 (0.254)
2219-T87 ALUMINUM BASE METAL	1.00 (2.54)	N/A
5Al-2.5 Sn (ELI) TITANIUM BASE & WELD METAL	0.35 (0.89)	0.053 (0.135)

NOTE: All Dimensions In Inches (Cm)
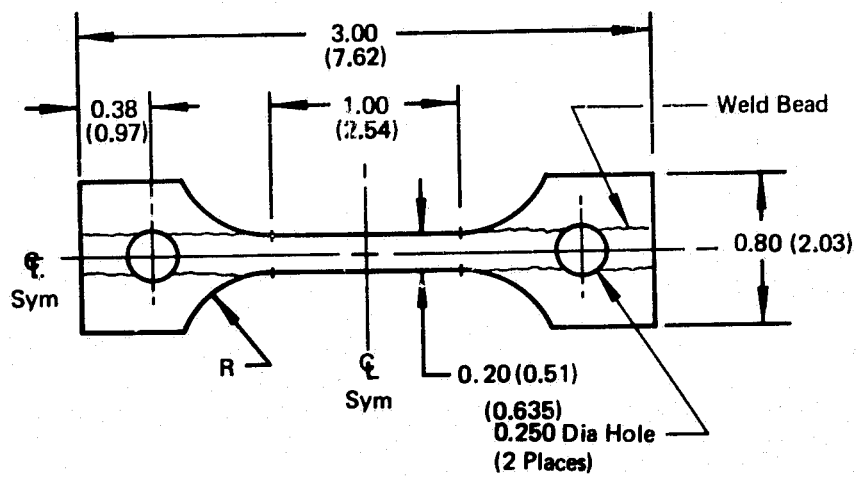
Figure C9: 5Al-2.5Sn (ELI) WELD METAL TENSILE SPECIMEN

NOTE: All dimensions in inches (Cm)
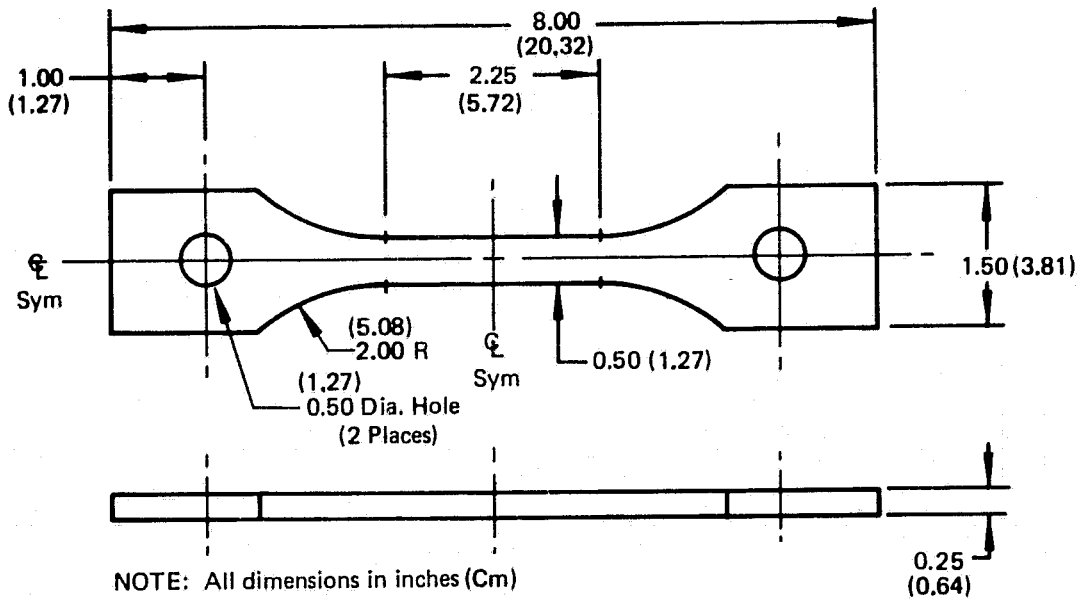
(a): Tensile specimen for *304 S.S., 5Al-2.5 Sn (ELI) titanium, 6Al-4V (ELI) annealed titanium, 2219-T87 aluminum and 2219-T6E46 aluminum*

NOTE: All Dimensions In Inches (Cm)
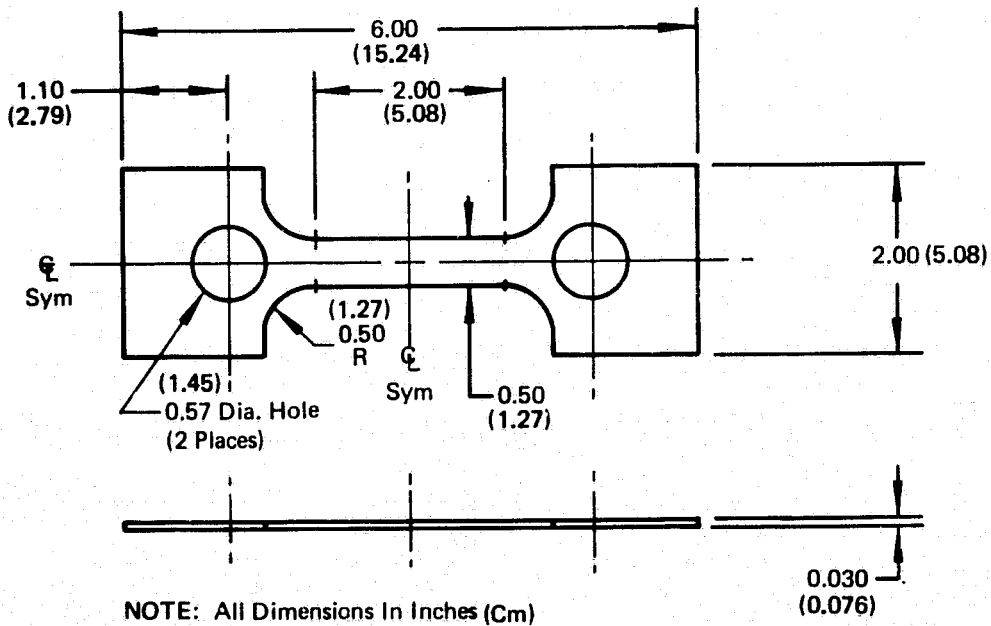
(b): Tensile specimen for *6Al-4V (ELI) STA titanium*

Figure C10: TENSILE SPECIMENS
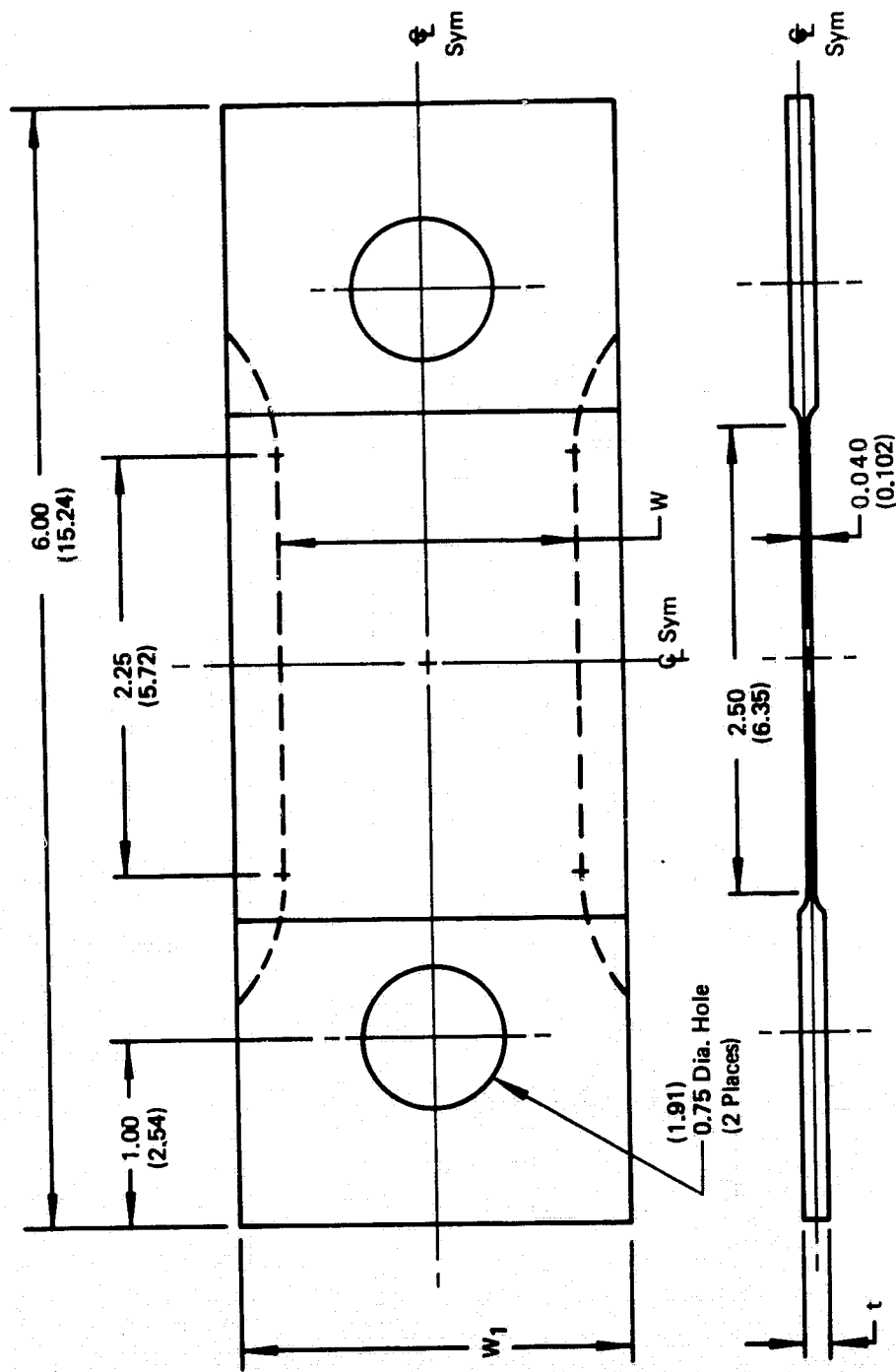
NOTE: All Dimensions In Inches(Cm)

△ See Tables for Width W

MATERIAL	W₁	W	t
2219-T87	2.00 (5.08)	△	0.125(0.318)
2219-T6E46	2.20 (5.59)		0.100(0.254)

Figure C11: ALUMINUM SUSTAIN LOAD SURFACE FLAWED SPECIMENS

113

NOTE: All Dimensions In Inches (Cm)

⚠ See Tables For Width W
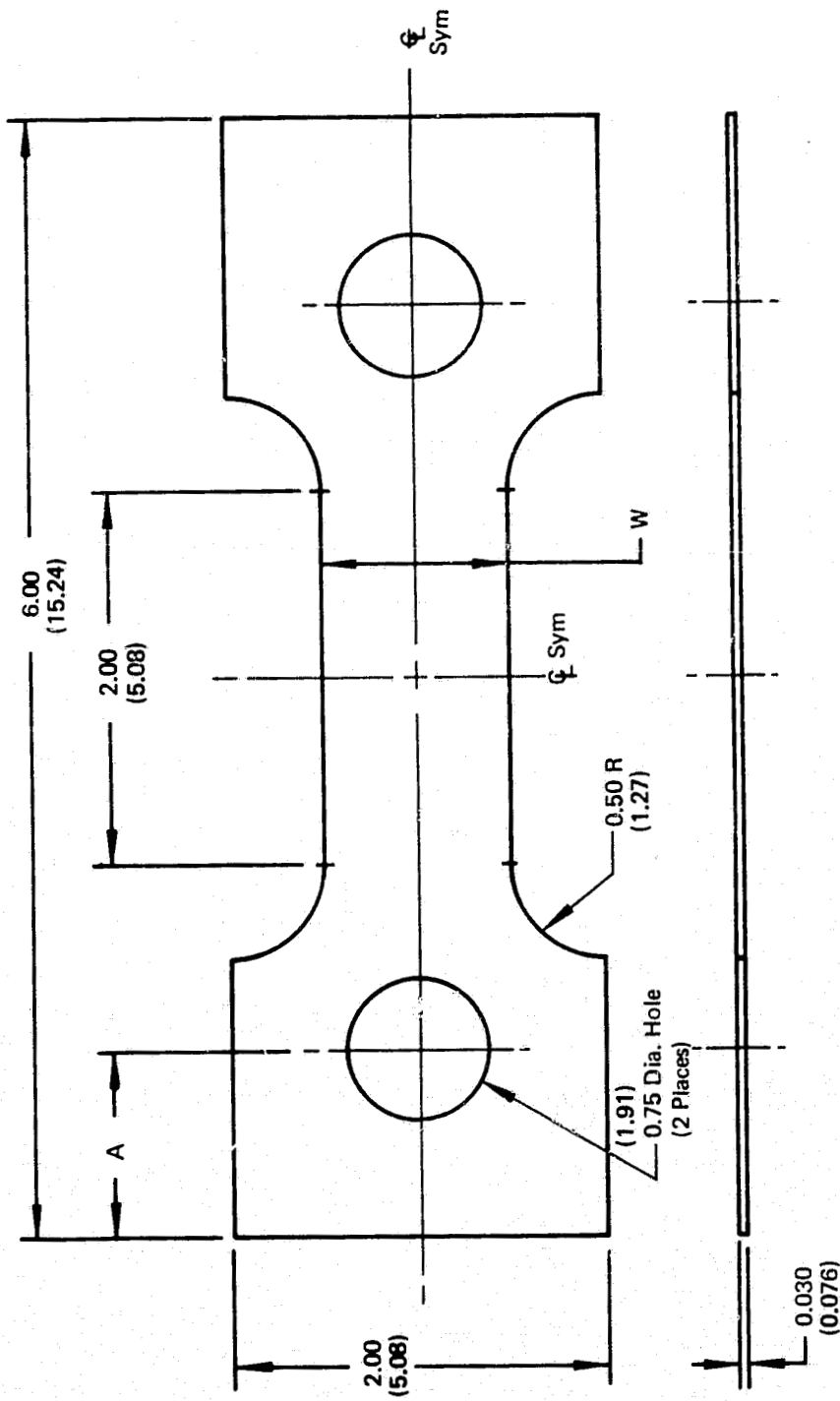
MATERIAL	A	W
5Al-2.5 Sn (ELI)	1.00 (2.54)	⚠
6Al-4V (ELI) ANNEALED	1.00 (2.54)	
6Al-4V (ELI) STA	1.10 (2.79)	

Figure C-12: TITANIUM SUSTAINED LOAD SURFACE FLAWED SPECIMEN

114

Table 2-1: TEST PROGRAM FOR EVALUATING STRESS CORROSION CRACKING RESISTANCE OF 2219-T87 ALUMINUM ALLOY BASE AND WELD METAL

| TEST ENVIRONMENT | | | | NUMBER OF BASE METAL/WELD METAL TESTS | |
MEDIUM	PHASE	TEMPERATURE, °F (°K)	GAGE PRESSURE, PSI (kN/m²)	DCB SPECIMENS (1.0 INCH THICK) (2.54 cm THICK)	SF SPECIMENS (0.625 INCH THICK) (1.59 cm THICK)
Distilled Water (DW)	Liquid	72 (295)	30 (20.7)	3/3	2/2
DW + 3½% NaCl	Liquid	72 (295)	30 (20.7)	3/3	2/2
Trichloroethylene	Liquid	72 (295)	30 (20.7)	3/3	2/2
Dye Penetrant (ZL-4B)	Liquid	72 (295)	30 (20.7)	3/3	2/2
Room Air	Gas	72 (295)	Ambient	0/0	3/2
Nitrogen	Liquid	-320 (78)	30 (20.7)	0/0	0/2
Hydrogen	Gas	~60 (288)	100 (69.0)	3/3	1/1
Hydrogen	Gas	~60 (288)	30 (20.7)	3/3	1/1
Hydrogen	Gas	-320 (78)	Ambient	3/3	2/2
Hydrogen	Gas	~-423 (20)	Ambient	0/0	3/5
Hydrogen	Liquid	-423 (20)	30 (20.7)	0/0	3/2
Oxygen	Gas	~60 (288)	30 (20.7)	3/3	2/2
Oxygen	Liquid	-320 (78)	30 (20.7)	3/3	2/2
Oxygen Diflouride	Gas	~60 (288)	30 (20.7)	3/3	2/2
Oxygen Diflouride	Liquid	-320 (78)	30 (20.7)	3/3	2/2
FLOX (80% F₂, 20% O₂)	Gas	~60 (288)	30 (20.7)	3/3	2/2
FLOX (80% F₂, 20% O₂)	Liquid	-320 (78)	30 (20.7)	3/3	2/2
Flourine	Gas	~60 (288)	30 (20.7)	3/3	0/0
Flourine	Liquid	-320 (78)	30 (20.7)	3/3	0/0
Argon	Gas	~60 (288)	30 (20.7)	0/0	3/0

NOTES:
(1) Crack Planes Parallel to Rolling Direction in Base Metal Specimens
(2) Cracks at Weld Centerline in Weld Metal Specimens
(3) All DCB Specimens Loaded in Room Air
(4) SF Specimens Loaded in Test Environment

Table 2-2: *TEST PROGRAM FOR EVALUATING STRESS CORROSION CRACKING RESISTANCE OF 5Al-2.5 Sn (ELI) TITANIUM ALLOY BASE AND WELD METAL*

TEST ENVIRONMENT				NUMBER OF BASE METAL/WELD METAL TESTS	
MEDIUM	PHASE	TEMPERATURE, °F (°K)	GAGE PRESSURE, PSI (kN/m²)	DCB SPECIMENS, 0.375 INCH THICK (1.59 cm THICK)	SF SPECIMENS, 0.375 INCH THICK (1.59 cm THICK)
Distilled Water (DW)	Liquid	72 (295)	30 (20.7)	3/3	1/2
DW + 3½% NaCl	Liquid	72 (295)	30 (20.7)	3/3	1/1
Acetone	Liquid	72 (295)	30 (20.7)	3/3	1/1
Methanol (MA)	Liquid	72 (295)	30 (20.7)	3/3	1/1
MA + 2% DW	Liquid	72 (295)	30 (20.7)	3/3	1/1
Ethanol (EA)	Liquid	72 (295)	30 (20.7)	3/3	1/1
EA + 2% DW	Liquid	72 (295)	30 (20.7)	3/3	1/1
Methyl Ethyl Ketone	Liquid	72 (295)	30 (20.7)	3/3	1/1
Dye Penetrant (ZL-2A)	Liquid	72 (295)	30 (20.7)	3/3	1/1
Room Air	Gas	72 (295)	Ambient	0/0	3/3
Argon	Gas	72 (295)	30 (20.7)	0/0	3/3
Helium	Gas	~60 (288)	30 (20.7)	3/3	1/2
Helium	Gas	-423 (20)	30 (20.7)	3/3	1/1
Helium	Gas	~60 (288)	1000 (689.5)	0/0	2/2
Nitrogen	Liquid	-320 (78)	Ambient	0/0	2/0
Hydrogen	Gas	~60 (288)	30 (20.7)	4/3	1/1
Hydrogen	Gas	~60 (288)	100 (69.0)	3/3	1/1
Hydrogen	Gas	-320 (78)	30 (20.7)	3/3	2/2
Hydrogen	Gas	~-423 (20)	100 (69.0)	3/3	4/4
Hydrogen	Liquid	-423 (20)	Ambient	0/0	2/2

NOTES:
(1) Crack Planes Perpendicular to Rolling Direction in All Base Metal Specimens
(2) Cracks at Weld Centerline in Weld Metal Specimens
(3) All DCB Specimens Loaded in Room Air
(4) All SF Specimens Loaded in Test Environment

Table 2-3: LOAD-IN-ENVIRONMENT TEST PROGRAM FOR 2219-T87 ALUMINUM AND 5Al-2.5 Sn (ELI) TITANIUM BASE METAL DCB SPECIMENS.

ALLOY	TEMP (°F)	PRESSURE (PSIG)	PHASE	MEDIUM	CRACK ORIENTATION	NUMBER OF TESTS	TEST DURATION (HRS)
				TEST ENVIRONMENT			
2219-T87 Aluminum	72	Amb	Liquid	Distilled Water (DW)	WR	1	100
					RW	1	100
				DW + 3 ½% NaCl	WR	1	100
					RW	1	100
				Acetone	WR	1	100
					RW	1	100
				Methanol + 2% DW	WR	1	100
					RW	1	100
				Methyl-Ethyl Ketone	WR	1	100
					RW	1	100
				Ethanol	WR	1	100
					RW	1	100
				Ethanol + 2% DW	WR	1	100
					RW	1	100
				Dye Penetrant (ZL-2A)	WR	1	100
					RW	1	100
Ti-5Al-2.5Sn(ELi)	72	Amb	Liquid	Distilled Water (DW)	WR	1	100
					RW	1	100
				DW + 3 ½% NaCl	WR	1	100
					RW	1	100
				Trichloroethylene	WR	1	100
					RW	1	100
				Dye Penetrant (ZL-4B)	WR	1	100
					RW	1	100

Table 2-4: *TEST PROGRAM FOR EVALUATING EFFECT OF SURFACE FLAWED SPECIMEN THICKNESS ON STRESS CORROSION CRACKING SUSCEPTIBILITY OF 5Al-2.5 Sn (ELI) TITANIUM ALLOY*

MATERIAL	TEST ENVIRONMENT	SPECIMEN THICKNESS (IN.)	LOADING SEQUENCE	NO. OF TESTS
5Al-2.5 Sn (ELI) TITANIUM BASE METAL WITH CRACK PLANE PERPENDICULAR TO THE LONGITUDINAL (ROLLING) DIRECTION	ARGON GAS AT 72°F METHANOL LIQUID AT 72°F	0.20 0.20	LOAD–UNLOAD SUSTAINED LOAD	1 2
	ARGON GAS AT 72°F METHANOL LIQUID AT 72°F	0.10 0.10	LOAD–UNLOAD SUSTAINED LOAD	1 2
	ARGON GAS AT 72°F METHANOL LIQUID AT 72°F	0.05 0.05	LOAD–UNLOAD SUSTAINED LOAD	1 2

118

Table 2-5: CHEMICAL COMPOSITIONS OF MATERIALS

ELEMENT (% BY WEIGHT EXCEPT AS NOTED)	2219 ALUMINUM PLATE		5Al-2.5Sn(ELI) TITANIUM SHEET (0.040 IN. THICK)	5Al-2.5Sn(ELI) TITANIUM PLATE (0.350 IN. THICK)	6Al-4V(ELI) TITANIUM PLATE
	MIN	MAX			
COPPER	5.8	6.8	—	—	—
SILICON	—	0.20	—	—	—
MANGANESE	0.20	0.40	0.003	<0.01	—
MAGNESIUM	—	0.02	—	—	—
IRON	—	0.30	0.07	0.19	0.06
CHROMIUM	—	—	—	—	—
ZINC	—	0.10	—	—	—
VANADIUM	0.05	0.15	—	—	4.0
ZIRCONIUM	0.10	0.25	—	—	—
CARBON	—	—	0.015	0.02	0.023
NITROGEN (PPM)	—	—	120	—	90
OXYGEN (PPM)	—	—	800	940	1,110
HYDROGEN (PPM)	—	—	110	94	50
PHOSPHOROUS	—	—	—	—	—
SULFUR	—	—	—	—	—
TIN	—	—	2.7	2.5	—
NICKEL	—	—	—	—	—
MOLYBDENUM	—	—	—	—	—
TITANIUM	0.02	0.10	REMAINDER	REM	REMAINDER
ALUMINUM	REMAINDER		5.9	5.1	5.9
OTHER	—	—	—	—	—

Table 2-6: MECHANICAL PROPERTIES OF MATERIALS

ALLOY	FORM	LOADING DIRECTION [T = Transverse / L = Longitudinal]	TEMPERATURE (°F)	ULTIMATE TENSILE STRENGTH (KSI)	0.2 PERCENT OFFSET YIELD STRENGTH (KSI)	ELONGATION IN 2.0 INCH GAGE LENGTH (%)
2219 Aluminum	1.0 Inch T87 Plate	T T T	72 -320 -423	69 86 101	55 66 69	8 12 11
	0.125 Inch T87 Plate	T T	72 -320	69 87	55 67	10 12
	1.0 Inch As-Welded GTA Weld	T T T	72 -320 -423	40 56 67	20 25 28	8 9 11
	0.125 Inch T6E46 Plate	T T	72 -320	66 81	48 57	12 13
5Al-2.5Sn(ELI) Titanium	0.35 Inch Plate	L L L	72 -320 -423	119 190 209	114 179 196	13 9 5
	0.04 Inch Sheet	T T	72 -320	117 180	112 173	14 16
	0.35 Inch GTA Weld	T T T	72 -320 -423	126 192 224	117 184 204	11 9 7
6Al-4V (ELI Titanium	0.375 Inch Plate	T T	72 -320	125 198	122 193	15 6
	0.375 STA Plate	T T	72 -320	162 225	150 214	9 4

Table 2-7: FRACTURE TOUGHNESS DATA FOR MATERIALS USED IN EVALUATING STRESS CORROSION CRACKING IN 2219-T87 ALUMINUM AND 5Al-2.5 Sn (ELI) TITANIUM

MATERIAL	TEST TEMP (°F)	SF SPECIMEN TESTS							DCB SPECIMEN TESTS			
		FRACTURE TOUGHNESS VALUES* FROM REF (KSI√IN.)				FRACTURE TOUGHNESS VALUES* FROM PRESENT PROGRAM (KSI√IN.)			FRACTURE TOUGHNESS VALUES FROM PRESENT PROGRAM (KSI√IN.)			
		LOADING DIREC-TION	NUMBER OF TESTS	RANGE OF VALUES	AVG. VALUE	NUMBER OF TESTS	RANGE OF VALUES	AVG. VALUE	TEST DIREC-TION	NUMBER OF TESTS	RANGE OF VALUES	AVG. VALUE
2219-T87 Aluminum Base Metal	72	Trans.	7	38-42	40	30	38-43	40	WR	2	31.6-32.2	32
	-320	Trans.	8	38-45	42	1	—	43	WR	2	38.4-37.7	38
	-423	Trans.	8	41-47	44	1	—	47	—	—	—	—
Ti-5Al-2.5Sn (ELI) Base Metal	72	Long.	—	—	—	—	—	—	RW	1	—	115
	-320	Long.	2	83-87	85	1	—	84	RW	1	—	59
	-423	Long.	8	59-64	61	1	—	70	RW	1	—	51
Ti-5Al-2.5Sn Weld Metal	72	—	—	—	—	—	—	—	—	—	—	—
	-320	—	—	—	85[a]	1	—	84	—	1	—	82
	-423	—	—	—	75[a]	1	—	70	—	1	—	58

a Obtained From Ref

* $K_{IE} = 1.1\,\sigma\,\sqrt{\pi a/Q}$; σ = Failure Stress

121

Table 2-8: SCC TEST RESULTS FOR 5Al-2.5 Sn (ELI) TITANIUM ALLOY BASE AND WELD METAL

ENVIRONMENT	BASE METAL				WELD METAL			
	DCB RESULTS [a,c]		SF RESULTS [b,c]		DCB RESULTS [e,f]		SF RESULTS [c,f]	
	CRACK GROWTH (IN.)	TEST DURATION (HRS)	CRACK GROWTH (IN.)	TEST DURATION (HRS)	CRACK GROWTH (IN.)	TEST DURATION (HRS)	CRACK GROWTH (IN.)	TEST DURATION (HRS)
DISTILLED WATER (DW)	0.16	118	NIL	16	0.06	240	NIL	24
SALT WATER	2.05	116	d	0.0083	0.13	150	d	0.17
METHANOL	1.58	238	0.05	16	0.33	68	0.07	0.6
METHANOL + 2% DW	1.66	118	d	5	0.32	166	d	2.2
ETHANOL + 2% DW	1.62	120	0.06	16	NIL	240	0.38	12
MEK	NIL	138	NIL	12	NIL	238	d	21.4
DYE PENETRANT (ZL-2A)	1.13	114	d	0.083	1.12	144	d	0.083
HYDROGEN GAS TEMP = AMB PRESS = 100 PSIG	0.47	24	NIL	10	NIL	30	NIL	9

NOTES:
a WR DIRECTION
b WT DIRECTION
c LOADED IN ENVIRONMENT
d SPECIMEN FAILED
e LOADED IN AIR
f WELD CENTERLINE

Table 2-9: RESULTS OF SF SPECIMEN THICKNESS EFFECT TESTS FOR RW DIRECTION OF Ti-5Al-2.5 Sn (ELI) PLATE IN LIQUID METHANOL AT 72°F

TEST NO.	SPECIMEN		TEST ENVIRONMENT	CRACK DIMENSIONS				PEAK STRESS LEVEL (KSI)	TIME AT PEAK STRESS (HRS)	K_I AT BEGINNING OF TEST (KSI√IN.)	K_I AT END OF TEST (KSI√IN.)	CRACK DEPTH GROWTH, Δa (IN.)
	GAGE THICKNESS (IN.)	GAGE WIDTH (IN.)		BEFORE TEST		AFTER TEST						
				DEPTH a (IN.)	LENGTH 2c (IN.)	DEPTH a (IN.)	LENGTH 2c (IN.)					
1	0.202	3.00	ARGON	0.074	0.410	0.083	0.410	75.0	0	40	45	0.009
2	0.201	3.00	METHANOL	0.080	0.400	0.102	0.400	80.0	23.1	45	56	0.022
3	0.201	3.00	METHANOL	0.078	0.400	0.094	0.400	70.0	15.9	39	45	0.016
4	0.103	3.00	ARGON	0.048	0.290	0.059	0.290	75.0	0	37	40	0.011
5	0.104	3.00	METHANOL	0.047	0.273	a	0.273	80.0	15.6	39	a	0.057
6	0.051	3.00	ARGON	0.035	0.182	0.044	0.182	75.0	0	40	—	0.009
7	0.050	3.00	METHANOL	0.038	0.178	a	0.178	80.0	20.5	47	a	0.012
8	0.051	3.00	METHANOL	0.035	0.186	a	0.186	70.0	16.5	38	a	0.016

a   CRACK GREW THROUGH SPECIMEN THICKNESS

* $K_I = 1.1 \, MK \, \sigma \sqrt{\dfrac{\pi a}{Q}}$; MK FROM REFERENCE 9

123

Table 2-10: RESULTS OF TESTS TO EVALUATE SURFACE FLAW GROWTH CHARACTERISTICS DURING RISING AND MONOTONIC LOADS

MATERIAL	ENVIRONMENT		SPECIMEN DETAILS			CRACK DIMENSIONS				APPLIED STRESS		RESULTS	
	MEDIUM	TEMPERATURE (°F)	IDENTIFICATION	GAGE WIDTH (IN.)	GAGE THICKNESS (IN.)	BEFORE TEST DEPTH, a (IN.)	BEFORE TEST WIDTH, 2c (IN.)	AFTER TEST DEPTH, a (IN.)	AFTER TEST WIDTH, 2c (IN.)	MAGNITUDE (KSI)	TIME AT PEAK STRESS (HRS)	K_I AT END OF TEST (KSI √IN.)	CRACK DEPTH GROWTH, Δa (IN.)
2219–T87 ALUMINUM BASE METAL (WR DIRECTION)	AIR	72	AR-2	6.00	0.606	0.252	0.925	0.260	0.925	44.5	0	36.7	0.008
			AR-3	5.98	0.607	0.243	0.925	0.251	0.925	44.5	1	36.7	0.008
			AR-4	6.00	0.591	0.249	0.915	0.259	0.915	44.5	20	37.3	0.010
	ARGON	72	AA-1	6.00	0.604	0.246	0.925	0.256	0.925	44.5	0	36.9	0.010
			AA-2	6.00	0.610	0.252	0.925	0.262	0.925	44.5	1	36.9	0.010
Al-2219 WELD METAL	AIR	72	WDF-1A	6.00	0.904	0.430	1.475	0.475	1.475	22.0	0	23.9	0.045
			WAP-2	5.99	0.913	0.415	1.470	0.440	1.470	22.0	16	23.9	0.040
Ti-5Al-2.5Sn ELI BASE METAL (RW DIRECTION)	AIR	72	TAR-1A	4.00	0.397	0.204	1.000	0.210	1.00	90.0	0	67.2	0.006
			TAR-3	4.00	0.399	0.168	0.945	0.196	0.950	86.0	1	67.2	0.028
			TAR-4	4.00	0.399	0.164	0.930	0.186	0.935	86.0	20	66.0	0.022
	ARGON	72	TAA-1	4.00	0.399	0.172	0.940	0.184	0.940	86.0	0	66.0	0.012
			TAA-2	4.00	0.399	0.188	0.990	0.204	0.990	86.0	1	68.6	0.016
			TAA-3	4.00	0.399	0.168	0.925	0.182	0.930	86.0	39	65.5	0.014
Ti-5Al-2.5Sn ELI WELD METAL	ARGON	72	TAAW-1	3.25	0.334	0.182	0.950	0.182	0.950	86.0	0	65.6	0
			TAAW-2	3.25	0.335	0.178	0.950	0.180	0.950	86.0	1	65.6	0.002
			TAAW-3	3.25	0.337	0.178	0.960	0.180	0.960	86.0	20	65.4	0.002
	AIR	72	TARW-3	3.25	0.334	0.175	0.945	0.175	0.945	86.0	1	64.8	0.002
			TARW-4	3.25	0.338	0.186	0.965	0.188	0.965	86.0	20	66.5	0.002

Table 2-11: RESULTS OF TESTS TO EVALUATE SURFACE FLAW GROWTH DURING RISING LOAD AT CRYOGENIC TEMPERATURES

MATERIAL	ENVIRONMENT		SPECIMEN DETAILS			CRACK DIMENSIONS				APPLIED STRESS		RESULTS	
	MEDIUM	TEMP (°F)	IDENTIFICATION	GAGE WIDTH (IN.)	GAGE THICKNESS (IN.)	BEFORE TEST DEPTH a (IN.)	BEFORE TEST LENGTH 2c (IN.)	AFTER TEST DEPTH a (IN.)	AFTER TEST LENGTH 2c (IN.)	MAGNITUDE (KSI)	TIME AT PEAK STRESS (HRS)	K_1 AT END OF TEST (KSI√IN.)	CRACK DEPTH GROWTH, Δa (IN.)
Al-2219-T87 (WR DIRECTION)	LH$_2$	-423	X-2	6.00	0.604	0.237	0.920	0.240	0.920	50.8	0	42.3	0.003
Al-2219 WELD METAL	O$_2$	-320	WS-1	6.00	0.903	0.430	1.46	0.465	1.46	25.0	0	27.3	0.035
	H$_2$	-320	WH-7	6.00	0.897	0.425	1.47	0.450	1.47	25.0	0	27.8	0.025
	LN$_2$	-320	WAN-2	6.00	0.915	0.422	1.49	0.467	1.49	25.0	0	27.5	0.045
	GH$_2$	-413	WH-10	6.00	0.909	0.417	1.47	0.460	1.47	25.0	0	26.9	0.045
			WH-2	6.00	0.900	0.420	1.48	0.430	1.48	22.0	0	23.2	0.011
Ti-5Al-2.5Sn (ELI), RW DIRECTION	GH$_2$	-413	TH-4	1.10	0.355	0.086	0.264	0.086	0.264	139.3	0	64.4	0

125

Table 2-12: SURFACE FLAW DEPTH GROWTH OBSERVED DURING TESTS OF 2219 WELD CENTERLINES

TEST TYPE	SPECIMEN IDENTIFICATION	MEDIUM	TEMPERATURE (°F)	PEAK STRESS LEVEL (KSI)	TIME AT PEAK STRESS (KSI)	CRACK DEPTH GROWTH (Δa) (IN.)
LOAD-UNLOAD	WPP-1A	AIR	72	22.0	0	0.045
	WH-7	GH_2	-320	25.0	0	0.025
	WAN-2	LN_2	-320	25.0	0	0.045
	WH-10	GH_2	-423	25.0	0	0.045
	WH-2	GH_2	-423	22.0	0	0.011
SUSTAINED LOAD	WS-1	H_2O +	72	22.0	24	0.075
	WS-2	3.5% NaCl	72	22.0	15	0.030
	WDW-2	DIST H_2O	72	22.0	16	0.035
	WT-2	TcE	72	22.0	12	0.030
	WDP-2	DYE PEN	72	22.0	16	0.035
	WOF-1 WOF-3	GOF_2	72	22.0	10	0.040
	WFX-1	GFLOX	72	22.0	7	0.030
	WFX-2				10	0.040
	WH-1	GH_2	72	22.0	15	0.035
	WH-3				10	0.030
	WO-1	GO_2	72	22.0	14	0.035
	WO-2				10	0.035
	WOF-4	LOF_2	-320	22.0	7	0.030
	WOF-6				10	0.040
	WFX-3	LFLOX	-320	22.0	8	0.025
	WFX-4				11	0.025
	WH-5	GH_2	-320	25.0	10	0.070
	WO-3	LO_2				0.060
	WH-14	GH_2	-413	22.0	10	0.020
	WH-8			25.0		0.100
	WH-11	WH-2	-423	22.0	12	0.020
	WO-4			25.0	11	0.070

126

Table 3-1: TEST PROGRAM FOR UPPER STAGE MATERIAL/ENVIRONMENT COMBINATIONS

MATERIAL	ENVIRONMENT			TEST DETAILS	
	MEDIUM	PHASE	TEMPERATURE (°F)	TEST DURATION (HRS)	NUMBER OF TESTS
ALUMINUM 2219-T6E46 BASE METAL	FLUORINE	GAS	−275	10	2
		LIQUID	−320	10	2
	FLOX (80% F₂ 20% O₂)	GAS	−275	10	2
				500	2
		LIQUID	−320	10	2
				500	2
ALUMINUM 2219-T87 BASE METAL	FLUORINE	GAS	−275	10	2
		LIQUID	−320	10	2
	FLOX	GAS	−275	10	2
				500	2
		LIQUID	−320	10	2
				500	2
	METHANE	GAS	−225	10	2
				40	2
				500	2
		LIQUID	−250	10	2
				40	2
				500	2
TITANIUM 5Al-2.5Sn (ELI) BASE METAL	METHANE	GAS	−225	10	2
				40	2
				500	2
		LIQUID	−250	10	2
				40	2
				500	2
TITANIUM 6Al-4V STA BASE METAL	METHANE	GAS	−225	10	2
				40	2
				500	2
		LIQUID	−250	10	2
				40	2
				500	2
TITANIUM 6Al-4V ANNEALED BASE METAL	METHANE	GAS	−225	10	2
				40	2
				500	2
		LIQUID	−250	10	2
				40	2
				500	2

127

Table 3-2: RESULTS OF -320°F PROOF OVERLOAD TESTS FOR 2219 ALUMINUM ALLOY SURFACE FLAWED SPECIMENS

| ALLOY | SPECIMEN | | | INITIAL FLAW | | TARGETED PEAK PROOF STRESS (KSI) | GROSS STRESS AT WHICH FLAW GREW THROUGH SPECIMEN THICKNESS (KSI) | GROSS STRESS AT WHICH SPECIMEN FAILED (KSI) | NOTES |
	NUMBER	WIDTH (IN.)	THICKNESS (IN.)	DEPTH, a (IN.)	WIDTH, 2c (IN.)				
2219-T87	A-5	2.00	0.041	0.029	0.315	59.0	a	55.3	
	A-7	2.00	0.041	0.028	0.276	59.0	a	57.4	
	A-4	2.00	0.041	0.026	0.255	59.0	b	a	
	A-8	2.00	0.040	0.024	0.240	59.0	59.0^c	63.0	
2219-T6E46	AL-1	2.20	0.039	0.022	0.210	46.0	b	a	
	AL-2	2.20	0.041	0.026	0.255	46.0	b	a	
	AL-4	2.20	0.041	0.028	0.300	46.0	b	a	
	AL-6	2.03	0.041	0.035	0.373	46.0	b	a	

NOTES

a NOT DETERMINED
b DID NOT GROW THROUGH THICKNESS AT PEAK STRESS
c GREW THROUGH AFTER 40 SECONDS AT 59 KSI

CRACK DIMENSIONS SELECTED FOR SUSTAINED LOAD TEST SPECIMENS

ALLOY	a(IN.)	2c(IN.)
T87	0.022	0.220
T6E46	0.035	0.350

Table 3-3: RESULTS OF -320°F PROOF OVERLOAD TESTS FOR TITANIUM ALLOY SURFACE FLAWED SPECIMENS

MATERIAL	SPECIMEN NUMBER	SPECIMEN WIDTH (IN.)	SPECIMEN THICKNESS (IN.)	INITIAL FLAW DEPTH, a (IN.)	INITIAL FLAW WIDTH, 2c (IN.)	TARGETED PEAK PROOF STRESS (KSI)	GROSS STRESS AT WHICH FLAW GREW THROUGH SPECIMEN THICKNESS (KSI)	GROSS STRESS AT WHICH SPECIMEN FAILED (KSI)	NOTES
5Al-2.5Sn (ELI) TITANIUM	5T-2	1.200	0.0319	0.019	0.186	128.0	a	—	a — DID NOT GROW THRU AT 128.0 KSI
	5T-3	1.200	0.0319	0.021	0.215	→	a	—	b — DID NOT GROW THRU PRIOR TO FAILURE. CRACK DIMENSIONS SELECTED FOR SUSTAIN LOAD TESTING a = 0.025", 2c = 0.200"
	5T-4	0.998	0.0315	0.020	0.210	→	a	—	
	5T-5	1.000	0.0314	0.022	0.240	→	b	166.0	
6Al-4V (ELI) TITANIUM ANNEALED	6AT-1	0.997	0.0326	0.018	0.182	160.0	158.5	161.5	c — DID NOT GROW THRU AT 160.0
	6AT-2	0.997	0.0315	0.021	0.220	→	142.7	152.9	d — DID NOT GROW THRU PRIOR TO FAILURE. CRACK DIMENSIONS SELECTED FOR SUSTAIN LOAD TESTING a = 0.020", 2c = 0.200"
	6AT-3	1.002	0.0315	0.017	0.172	→	c	—	
	6AT-4	1.003	0.0315	0.017	0.166	→	c	194.0	
	6AT-5	1.003	0.0315	0.021	0.255	→	d	170.0	
6Al-4V (ELI) TITANIUM STA	STA-1	0.833	0.0302	0.015	0.180	180.0	e	171.5	e — DID NOT GROW THRU PRIOR TO FAILURE. CRACK DIMENSIONS SELECTED FOR SUSTAIN LOAD TESTING a = 0.013", 2c = 0.130"
	STA-2	0.833	0.0302	0.013	0.147	→	e	196.0	

Table 3-4: RESULTS OF SUSTAINED LOAD TESTS OF UPPER STAGE MATERIAL/ENVIRONMENT COMBINATIONS

ALLOY	THICKNESS (IN.)	FLAW SIZE		TEST CONDITIONS					RESULTS
		DEPTH a (IN.)	LENGTH 2c (IN.)	MEDIUM	TEMP (°F)	PROOF STRESS* (KSI)	SUSTAINED STRESS (KSI)	TEST DURATION (HRS)	
2219-T6E46 BASE METAL	0.04	0.033	0.36	GF_2	-275	46.0	39.0	10	
		0.033	0.39	LF_2	-320	46.0	38.9	10	
	0.04	0.032	0.37	GFLOX	-275	46.0	39.0	500	
		0.033	0.40	LFLOX	-320	46.0	39.0	500	
2219-T87 BASE METAL	0.04	0.020	0.25	GF_2	-275	59.0	50.9	10	SURFACE FLAWS DID NOT GROW THROUGH PARENT SPECIMEN THICKNESS IN ANY OF THESE SUSTAINED LOAD TESTS
		0.020	0.24	LF_2	-320	59.0	51.1	10	
		0.021	0.23	GFLOX	-275	59.0	51.1	500	
		0.023	0.25	LFLOX	-320	59.0	51.0	500	
		0.021	0.25	GCH_4	-225	59.0	51.0	500	
		0.021	0.24	LCH_4	-250	59.0	51.1	500	
TITANIUM 5Al-2.5Sn ELI	0.032	0.022	0.22	GCH_4	-225	128.0	95.0	500	
		0.022	0.21	LCH_4	-250	128.0	95.0	500	
TITANIUM 6Al-4V (ELI) STA	0.032	0.013	0.16	GCH_4	-225	182.0	150.0	500	
		0.012	0.15	LCH_4	-250	182.0	150.2	500	
TITANIUM 6Al-4V (ELI) ANNEALED	0.032	0.022	0.22	GCH_4	-225	160.0	125.1	500	
		0.018	0.22	LCH_4	-250	160.0	125.0	500	

*ALL SPECIMENS PROOF LOADED AT -320°F BEFORE SUSTAINED LOAD TEST

130

Table A1:   2219-T87 ALUMINUM BASE METAL STRESS COR
FOR NONHAZARDOUS ENVIRONMENTS

ENVIRONMENT				DCB SPECIMEN DATA												SPECI	
				SPECIMEN DETAILS							TEST DATA						
MEDIUM	PHASE	TEMPERATURE (°F)	PRESSURE (psig)	IDENTIFICATION	GROOVE SHAPE	THICKNESS, b (inch)	NET THICKNESS AT GROOVE, b_n (inch)	HEIGHT, h (inch)	INITIAL CRACK LENGTH, a_i (inch)	LOADING MEDIUM	JAW DISPLACEMENT (inch)	TEST DURATION (hours)	FINAL CRACK LENGTH, a_f (inch)	LOAD TO EFFECT JAW DISPLACEMENT (pounds)	IDENTIFICATION	CONFIGURATION (Figure Number)	THICKNESS
DISTILLED WATER + 3.5% NaCl	LIQUID	AMB	30	S-2	U	0.993	0.785	1.50	1.70	R.T. AIR	0.031	49.5	1.72	4725	AS-1		0.59
				S-3	U	0.978	0.776	↑	1.70	↑	↑	71.6	1.77	4405			
				S-4	U	0.987	0.778		1.69			262.1	1.80	4505			
DISTILLED WATER	LIQUID	AMB	30	DW-1	U	0.984	0.777		1.70			48.0	1.76	4710	AW-1 AW-2		0.60 0.60
				DW-2	U	0.984	0.778		1.73			71.1	1.82	4505			
				DW-3	U	0.990	0.780		1.69			139.2	1.77	4625			
TRICHLORO-ETHYLENE	LIQUID	AMB	30	T-1	U	0.988	0.778		1.70			71.0	1.76	4550	AT-1 AT-2		0.5 0.6
				T-2	U	0.978	0.770		1.66			115.0	1.86	4335			
				T-3	U	0.985	0.777		1.70			286.7	1.80	4400			
DYE PENETRANT	LIQUID	AMB	30	DP-1	U	0.990	0.783		1.70			66.1	1.76	4710	AD-1 AD-2		0.6 0.6
				DP-2	U	0.988	0.785	↓	1.70	↓	↓	93.6	1.76	4530			
				DP-3	U	0.984	0.777	1.50	1.69	R.T. AIR	0.031	237.8	1.76	4540			

* 5.0 AND 10.0 HOUR SUSTAIN CYCLES

FOLDOUT FRAME   1

AM BASE METAL STRESS CORROSION DATA
VARIOUS ENVIRONMENTS

LENGTH, a_f (inch)	LOAD TO EFFECT JAW DISPLACEMENT (pounds)	SURFACE FLAWED SPECIMEN DATA — SPECIMEN DETAILS — IDENTIFICATION	CONFIGURATION (Figure Number)	THICKNESS (inch)	WIDTH (inch)	INITIAL FLAW DEPTH, a_i (inch)	INITIAL FLAW LENGTH, $2c_i$ (inch)	LOADING MEDIUM	GROSS STRESS (ksi)	TEST DURATION (hours)	FLAW DEPTH AFTER TEST RUN, a_f (inch)	FLAW LENGTH AFTER TEST RUN, $2c_f$ (inch)	FLAW DEPTH AFTER FATIGUE MARKING, a_{cr} (inch)	FLAW LENGTH AFTER FATIGUE MARKING, $2c_{cr}$ (inch)	AMBIENT TEMP. FAILURE LOAD (kips)
.72	4725														
.77	4405	AS-1		0.599	6.00	0.249	0.920		44.6	16.0	0.253	0.920	0.291	1.01	164.8
.80	4505														
.76	4710														
.82	4505	AW-1		0.600	6.00	0.255	0.925		44.6	16.0	0.263	0.925	0.291	1.00	170.2
.77	4625	AW-2		0.605	6.00	0.246	0.925		44.6	27.1	0.251	0.925	0.300	1.00	170.0
.76	4550														
.86	4335	AT-1		0.589	6.01	0.264	0.923	TEST ENVIRONMENT	44.6	16.2	0.269	0.923	0.330	1.06	158.4
.80	4400	AT-2		0.603	6.00	0.252	0.925		42.0	15.7	0.257	0.925	0.304	1.03	162.2
.76	4710														
.76	4530	AD-1		0.603	6.00	0.264	0.925		44.6	15.0*	0.274	0.925	0.377	1.10	149.4
.76	4540	AD-2		0.604	6.00	0.264	0.930		42.0	16.1	0.269	0.930	0.304	1.03	168.0

Table A2: 2219-T87 ALUMINUM BASE METAL STRESS CORRO
FOR HYDROGEN AND OXYGEN

ENVIRONMENT				DCB SPECIMEN DATA												SPECIME	
				SPECIMEN DETAILS							TEST DATA						
MEDIUM	PHASE	TEMPERATURE (°F)	PRESSURE (psig)	IDENTIFICATION	GROOVE SHAPE	THICKNESS, b (inch)	NET THICKNESS AT GROOVE, b_n (inch)	HEIGHT, h (inch)	INITIAL CRACK LENGTH, a_i (inch)	LOADING MEDIUM	JAW DISPLACEMENT (inch)	TEST DURATION (hours)	FINAL CRACK LENGTH, a_f (inch)	LOAD TO EFFECT JAW DISPLACEMENT (pounds)	IDENTIFICATION	CONFIGURATION (Figure Number)	THICKNESS (inch)
HYDROGEN	GAS	AMB	30	H-1	U	0.990	0.780	1.50	1.68	R.T. AIR	0.031	4.0	1.75	4870	H-1		0.601
				H-2	U	0.985	0.780	↑	1.71	↑	0.031	21.0	1.78	4650			
				H-3	U	0.978	0.775		1.69			28.0	1.76	4840			
	GAS	AMB	100	H-4	U	0.986	0.775		1.74		0.031	7.0	1.79	4710	H-2		0.603
				H-5	U	0.978	0.775		1.74		0.031	23.5	1.78	4500			
				H-6	U	0.985	0.775		1.73		0.032	30.7	1.81	4690			
	GAS	-320	30	H-7	U	0.984	0.775		1.74		0.035	43.8	1.80	5862	H-3		0.600
				H-8	U	0.985	0.775	↓	1.70	↓	0.035	43.8	1.74	6250	H-4		0.600
				H-9	U	0.982	0.775	1.50	1.69	R.T. AIR	0.035	43.8	1.72	6363			
	GAS	-413	AMB												H-5		0.599
															H-7		0.605
															H-10		0.600
	LIQUID	-423	AMB												X-2		0.604
															H-9		0.600
															H-8		0.598
OXYGEN	GAS	AMB	30	O-1	U	0.985	0.775	1.50	1.70	R.T. AIR	0.031	8.3	1.77	4650	O-1		0.602
				O-2	U	0.981	0.775	↑	1.71	↑	0.031	23.8	1.81	4520	O-2		0.600
				O-3	U	0.982	0.770		1.70		0.031	32.3	1.76	4470			
	LIQUID	-320	30	O-4	U	0.988	0.775		1.70		0.035	49.5	1.99	5021	O-3		0.600
				O-5	U	0.987	0.775	↓	1.70	↓	0.035	49.5	1.85	5555	O-4		0.599
				O-6	U	0.985	0.770	1.50	1.67	R.T. AIR	0.035	49.5	1.87	5450			

*LOAD-UNLOAD

| | LOAD TO EFFECT JAW DISPLACEMENT (pounds) | SURFACE FLAWED SPECIMEN DATA | | | | | | | | | | | | |
| | | SPECIMEN DETAILS | | | | | | TEST DATA | | | | | | |
(inch)		IDENTIFICATION	CONFIGURATION (Figure Number)	THICKNESS (inch)	WIDTH (inch)	INITIAL FLAW DEPTH, a_i (inch)	INITIAL FLAW LENGTH, $2c_i$ (inch)	LOADING MEDIUM	GROSS STRESS (ksi)	TEST DURATION (hours)	FLAW DEPTH AFTER TEST RUN, a_f (inch)	FLAW LENGTH AFTER TEST RUN, $2c_f$ (inch)	FLAW DEPTH AFTER FATIGUE MARKING, a_{cr} (inch)	FLAW LENGTH AFTER FATIGUE MARKING, $2c_{cr}$ (inch)	AMBIENT TEMP. FAILURE LOAD (kips)
	4870 / 4650 / 4840	H-1		0.601	6.00	0.243	0.920	↑	44.6	10.0	0.246	0.920	0.320	1.05	162.0
	4710 / 4500 / 4690	H-2		0.603	6.00	0.240	0.920		44.6	10.0	0.243	0.920	0.320	1.09	161.0
	5862	H-3		0.600	6.00	0.242	0.920		47.0	1.0	0.248	0.920	0.323	1.03	161.0
	6250 / 6363	H-4		0.600	6.00	0.261	0.920		47.0	20.1	0.267	0.920	0.320	1.03	161.0
		H-5		0.599	6.00	0.240	0.910		50.8	20.0	0.246	0.910	0.365	1.09	156.0
		H-7		0.605	6.00	0.268	0.935		50.8	10.0	0.270	0.935	0.350	1.12	153.0
		H-10		0.600	6.00	0.243	0.970		45.1	1.0	0.243	0.970	0.332	1.07	156.5
		X-2		0.604	6.00	0.237	0.920		50.8	*	0.240	0.920	0.353	1.13	151.0
		H-9		0.600	6.01	0.243	0.940	TEST ENVIRONMENT	50.8	20.0	0.249	0.940	0.340	1.13	153.0
		H-8		0.598	6.00	0.252	0.925		50.8	1.0	0.258	0.925	0.330	1.08	154.5
7	4650	O-1		0.602	6.00	0.246	0.930		44.6	10.0	0.255	0.930	0.315	1.08	162.0
1	4520	O-2		0.600	6.00	0.249	0.920		44.6	12.0	0.258	0.920	0.343	1.11	159.0
6	4470														
9	5021	O-3		0.600	6.00	0.252	0.925		47.0	10.0	0.258	0.925	0.344	1.08	158.0
35	5555	O-4		0.599	6.00	0.252	0.920		47.0	10.0	0.261	0.920	0.365	1.14	150.4
87	5460														

133

FOLDOUT FRAME 2

ENVIRONMENT				DCB SPECIMEN DATA												SPECIMEN		
				SPECIMEN DETAILS							TEST DATA							
MEDIUM	PHASE	TEMPERATURE (°F)	PRESSURE (psig)	IDENTIFICATION	GROOVE SHAPE	THICKNESS, b (inch)	NET THICKNESS AT GROOVE, b_n (inch)	HEIGHT, h (inch)	INITIAL CRACK LENGTH, a_i (inch)	LOADING MEDIUM	JAW DISPLACEMENT (inch)	TEST DURATION (hours)	FINAL CRACK LENGTH, a_f (inch)	LOAD TO EFFECT JAW DISPLACEMENT (pounds)	IDENTIFICATION	CONFIGURATION (Figure Number)	THICKNESS (inch)
OXYGEN/DIFLUORIDE	GAS	AMB	30	OF-1	U	0.986	0.775	1.50	1.68	R.T. AIR	0.033	26.0	1.76	4910	OF-1		0.595
				OF-2	U	0.987	0.780	↑	1.71	↑	0.031	26.0	1.76	4300	OF-3		0.596
				OF-3	U	0.986	0.775		1.70		0.031	26.0	1.78	4460			
	LIQUID	-320	30	OF-4	U	0.986	0.775		1.69		0.035	31.5	1.82	5718	OF-2		0.601
				OF-5	U	0.988	0.775		1.68		0.035	31.5	1.82	5718	OF-4		0.604
				OF-6	U	0.989	0.780		1.71		0.035	31.5	1.82	5718			
FLOX	GAS	AMB	30	FX-1	U	0.979	0.770		1.70		0.031	28.0	1.73	4650	X-1		0.602
				FX-2	U	0.990	0.775		1.67		0.031	28.0	1.72	4620	FX-2		0.598
				FX-3	U	0.983	0.775		1.70		0.031	28.0	1.76	4550	FX-1		0.598
	LIQUID	-320	30	FX-4	U	0.989	0.775		1.69		0.035	31.0	1.83	5720	FX-3		0.597
				FX-5	U	0.990	0.775		1.72		0.035	31.0	1.77	6005	FX-4		0.600
				FX-6	U	0.990	0.780		1.69		0.035	31.0	1.78	5982			
FLUORINE	GAS	AMB	30	FL-1	U	0.985	0.775		1.70		0.031	33.0	1.75	4570			
				FL-2	U	0.986	0.775		1.68		0.031	33.0	1.76	4410			
				FL-3	U	0.986	0.775		1.69		0.031	33.0	1.75	4400			
	LIQUID	-320	30	FL-4	U	0.988	0.775		1.68		0.035	42.5	1.75	6183			
				FL-5	U	0.981	0.770	↓	1.71	↓	0.035	42.5	1.89	5319			
				FL-6	U	0.991	0.775	1.50	1.69	R.T. AIR	0.035	42.5	1.86	5500			

PRECEDING PAGE BLANK NOT FILMED

FOLDOUT FRAME   /

	LOAD TO EFFECT JAW DISPLACEMENT (pounds)	SURFACE FLAWED SPECIMEN DATA													
(inch)		SPECIMEN DETAILS							TEST DATA						
		IDENTIFICATION	CONFIGURATION (Figure Number)	THICKNESS (inch)	WIDTH (inch)	INITIAL FLAW DEPTH, a_i (inch)	INITIAL FLAW LENGTH, $2c_i$ (inch)	LOADING MEDIUM	GROSS STRESS (ksi)	TEST DURATION (hours)	FLAW DEPTH AFTER TEST RUN, a_f (inch)	FLAW LENGTH AFTER TEST RUN, $2c_f$ (inch)	FLAW DEPTH AFTER FATIGUE MARKING, a_{cr} (inch)	FLAW LENGTH AFTER FATIGUE MARKING, $2c_{cr}$ (inch)	AMBIENT TEMP. FAILURE LOAD (kips)
	4910	OF-1		0.595	5.97	0.243	0.925	↑	44.6	11.0	0.249	0.925	0.320	1.01	158.4
	4300	OF-3		0.596	6.00	0.243	0.915		44.6	10.4	0.249	0.915	0.320	1.02	156.6
	4460														
	5718	OF-2		0.601	5.97	0.240	0.925		47.0	10.0	0.249	0.925	0.320	1.00	159.6
	5718	OF-4		0.604	6.00	0.243	0.920		47.0	10.1	0.249	0.920	0.370	1.20	144.4
	5718														
	4650	X-1		0.602	6.00	0.243	0.920		44.6	10.0	0.246	0.920	0.310	1.08	161.0
	4620	FX-2		0.598	6.00	0.237	0.915		44.6	8.0	0.240	0.915	0.325	1.09	164.2
	4550	FX-1		0.598	6.00	0.240	0.915		44.6	0.3	0.246	0.915	0.370	1.34	142.4
	5720	FX-3		0.597	6.00	0.237	0.920		47.0	8.0	0.240	0.920	0.345	1.08	162.2
	6005	FX-4		0.600	6.00	0.246	0.920		47.0	10.1	0.249	0.920	0.365	1.07	157.8
	5982														
	4570							SEE SECTION 2.3.2							
	4410														
	4400														
	6183														
	5319														
	5500														

135

| ENVIRONMENT | | | | DCB SPECIMEN DATA | | | | | | | | | | | | SPECIMEN | |
| | | | | SPECIMEN DETAILS | | | | | | | TEST DATA | | | | | | | |
MEDIUM	PHASE	TEMPERATURE (°F)	PRESSURE (psig)	IDENTIFICATION	GROOVE SHAPE	THICKNESS, b (inch)	NET THICKNESS AT GROOVE, b_n (inch)	HEIGHT, h (inch)	INITIAL CRACK LENGTH, a_i (inch)	LOADING MEDIUM	JAW DISPLACEMENT (inch)	TEST DURATION (hours)	FINAL CRACK LENGTH, a_f (inch)	LOAD TO EFFECT JAW DISPLACEMENT (pounds)	IDENTIFICATION	CONFIGURATION (Figure Number)	THICKNESS (inch)	WIDTH
DISTILLED WATER + 3.5% NaCl	LIQUID	AMB	30	WS-1	V	0.951	0.765	1.50	1.72	R.T. AIR	0.035	143.0	1.73	4570	WS-1		0.898	5
				WS-2	V	0.951	0.765	↑	1.76	↑	0.035	239.5	1.77	4550	WS-2		0.902	5
				WS-3	V	0.951	0.765		1.79		0.037	407.8	1.82	4710				
DISTILLED WATER	LIQUID	AMB	30	WDW-1	V	0.954	0.765		1.78		0.035	143.0	1.78	4650	WDW-1		0.909	5
				WDW-2	V	0.951	0.760		1.86		0.035	239.3	1.86	4480	WDW-2		0.900	5
				WDW-3	V	0.953	0.770		1.85		0.035	407.0	1.85	4550				
TRICHLORO-ETHYLENE	LIQUID	AMB	30	WT-1	V	0.952	0.765		1.85		0.035	71.5	1.85	4480	WT-1		0.901	5
				WT-2	V	0.952	0.765		1.83		0.035	168.5	1.83	4400	WT-2		0.898	5
				WT-3	V	0.953	0.765		1.83		0.034	336.1	1.83	4550				
DYE PENETRANT	LIQUID	AMB	30	WDP-1	V	0.952	0.765		1.74		0.035	71.0	1.78	4930	WDP-1		0.899	5
				WDP-2	V	0.953	0.765	↓	1.83	↓	0.035	168.0	1.90	4720	WDP-2		0.900	5
				WDP-3	V	0.953	0.765	1.50	1.71	R.T. AIR	0.035	335.4	1.89	4680				

▷ SPECIMENS LOADED THAN UNLOADED IMMEDIATELY

		SURFACE FLAWED SPECIMEN DATA												
	SPECIMEN DETAILS							TEST DATA						
LOAD TO EFFECT JAW DISPLACEMENT (pounds)	IDENTIFICATION	CONFIGURATION (Figure Number)	THICKNESS (inch)	WIDTH (inch)	INITIAL FLAW DEPTH, a_i (inch)	INITIAL FLAW LENGTH, $2c_i$ (inch)	LOADING MEDIUM	GROSS STRESS (ksi)	TEST DURATION (hours)	FLAW DEPTH AFTER TEST RUN, a_f (inch)	FLAW LENGTH AFTER TEST RUN, $2c_f$ (inch)	FLAW DEPTH AFTER FATIGUE MARKING, a_{cr} (inch)	FLAW LENGTH AFTER FATIGUE MARKING, $2c_{cr}$ (inch)	AMBIENT TEMP. FAILURE LOAD (kips)
4570	WS–1		0.898	5.90	0.420	1.475		22.0	23.9	0.495	1.475	0.770	2.50	98.0
4550	WS–2		0.902	5.90	0.435	1.465		22.0	14.6	0.465	1.465	0.620	1.80	119.0
4710														
4650	WDW–1		0.909	5.90	0.415	1.475		21.0	▷	0.457	1.475	0.690	2.08	105.0
4480	WDW–2		0.900	5.90	0.420	1.475		22.0	15.8	0.455	1.475	0.620	1.85	114.6
4550														
4480	WT–1		0.901	5.90	0.430	1.475		18.0	▷	0.440	1.475	0.710	2.05	104.0
4400	WT–2		0.898	5.90	0.425	1.480	TEST ENVIRONMENT	22.0	12.0	0.455	1.480	0.770	2.35	100.0
4550														
4930	WDP–1		0.899	5.90	0.425	1.465		20.0	▷	0.447	1.465	0.740	2.18	105.0
4720	WDP–2		0.900	5.90	0.430	1.460		22.0	16.0	0.463	1.460	0.580	1.80	116.0
4680														

137

ENVIRONMENT				DCB SPECIMEN DATA											SPECIM...		
				SPECIMEN DETAILS							TEST DATA						
MEDIUM	PHASE	TEMPERATURE (°F)	PRESSURE (psig)	IDENTIFICATION	GROOVE SHAPE	THICKNESS, b (inch)	NET THICKNESS AT GROOVE, b_n (inch)	HEIGHT, h (inch)	INITIAL CRACK LENGTH, a_i (inch)	LOADING MEDIUM	JAW DISPLACEMENT (inch)	TEST DURATION (hours)	FINAL CRACK LENGTH, a_f (inch)	LOAD TO EFFECT JAW DISPLACEMENT (pounds)	IDENTIFICATION	CONFIGURATION (Figure Number)	THICKNESS (inch)
HYDROGEN	GAS	AMB	30	WH-1	V	0.952	0.770	1.50	1.75	R.T. AIR	0.036	6.8	1.75	5150			
				WH-2	V	0.954	0.770	↑	1.83	↑	0.035	23.0	1.83	5100	WH-1		0.908
				WH-3	V	0.954	0.775		1.80		0.035	30.5	1.80	4550			
	GAS	AMB	100	WH-4	V	0.954	0.770		1.89		0.035	6.0	1.89	4130			
				WH-5	V	0.954	0.770		1.78		0.035	22.8	1.78	4500	WH-3		0.904
				WH-6	V	0.953	0.765		1.87		0.035	30.3	1.87	4470			
	GAS	-320	30	WH-7	V	0.952	0.770		1.89		0.035	43.7	1.89	4275	WH-5		0.90
				WH-8	V	0.951	0.770	↓	1.86		0.035	43.7	1.86	4355	WH-7		0.89
				WH-9	V	0.952	0.770	1.50	1.91		0.035	43.7	1.91	4225			
	GAS	-413	AMB												WH-8		0.89
															WH-14		0.91
															WH-10		0.90
															W423-2		0.90
															WH-9		0.90
	GAS	-423	AMB												WH-11		0.90
															WO-4		0.92
OXYGEN	GAS	AMB	30	WO-1	V	0.953	0.765	1.50	1.80		0.035	7.3	1.86	4560	WO-1		0.89
				WO-2	V	0.952	0.760	↑	1.71		0.035	23.3	1.71	4950	WO-2		0.90
				WO-3	V	0.952	0.770		1.78		0.035	30.8	1.78	4540			
	LIQUID	-320	30	WO-4	V	0.952	0.765		1.84		0.035	49.5	1.84	4355	WO-3		0.89
				WO-5	V	0.953	0.760	↓	1.90	↓	0.035	49.5	1.90	4250	WS-1		0.90
				WO-6	V	0.953	0.760	1.50	1.90	R.T. AIR	0.034	49.5	1.90	4250			

* SPECIMENS LOADED TO INDICATED STRESS LEVEL THAN UNLOADED IMMEDIATELY

** SPECIMEN FAILED 3 MINUTES AFTER MAXIMUM LOAD WAS OBTAINED

PRECEDING PAGE BLANK NOT FILMED

FOLDOUT FRAME

FINAL CRACK LENGTH, a_f (inch)	LOAD TO EFFECT JAW DISPLACEMENT (pounds)	SURFACE FLAWED SPECIMEN DATA													
		SPECIMEN DETAILS							TEST DATA						
		IDENTIFICATION	CONFIGURATION (Figure Number)	THICKNESS (inch)	WIDTH (inch)	INITIAL FLAW DEPTH, a_i (inch)	INITIAL FLAW LENGTH, $2c_i$ (inch)	LOADING MEDIUM	GROSS STRESS (ksi)	TEST DURATION (hours)	FLAW DEPTH AFTER TEST RUN, a_f (inch)	FLAW LENGTH AFTER TEST RUN, $2c_f$ (inch)	FLAW DEPTH AFTER FATIGUE MARKING, a_{cr} (inch)	FLAW LENGTH AFTER FATIGUE MARKING, $2c_{cr}$ (inch)	AMBIENT TEMP. FAILURE LOAD (kips)
1.75 / 5150, 1.83 / 5100, 1.80 / 4550		WH-1		0.908	5.90	0.440	1.500		22.0	13.4	0.475	1.500	0.490	1.52	134.0
1.89 / 4130, 1.78 / 4500, 1.87 / 4470		WH-3		0.900	5.90	0.440	1.480		22.0	14.9	0.470	1.480	0.540	1.59	126.0
1.89 / 4275		WH-5		0.905	5.90	0.425	1.475	TEST ENVIRONMENT	25.0	10.0	0.536	1.475	0.570	1.80	114.5
1.86 / 4355		WH-7		0.897	5.90	0.425	1.470		25.0	*	0.450	1.470	0.540	1.67	122.0
1.91 / 4225		WH-8		0.890	5.90	0.410	1.465		25.0	10.0	0.480	1.465	0.590	1.75	110.0
		WH-14		0.913	5.88	0.400	1.480		22.0	10.0	0.420	1.480	0.630	1.78	111.0
		WH-10		0.909	5.90	0.417	1.465		25.0	*	0.462	1.465	0.580	1.68	120.0
		W423-2		0.900	5.90	0.420	1.480		22.0	*	0.431	1.480	0.640	1.82	112.0
		WH-9		0.903	5.89	0.415	1.460		26.5	**0.05			SPECIMEN FAILED		
		WH-11		0.902	5.90	0.433	1.475		22.0	12.3	0.453	1.475	0.630	1.80	111.6
		WO-4		0.921	5.90	0.425	1.480		25.6	11.1	0.495	1.490	0.590	1.68	120.4
1.86 / 4560		WO-1		0.893	5.90	0.425	1.475		22.0	13.5	0.460	1.475	0.560	1.70	120.4
1.71 / 4950, 1.78 / 4540		WO-2		0.906	5.88	0.450	1.485		22.0	9.8	0.485	1.485	0.590	1.95	118.0
1.84 / 4355		WO-3		0.895	5.90	0.410	1.485		25.0	10.0	0.470	1.485	0.570	1.72	118.0
1.90 / 4250, 1.90 / 4250		WS-1		0.903	5.90	0.430	1.460		25.0	*	0.465	1.460	0.710	2.20	100.0

139

Table A6: 2219 ALUMINUM WELD METAL STRESS CORROSION DA[TA]
FLUORINE, FLOX AND OF$_2$

ENVIRONMENT				DCB SPECIMEN DATA											SPECIME[N]		
				SPECIMEN DETAILS							TEST DATA						
MEDIUM	PHASE	TEMPERATURE (°F)	PRESSURE (psig)	IDENTIFICATION	GROOVE SHAPE	THICKNESS, b (inch)	NET THICKNESS AT GROOVE, b_n (inch)	HEIGHT, h (inch)	INITIAL CRACK LENGTH, a_i (inch)	LOADING MEDIUM	JAW DISPLACEMENT (inch)	TEST DURATION (hours)	FINAL CRACK LENGTH, a_f (inch)	LOAD TO EFFECT JAW DISPLACEMENT (pounds)	IDENTIFICATION	CONFIGURATION (Figure Number)	THICKNESS (inch)
OXYGEN/DIFLUORIDE	GAS	AMB	30	WOF-1	V	0.954	0.750	1.50	1.78	R. T. AIR	0.035	26.0	1.78	4550	WOF-2		0.917
				WOF-2	V	0.953	0.755	↑	1.84	↑	0.035	26.0	1.84	4290	WOF-1		0.900
				WOF-3	V	0.954	0.760		1.90		0.035	26.0	1.90	4350	WOF-5		0.924
	LIQUID	-320	30	WOF-4	V	0.950	0.755		1.82		0.035	31.5	1.82	4130	WOF-4		0.908
				WOF-5	V	0.954	0.760		1.96		0.035	31.5	1.96	4500	WOF-6		0.898
				WOF-6	V	0.952	0.760		1.75		0.035	31.5	1.75	4470			
FLOX	GAS	AMB	30	WFX-1	V	0.953	0.770		1.76		0.035	28.0	1.77	4410	WFX-1		0.908
				WFX-2	V	0.951	0.775		1.80		0.035	28.0	1.84	3950	WFX-2		0.905
				WFX-3	V	0.951	0.755		1.85		0.035	28.0	1.87	4050			
	LIQUID	-320	30	WFX-4	V	0.954	0.760		1.83		0.035	31.0	1.84	4420	WFX-3		0.910
				WFX-5	V	0.953	0.755		1.84		0.035	31.0	1.87	4325	WFX-4		0.895
				WFX-6	V	0.953	0.755		1.82		0.035	31.0	1.82	4420			
FLUORINE	GAS	AMB	30	WFL-1	V	0.952	0.750		1.82		0.035	33.0	1.82	4040			
				WFL-2	V	0.953	0.750		1.68		0.035	33.0	1.68	4580			
				WFL-3	V	0.948	0.755		1.85		0.035	33.0	1.85	4110			
	LIQUID	-320	30	WFL-4	V	0.952	0.755		1.74		0.035	42.5	1.74	4825			
				WFL-5	V	0.954	0.760	↓	1.80	↓	0.035	42.5	1.80	4565			
				WFL-6	V	0.951	0.770	1.50	1.81	R. T. AIR	0.035	42.5	1.81	4525			

	SURFACE FLAWED SPECIMEN DATA												
(pounds)	SPECIMEN DETAILS						TEST DATA						
(pounds)	IDENTIFICATION	CONFIGURATION (Figure Number)	THICKNESS (inch)	WIDTH (inch)	INITIAL FLAW DEPTH, a_i (inch)	INITIAL FLAW LENGTH, $2c_i$ (inch)	LOADING MEDIUM	GROSS STRESS (ksi)	TEST DURATION (hours)	FLAW DEPTH AFTER TEST RUN, a_f (inch)	FLAW LENGTH AFTER TEST RUN, $2c_f$ (inch)	FLAW DEPTH AFTER FATIGUE MARKING, a_{cr} (inch)	FLAW LENGTH AFTER FATIGUE MARKING, $2c_{cr}$ (inch)	AMBIENT TEMP. FAILURE LOAD (kips)
50	WOF–2		0.917	5.90	0.430	1.475		22.0	9.6	0.470	1.475	0.560	1.65	128.0
00	WOF–1		0.900	5.90	0.425	1.475		22.0	10.0	0.465	1.475	0.900	2.65	87.0
50	WOF–5		0.924	5.90	0.425	1.480		22.0	10.1	0.465	1.480	0.720	2.15	104.2
30	WOF–4		0.908	5.90	0.423	1.475		22.0	6.6	0.453	1.475	0.520	1.60	124.8
00	WOF–6		0.898	5.90	0.415	1.470		22.0	10.0	0.435	1.470	0.580	1.70	113.0
70														
10	WFX–1		0.908	5.90	0.425	1.465		22.0	3.0	0.465	1.465	0.580	1.68	121.0
60	WFX–2		0.905	5.90	0.420	1.450		22.0	10.0	0.460	1.450	0.650	1.95	113.0
50														
20	WFX–3		0.910	5.90	0.425	1.470		22.0	8.0	0.450	1.470	0.580	1.70	118.0
25	WFX–4		0.895	5.90	0.420	1.460		22.0	11.3	0.445	1.470	0.600	1.90	120.0
20														
40														
30							SEE SECTION 2.3.2							
10														
25														
65														
25														

141

Table A7a: 5Al-2.5Sn (ELI) TITANIUM BASE METAL STRESS CORROSIO
FOR NONHAZARDOUS ENVIRONMENTS

MEDIUM	PHASE	TEMPERATURE (°F)	PRESSURE (psig)	IDENTIFICATION	GROOVE SHAPE	THICKNESS, b (inch)	NET THICKNESS AT GROOVE, b_n (inch)	HEIGHT, h (inch)	INITIAL CRACK LENGTH, a_i (inch)	LOADING MEDIUM	JAW DISPLACEMENT (inch)	TEST DURATION (hours)	FINAL CRACK LENGTH, a_f (inch)	LOAD TO EFFECT JAW DISPLACEMENT (pounds)	IDENTIFICATION	CONFIGURATION (Figure Number)	THICKNESS (inch)	WIDTH
DISTILLED WATER	LIQUID	AMB	30	TW-1	V	0.348	0.240	1.50	1.65	R.T. AIR	0.058	74.2	1.73	5600				
				TW-2	V	0.348	0.241	↑	1.65	↑	0.059	142.6	1.67	5650	TDW-1		0.398	4.
				TW-3	V	0.348	0.240		1.66		0.059	237.6	1.71	5750				
DISTILLED WATER & 3.5% NaCl	LIQUID	AMB	30	TS-1	V	0.346	0.240		1.67		0.058	71.9	1.73	5410				
				TS-2	V	0.346	0.240		1.66		0.058	136.8	1.72	5560	TS-1		0.399	4.
				TS-3	V	0.346	0.238		1.68		0.058	233.3	1.72	5680				
ACETONE	LIQUID	AMB	30	TA-1	V	0.348	0.238		1.66		0.059	72.6	1.68	5760				
				TA-2	V	0.346	0.238		1.65		0.060	130.3	1.68	5730	TA-1		0.395	4.
				TA-3	V	0.346	0.240		1.66		0.059	232.9	1.71	5560				
METHYL ALCOHOL	LIQUID	AMB	30	TM-1	V	CRACK GREW OUT OF PLANE					0.059			2440				
				TM-2	V	0.348	0.240		1.64		0.049	136.9	2.42	3950	TM-1		0.399	4.
				TM-4	V	0.348	0.233		1.76		0.049	237.5	3.30	1450				
METHYL ALCOHOL (DILUTE)	LIQUID	AMB	30	TMD-1	V	0.344	0.236		1.64		0.057	90.3	1.73	5230				
				TMD-2	V	0.346	0.236		1.63		0.059	162.2	1.72	5420	TMD-1		0.391	4.
				TMD-3	V	0.349	0.240		1.63		0.059	258.3	1.72	5450				
METHYL ETHYL KETONE	LIQUID	AMB	30	TME-1	V	0.346	0.240		1.66		0.058	70.0	1.70	5500				
				TME-2	V	0.344	0.240		1.64		0.059	146.1	1.70	5600	TME-1		0.398	4.
				TME-3	V	0.346	0.238		1.65		0.060	237.6	1.73	5470				
ETHYL ALCOHOL	LIQUID	AMB	30	TE-1	V	0.348	0.240		1.66		0.059	68.0	1.77	5350				
				TE-2	V	0.346	0.238	↓	1.64	↓	0.059	143.8	1.66	5680	TE-1		0.395	4
				TE-3	V	0.348	0.240	1.50	1.64	R.T. AIR	0.059	235.6	1.67	5570				

FOLDOUT FRAME

(inch)	LOAD TO EFFECT JAW DISPLACEMENT (pounds)	SURFACE FLAWED SPECIMEN DATA													
		SPECIMEN DETAILS							TEST DATA						
		IDENTIFICATION	CONFIGURATION (Figure Number)	THICKNESS (inch)	WIDTH (inch)	INITIAL FLAW DEPTH, a_i (inch)	INITIAL FLAW LENGTH, $2c_i$ (inch)	LOADING MEDIUM	GROSS STRESS (ksi)	TEST DURATION (hours)	FLAW DEPTH AFTER TEST RUN, a_f (inch)	FLAW LENGTH AFTER TEST RUN, $2c_f$ (inch)	FLAW DEPTH AFTER FATIGUE MARKING, a_{cr} (inch)	FLAW LENGTH AFTER FATIGUE MARKING, $2c_{cr}$ (inch)	AMBIENT TEMP. FAILURE LOAD (kips)
	5600														
	5650	TDW-1		0.398	4.00	0.156	0.930	↑	86.0	16.0	0.184	0.930	THRU	1.43	74.8
	5750														
3	5410														
2	5560	TS-1		0.399	4.00	0.156	0.935		86.0	0.01	SPECIMEN FAILED DURING SUSTAINED LOADING				
2	5680														
3	5760														
3	5730	TA-1		0.395	4.00	0.157	0.940		86.0	12.1	0.186	0.945	THRU	1.41	76.2
1	5560														
	2440														
2	3950	TM-1		0.399	4.00	0.166	0.935		86.0	16.2	0.214	1.100	THRU	1.72	65.0
0	1450														
3	5230														
2	5420	TMD-1		0.391	4.00	0.152	0.870	TEST ENVIRONMENT	86.0	5.0	SPECIMEN FAILED DURING SUSTAINED LOADING				
2	5450														
0	5500														
0	5600	TME-1		0.398	4.00	0.166	0.940		86.0	12.0	0.196	1.035	THRU	1.48	74.3
73	5470														
77	5350														
66	5680	TE-1		0.395	4.00	0.170	0.950		86.0	14.5	0.200	0.960	THRU	1.37	76.6
67	5570														

143

Table A7b: 5Al-2.5Sn (ELI) TITANIUM BASE METAL STRESS CORROSION DA... FOR NONHAZARDOUS ENVIRONMENTS (Cont.)

MEDIUM	PHASE	TEMPERATURE (°F)	PRESSURE (psig)	IDENTIFICATION	GROOVE SHAPE	THICKNESS, b (inch)	NET THICKNESS AT GROOVE, b_n (inch)	HEIGHT, h (inch)	INITIAL CRACK LENGTH, a_i (inch)	LOADING MEDIUM	JAW DISPLACEMENT (inch)	TEST DURATION (hours)	FINAL CRACK LENGTH, a_f (inch)	LOAD TO EFFECT JAW DISPLACEMENT (pounds)	IDENTIFICATION	CONFIGURATION (Figure Number)	THICKNESS (inch)	WIDTH (inch)
ALCOHOL (DILUTE)	LIQUID	AMB	30	TED-1	V	0.348	0.240	1.50	1.65	R.T. AIR	0.059	77.0	1.68	5650				
				TED-2	V	0.348	0.240	↑	1.62	↑	0.059	144.7	1.68	5615	TED-1		0.392	4.00
				TED-3	V	0.348	0.240		1.62		0.059	239.7	1.66	5620				
PENETRANT	LIQUID	AMB	30	TD-1	V	0.344	0.238		1.64		0.059	69.0	1.76	5640				
				TD-2	V	0.347	0.240	↓	1.64	↓	0.059	145.0	1.73	5880	TDP-1		0.396	4.00
				TD-3	V	0.346	0.240	1.50	1.59	R.T. AIR	0.059	236.3	1.69	5840				

FOLDOUT FRAME

		SURFACE FLAWED SPECIMEN DATA													
DATA		SPECIMEN DETAILS							TEST DATA						
FINAL CRACK LENGTH, a_f (inch)	LOAD TO EFFECT JAW DISPLACEMENT (pounds)	IDENTIFICATION	CONFIGURATION (Figure Number)	THICKNESS (inch)	WIDTH (inch)	INITIAL FLAW DEPTH, a_i (inch)	INITIAL FLAW LENGTH, $2c_i$ (inch)	LOADING MEDIUM	GROSS STRESS (ksi)	TEST DURATION (hours)	FLAW DEPTH AFTER TEST RUN, a_f (inch)	FLAW LENGTH AFTER TEST RUN, $2c_f$ (inch)	FLAW DEPTH AFTER FATIGUE MARKING, a_{cr} (inch)	FLAW LENGTH AFTER FATIGUE MARKING, $2c_{cr}$ (inch)	AMBIENT TEMP. FAILURE LOAD (kips)
1.68	5630														
1.68	5615	TED-1		0.392	4.00	0.178	0.965	TEST ENVIRONMENT	86.0	16.0	0.238	1.250	THRU	1.52	70.1
1.66	5620														
1.76	5640														
1.73	5880	TDP-1		0.396	4.00	0.204	1.035		86.0	0.08	SPECIMEN FAILED DURING SUSTAINED LOADING				
1.69	5840														

145

Table A8: 5Al–2.5Sn (ELI) TITANIUM BASE METAL STRESS COR
DATA FOR HYDROGEN AND HELIUM

ENVIRONMENT				DCB SPECIMEN DATA												SPECIMEN			
				SPECIMEN DETAILS							TEST DATA								
MEDIUM	PHASE	TEMPERATURE (°F)	PRESSURE (psig)	IDENTIFICATION	GROOVE SHAPE	THICKNESS, b (inch)	NET THICKNESS AT GROOVE, b_n (inch)	HEIGHT, h (inch)	INITIAL CRACK LENGTH, a_i (inch)	LOADING MEDIUM	JAW DISPLACEMENT (inch)	TEST DURATION (hours)	FINAL CRACK LENGTH, a_f (inch)	LOAD TO EFFECT JAW DISPLACEMENT (pounds)	IDENTIFICATION	CONFIGURATION (Figure Number)	THICKNESS (inch)	WIDTH
HYDROGEN	GAS	AMB	30	TH–1	V	0.347	0.248	1.50	1.65	R.T. AIR	0.059	6.0	1.76	5530	TH–9		0.399	4.
				TH–2	V	0.347	0.244	↑	1.67	↑	0.059	21.0	1.72	5400				
				TH–3	V	0.347	0.240		1.68		0.059	30.0	1.73	5520				
	GAS	AMB	100	TH–4	V	0.347	0.244		1.67		0.059	6.5	1.73	5630	TAR–2		0.396	4.
				TH–5	V	0.348	0.244		1.63		0.059	23.5	2.10	3980				
				TH–6	V	0.348	0.238		1.62		0.059	30.5	1.64	5290				
				THE–5	V	0.347	0.244		1.62		0.059	32.8	2.02	4780				
	GAS	–320	30	TH–7	V	0.347	0.248		1.63		0.031	31.8	1.65	3460	T320–4		0.357	2
				TH–8	V	0.345	0.246		1.63		0.031	31.8	1.63	3525	T320–6		0.354	2
				TH–9	V	0.348	0.246		1.66		0.031	31.8	1.66	3415				
	GAS	–413	AMB	TH–10	V	0.343	0.240		1.66		0.027	46.0	1.66	2970	TH–1		0.355	1
				TH–11	V	0.345	0.244	↓	1.66		0.027	46.0	1.72	2805	TH–2 / TH–3		0.356 / 0.356	1 / 1
				TH–12	V	0.350	0.246	1.50	1.65		0.027	46.0	1.65	3010	TH–4		0.355	1
	LIQUID	–423	AMB												TH–5		0.355	1
															TH–6		0.355	1
HELIUM	GAS	AMB	30	THE–1	V	0.348	0.248	1.50	1.69		0.059	6.0	1.72	5480	TAR–1		0.398	4
				THE–2	V	0.344	0.246	↑	1.65		0.059	23.0	1.68	5500				
				THE–3	V	0.347	0.250		1.66		0.059	30.5	1.69	5540				
	GAS	–423	30	THE–7	V	0.347	0.244		1.66		0.027	42.3	1.69	2885	THE–4		0.355	1
				THE–8	V	0.345	0.244	↓	1.61		0.027	42.3	1.62	3100				
				THE–9	V	0.347	0.246	1.50	1.64	↓	0.027	42.3	1.65	3010				
	GAS	AMB	1000							R.T. AIR					THE–2		0.395	4
															THE–3		0.388	4

*LOAD-UNLOAD

(hours)	FINAL CRACK LENGTH, a_f (inch)	LOAD TO EFFECT JAW DISPLACEMENT (pounds)	SURFACE FLAWED SPECIMEN DATA													
			SPECIMEN DETAILS						LOADING MEDIUM	TEST DATA						
			IDENTIFICATION	CONFIGURATION (Figure Number)	THICKNESS (inch)	WIDTH (inch)	INITIAL FLAW DEPTH, a_i (inch)	INITIAL FLAW LENGTH, $2c_i$ (inch)		GROSS STRESS (ksi)	TEST DURATION (hours)	FLAW DEPTH AFTER TEST RUN, a_f (inch)	FLAW LENGTH AFTER TEST RUN, $2c_f$ (inch)	FLAW DEPTH AFTER FATIGUE MARKING, a_{cr} (inch)	FLAW LENGTH AFTER FATIGUE MARKING, $2c_{cr}$ (inch)	AMBIENT TEMP. FAILURE LOAD (kips)
	1.76	5530	TH-9		0.399	4.00	0.164	0.960	↑	80.0	12.0	0.174	0.960	THRU	1.61	110.2
	1.72	5400														
	1.73	5520														
	1.73	5630	TAR-2		0.396	4.01	0.168	0.940		80.0	10.0	0.181	0.940	THRU	1.63	108.3
	2.10	3980														
	1.64	5290														
	2.02	4780														
	1.65	3460	T320-4		0.357	2.50	0.121	0.525		126.0	10.0	0.126	0.525	THRU	0.950	79.8
	1.63	3525	T320-6		0.354	2.50	0.117	0.525		126.0	10.1	0.124	0.525	THRU	0.980	77.0
	1.66	3415														
	1.66	2970	TH-1		0.355	1.10	0.087	0.261		139.3	1.0	0.087	0.261	0.140	0.325	43.4
	1.72	2805	TH-2		0.356	1.10	0.084	0.255		139.3	20.0	0.084	0.255	0.097	0.275	44.9
			TH-3		0.356	1.10	0.085	0.261		123.8	10.0	0.085	0.261	0.158	0.340	42.5
	1.65	3010	TH-4		0.355	1.10	0.086	0.264		139.3	*	0.086	0.264	0.136	0.330	42.1
			TH-5		0.355	1.10	0.081	0.255		139.3	20.0	0.081	0.255	0.200	0.430	39.7
			TH-6		0.355	1.10	0.090	0.285		139.3	1.0	0.090	0.285	0.135	0.320	43.3
.0	1.72	5480	TAR-1		0.398	4.00	0.178	0.950	TEST ENVIRONMENT	80.0	10.0	0.188	0.950	THRU	1.50	114.8
.0	1.68	5500														
.5	1.69	5540														
.3	1.69	2885	THE-4		0.355	1.10	0.089	0.264		139.3	10.0	0.089	0.264	0.123	0.285	44.3
.3	1.62	3100														
.3	1.65	3010														
			THE-2		0.395	4.00	0.166	0.970		80.0	12.0	0.191	0.970	THRU	1.42	116.7
			THE-3		0.388	4.00	0.174	0.950		80.0	12.0	0.189	0.950	THRU	1.40	117.0

ENVIRONMENT				DCB SPECIMEN DATA												SPECIME		
				SPECIMEN DETAILS							TEST DATA							
MEDIUM	PHASE	TEMPERATURE (°F)	PRESSURE (psig)	IDENTIFICATION	GROOVE SHAPE	THICKNESS, b (inch)	NET THICKNESS AT GROOVE, b_n (inch)	HEIGHT, h (inch)	INITIAL CRACK LENGTH, a_i (inch)	LOADING MEDIUM	JAW DISPLACEMENT (inch)	TEST DURATION (hours)	FINAL CRACK LENGTH, a_f (inch)	LOAD TO EFFECT JAW DISPLACEMENT (pounds)	IDENTIFICATION	CONFIGURATION (Figure Number)	THICKNESS (inch)
DYE PENETRANT	LIQUID	AMB	30	TWD-1	V	0.310	0.232	1.50	1.73	R. T. AIR	0.069	65.6	2.68	2810	TDPW-1		0.334
				TWD-2	V	0.316	0.220	↑	1.68	↑	0.070	144.0	2.80	2600	TDPW-2		0.338
				TWD-3	V	0.316	0.230		1.65		0.070	238.1	2.87	3050			
DISTILLED WATER	LIQUID	AMB	30	TWW-1	V	0.317	0.228		1.65		0.071	71.6	1.73	5820			
				TWW-2	V	0.317	0.225		1.64		0.070	146.6	1.68	5680	TDWW-1		0.338
				TWW-3	V	0.317	0.227		1.65		0.070	237.5	1.76	5880			
DISTILLED WATER + 3.5% NaCl WATER	LIQUID	AMB	30	TWS-1	V	0.317					0.070						
				TWS-2	V	0.317	0.225		1.67		0.071	148.6	1.82	5280	TSW-1		0.334
				TWS-3	V	0.318	0.230		1.62		0.068	239.6	1.70	5420			
METHYL ALCOHOL	LIQUID	AMB	30	TWM-1	V	0.317	0.226		1.67		0.059	236.0	2.08	3500			
				TWM-2	V	0.315	0.223		1.68		0.063	141.3	1.92	4450	TMW-1		0.329
				TWM-3	V	0.310	0.228		1.70		0.064	67.5	2.03	4250			
METHYL ALCOHOL (DILUTE)	LIQUID	AMB	30	TWMD-1	V	0.313	0.231		1.68		0.071	71.3	1.95	5070			
				TWMD-2	V	0.316	0.233		1.75		0.071	166.5	2.07	4680	TMDW-1		0.333
				TWMD-3	V	0.317	0.224		1.70		0.071	234.7	1.97	4890			
ACETONE	LIQUID	AMB	30	TWA-1	V	0.317	0.228		1.72		0.069	70.7	1.72	5720			
				TWA-2	V	0.317	0.222		1.70		0.070	145.6	1.73	5510	TAW-1		0.333
				TWA-3	V	0.318	0.225		1.68		0.070	236.6	1.79	5550			
ETHYL ALCOHOL	LIQUID	AMB	30	TWE-1	V	0.317	0.222		1.68		0.072	65.6	1.76	5760			
				TWE-2	V	0.316	0.227	↓	1.70	↓	0.070	143.5	1.77	5560	TEW-1		0.327
				TWE-3	V	0.317	0.227	1.50	1.70	R. T. AIR	0.072	237.7	1.81	5190			

FOLDOUT FRAME

		SURFACE FLAWED SPECIMEN DATA												
TA		SPECIMEN DETAILS						TEST DATA						
LENGTH, a_f (inch)	LOAD TO EFFECT JAW DISPLACEMENT (pounds)	IDENTIFICATION	CONFIGURATION (Figure Number)	THICKNESS (inch)	WIDTH (inch)	INITIAL FLAW DEPTH, a_i (inch)	INITIAL FLAW LENGTH, $2c_i$ (inch)	LOADING MEDIUM	GROSS STRESS (ksi)	TEST DURATION (hours)	FLAW DEPTH AFTER TEST RUN, a_f (inch)	FLAW LENGTH AFTER TEST RUN, $2c_f$ (inch)	FLAW DEPTH AFTER FATIGUE MARKING, a_{cr} (inch)	FLAW LENGTH AFTER FATIGUE MARKING, $2c_{cr}$ (inch)	AMBIENT TEMP. FAILURE LOAD (kips)
.68	2810	TDPW-1		0.334	3.26	0.174	0.950	↑	86.0	0.08	SPECIMEN FAILED DURING SUSTAINED LOADING				
.80	2600	TDPW-2		0.338	3.25	0.173	0.955		55.0	47.0	0.300	1.090	THRU	1.12	93.2
.87	3050														
.73	5820														
.68	5680	TDWW-1		0.338	3.25	0.176	0.950		86.0	24.0	0.179	0.950	THRU	1.29	80.6
.76	5880														
.82	5280	TSW-1		0.334	3.25	0.174	0.940		86.0	0.02	SPECIMEN FAILED DURING SUSTAINED LOADING				
.70	5420														
.08	3500														
.92	4450	TMW-1		0.329	3.25	0.172	0.955		86.0	0.6	0.240	0.970	THRU	1.26	78.8
.03	4250														
.95	5070														
.07	4680	TMDW-1		0.333	3.25	0.170	0.960		86.0	2.2	SPECIMEN FAILED DURING SUSTAINED LOADING				
.97	4890														
.72	5720								TEST ENVIRONMENT							
.73	5510	TAW-1		0.333	3.25	0.174	0.960		86.0	18.2	0.177	0.960	THRU	1.37	74.2
.79	5550														
.76	5760														
.77	5560	TEW-1		0.327	3.25	0.185	0.945		86.0	121.0	0.190	0.945	THRU	1.29	78.2
.81	5190														

FOLDOUT FRAME 2

ENVIRONMENT				DCB SPECIMEN DATA												SPECIM		
				SPECIMEN DETAILS							TEST DATA							
MEDIUM	PHASE	TEMPERATURE (°F)	PRESSURE (psig)	IDENTIFICATION	GROOVE SHAPE	THICKNESS, b (inch)	NET THICKNESS AT GROOVE, b_n (inch)	HEIGHT, h (inch)	INITIAL CRACK LENGTH, a_i (inch)	LOADING MEDIUM	JAW DISPLACEMENT (inch)	TEST DURATION (hours)	FINAL CRACK LENGTH, a_f (inch)	LOAD TO EFFECT JAW DISPLACEMENT (pounds)	IDENTIFICATION	CONFIGURATION (Figure Number)	THICKNESS (inch)
ETHYL ALCOHOL (DILUTE)	LIQUID	AMB	AMB	TWED-1	V	0.317	0.225	1.50	1.66	R. T. AIR	0.071	71.8	1.73	5800	TEDW-1		0.324
				TWED-2	V	0.316	0.225	↑	1.68	↑	0.071	167.0	1.75	5580			
				TWED-3	V	0.317	0.227		1.68		0.071	234.8	1.76	5540			
METHYL ETHYL KETONE	LIQUID	AMB	AMB	TWME-1	V	0.316	0.248		1.66		0.071	66.8	1.73	5910	TMEW-1		0.337
				TWME-2	V	0.318	0.238	↓	1.71	↓	0.070	145.1	1.76	5730			
				TWME-3	V	0.317	0.234	1.50	1.70	R. T. AIR	0.069	239.1	1.78	5540			

PRECEDING PAGE BLANK NOT FILMED

FOLDOUT FRAME

...A		SURFACE FLAWED SPECIMEN DATA														
LENGTH, a_i (inch)	LOAD TO EFFECT JAW DISPLACEMENT (pounds)	SPECIMEN DETAILS							TEST DATA							
		IDENTIFICATION	CONFIGURATION (Figure Number)	THICKNESS (inch)	WIDTH (inch)	INITIAL FLAW DEPTH, a_i (inch)	INITIAL FLAW LENGTH, $2c_i$ (inch)	LOADING MEDIUM	GROSS STRESS (ksi)	TEST DURATION (hours)	FLAW DEPTH AFTER TEST RUN, a_f (inch)	FLAW LENGTH AFTER TEST RUN, $2c_f$ (inch)	FLAW DEPTH AFTER FATIGUE MARKING, a_{cr} (inch)	FLAW LENGTH AFTER FATIGUE MARKING, $2c_{cr}$ (inch)	AMBIENT TEMP. FAILURE LOAD (kips)
3	5800														
5	5580	TEDW-1		0.324	3.26	0.172	0.945	TEST ENVIRONMENT	86.0	12.0	0.210	0.970	THRU	1.21	78.9
6	5540														
3	5910														
6	5730	TMEW-1		0.337	3.25	0.173	0.940		86.0	21.4	SPECIMEN FAILED DURING SUSTAINED LOADING				
8	5540														

Table A10: 5Al-2.5Sn (ELI) TITANIUM WELD METAL STRESS CORROSIO[...]
FOR HYDROGEN AND HELIUM

MEDIUM	PHASE	TEMPERATURE (°F)	PRESSURE (psig)	IDENTIFICATION	GROOVE SHAPE	THICKNESS, b (inch)	NET THICKNESS AT GROOVE, b_n (inch)	HEIGHT, h (inch)	INITIAL CRACK LENGTH, a_i (inch)	LOADING MEDIUM	JAW DISPLACEMENT (inch)	TEST DURATION (hours)	FINAL CRACK LENGTH, a_f (inch)	LOAD TO EFFECT JAW DISPLACEMENT (pounds)	IDENTIFICATION	CONFIGURATION (Figure Number)	THICKNESS (inch)	WIDTH
HYDROGEN	GAS	AMB	30	TWH-1	V	0.316	0.228	1.50	1.66	R.T. AIR	0.070	8.8	1.74	5980	TWH-1A		0.334	3.
	GAS	AMB	30	TWH-2	V	0.318	0.224	↑	1.68	↑	0.070	23.5	1.80	5580				
	GAS	AMB	30	TWH-3	V	0.317	0.228		1.70		0.070	32.8	1.88	5460				
	GAS	AMB	100	TWH-4	V	0.318	0.226		1.72		0.070	9.0	1.86	5380	TWH-3A		0.344	3.
	GAS	AMB	100	TWH-5	V	0.317	0.222		1.68		0.070	23.5	1.84	5310				
	GAS	AMB	100	TWH-6	V	0.316	0.226		1.68		0.070	2.8	1.81	5400				
	GAS	-320	30	TWH-7	V	0.319	0.226		1.68		0.042	31.9	1.78	4125	TWH-31		0.331	2.
	GAS	-320	30	TWH-8	V	0.319	0.228		1.68		0.042	31.9	1.79	4080	TWH-35		0.338	2.
	GAS	-320	30	TWH-9	V	0.316	0.224		1.68		0.042	31.9	1.68	4200				
	GAS	-413	AMB	TWH-10	V	0.317	0.222		1.67		0.033	46.0	1.67	3310	TWH-1		0.339	1.
	GAS	-413	AMB	TWH-11	V	0.315	0.226	↓	1.66		0.033	46.0	1.66	3320	TWH-2 TWH-3		0.338 0.337	1. 1.
	GAS	-413	AMB	TWH-12	V	0.317	0.230	1.50	1.65		0.033	46.0	1.82	3180	TWH-4		0.335	1.
	LIQUID	-423	AMB												TWH-5		0.331	1.
															TWH-6		0.338	1.
HELIUM	GAS	AMB	30	TWHE-1	V	0.316	0.226	1.50	1.63		0.070	7.0	1.72	5900	TWHE-1		0.337	3.
	GAS	AMB	30	TWHE-2	V	0.318	0.218	↑	1.67		0.070	23.5	1.86	5720	W-22		0.337	3.
	GAS	AMB	30	TWHE-3	V	0.316	0.226		1.63		0.070	31.0	1.88	5500				
	GAS	-423	30	TWHE-4	V	0.318	0.223		1.67		0.033	42.3	1.72	3270	TWH-36		0.338	1.
	GAS	-423	30	TWHE-5	V	0.316	0.224	↓	1.64	↓	0.033	42.3	1.82	3180				
	GAS	-423	30	TWHE-6	V	0.315	0.224	1.50	1.66	R.T. AIR	0.033	42.3	1.74	3170				
	GAS	AMB	1000												W-23		0.341	3.
															W-24		0.337	3.

FOLDOUT FRAME

...NIUM WELD METAL STRESS CORROSION DATA
...O HELIUM

(hours)	FINAL CRACK LENGTH, a_f (inch)	LOAD TO EFFECT JAW DISPLACEMENT (pounds)	IDENTIFICATION	CONFIGURATION (Figure Number)	THICKNESS (inch)	WIDTH (inch)	INITIAL FLAW DEPTH, a_i (inch)	INITIAL FLAW LENGTH, $2c_i$ (inch)	LOADING MEDIUM	GROSS STRESS (ksi)	DURATION (hours)	FLAW DEPTH AFTER TEST RUN, a_f (inch)	FLAW LENGTH AFTER TEST RUN, $2c_f$ (inch)	FLAW DEPTH AFTER FATIGUE MARKING, a_{cr} (inch)	FLAW LENGTH AFTER FATIGUE MARKING, $2c_{cr}$ (inch)	AMBIENT TEMP. FAILURE LOAD (kips)
8	1.74	5980														
5	1.80	5580	TWH-1A		0.334	3.25	0.176	0.955		80.0	9.0	0.176	0.955	THRU	1.24	85.8
8	1.88	5460														
0	1.86	5380														
5	1.84	5310	TWH-3A		0.344	3.25	0.170	0.945		80.0	8.7	0.170	0.945	THRU	1.25	88.0
8	1.81	5400														
9	1.78	4125	TWH-31		0.331	2.31	0.120	0.523		95.4	12.0	0.120	0.523	0.174	0.560	84.8
9	1.79	4080	TWH-35		0.338	2.30	0.132	0.530		95.4	12.0	0.132	0.530	0.250	0.620	81.2
9	1.68	4200														
0	1.67	3310	TWH-1		0.339	1.10	0.095	0.270		124.0	0.5	0.099	0.270	0.212	0.450	39.1
0	1.66	3320	TWH-2		0.338	1.10	0.090	0.264		124.0	11.9	0.090	0.264	0.138	0.336	42.7
0	1.82	3180	TWH-3		0.337	1.10	0.092	0.272		110.0	11.0	0.092	0.272	0.153	0.435	40.5
			TWH-4		0.335	1.10	0.092	0.264		124.0	—	0.092	0.264	0.152	0.425	40.2
			TWH-5		0.331	1.10	0.090	0.266		124.0	1.0	0.090	0.266	0.178	0.430	41.7
			TWH-6		0.338	1.10	0.090	0.264		124.0	8.6	0.090	0.264	0.193	0.560	39.0
0	1.72	5900	TWHE-1		0.337	3.25	0.170	0.950		85.0	15.1	0.170	0.950	0.257	1.12	100.5
5	1.86	5720	W-22		0.337	3.25	0.176	0.940	TEST ENVIRONMENT	86.0	10.0	0.182	0.940	0.294	1.04	99.3
0	1.88	5500														
3	1.72	3270	TWH-36		0.338	1.10	0.090	0.255		124.0	10.0	0.090	0.255	0.174	0.347	42.8
3	1.82	3180														
3	1.74	3170														
			W-23		0.341	3.25	0.170	0.950		86.0	10.0	0.180	0.950	0.234	0.98	109.5
			W-24		0.337	3.25	0.178	0.950		86.0	10.0	0.193	0.950	0.231	1.00	106.5

ENVIRONMENT				DCB SPECIMEN DATA												SPECIMEN		
				SPECIMEN DETAILS							TEST DATA							
MEDIUM	PHASE	TEMPERATURE (°F)	PRESSURE (psig)	IDENTIFICATION	GROOVE SHAPE	THICKNESS, b (inch)	NET THICKNESS AT GROOVE, b_n (inch)	HEIGHT, h (inch)	INITIAL CRACK LENGTH, a_i (inch)	LOADING MEDIUM	JAW DISPLACEMENT (inch)	TEST DURATION (hours)	FINAL CRACK LENGTH, a_f (inch)	LOAD TO EFFECT JAW DISPLACEMENT (pounds)	IDENTIFICATION	CONFIGURATION (Figure Number)	THICKNESS (inch)
3.5% NaCl	LIQUID	AMB	AMB	ST-1	V	0.983	0.780	1.50	1.66		0.036	91.2	2.09	4160			
				SL-1	V	0.985	0.775		1.64		0.034	90.5	1.68	5600			
DISTILLED WATER	LIQUID	AMB	AMB	DWT-1	V	0.984	0.775		1.65	TEST ENVIRONMENT	0.036	90.3	2.08	3980			
				DWL-1	V	0.983	0.780		1.65		0.034	90.2	1.72	4480			
TRICHLO-ROETHY-LENE	LIQUID	AMB	AMB	TT-1	V	0.983	0.775		1.69		0.034	89.8	2.14	4000			
				TL-1	V	0.978	0.780		1.65		0.035	89.6	1.66	4660			
DYE PENE-TRANT	LIQUID	AMB	AMB	DPT-1	V	0.983	0.775		1.63		0.033	89.2	1.97	4500			
				DPL-1	V	0.983	0.775	1.50	1.65		0.034	89.1	1.71	5610			

FOLDOUT FRAME

| | TEST DATA | | SURFACE FLAWED SPECIMEN DATA | | | | | | | | TEST DATA | | | | | |
| | | | | SPECIMEN DETAILS | | | | | | | | | | | | |
TEST DURATION (hours)	FINAL CRACK LENGTH, a_f (inch)	LOAD TO EFFECT JAW DISPLACEMENT (pounds)	IDENTIFICATION	CONFIGURATION (Figure Number)	THICKNESS (inch)	WIDTH (inch)	INITIAL FLAW DEPTH, a_i (inch)	INITIAL FLAW LENGTH, $2c_i$ (inch)	LOADING MEDIUM	GROSS STRESS (ksi)	TEST DURATION (hours)	FLAW DEPTH AFTER TEST RUN, a_f (inch)	FLAW LENGTH AFTER TEST RUN, $2c_f$ (inch)	FLAW DEPTH AFTER FATIGUE MARKING, a_{cr} (inch)	FLAW LENGTH AFTER FATIGUE MARKING, $2c_{cr}$ (inch)	AMBIENT TEMP. FAILURE LOAD (kips)
91.2	2.09	4160														
90.5	1.68	5600														
90.3	2.08	3980														
90.2	1.72	4480														
89.8	2.14	4000														
89.6	1.66	4660														
89.2	1.97	4500														
89.1	1.71	5610														

ENVIRONMENT				DCB SPECIMEN DATA											SPEC		
				SPECIMEN DETAILS							TEST DATA						
MEDIUM	PHASE	TEMPERATURE (°F)	PRESSURE (psig)	IDENTIFICATION	GROOVE SHAPE	THICKNESS, b (inch)	NET THICKNESS AT GROOVE, b_n (inch)	HEIGHT, h (inch)	INITIAL CRACK LENGTH, a_i (inch)	LOADING MEDIUM	JAW DISPLACEMENT (inch)	TEST DURATION (hours)	FINAL CRACK LENGTH, a_f (inch)	LOAD TO EFFECT JAW DISPLACEMENT (pounds)	IDENTIFICATION	CONFIGURATION (Figure Number)	THICKNESS
DISTILLED WATER		AMB	AMB	TWT–1	V	0.325	0.232	1.50	1.61		0.059	118.0	1.63	5140			
				TWL–1	V	0.322	0.224		1.59		0.058	118.2	1.75	4950			
3.5% NaCl		AMB	AMB	TST–1	V	0.323	–		–		0.058	116.3	$\boxed{1}$	–			
				TSL–1	V	0.323	0.228		1.60		0.058	116.2	3.65	1250			
ACETONE		AMB	AMB	TAT–1	V	0.322	0.236		1.62		0.058	115.3	1.66	5120			
				TAL–1	V	0.321	0.236		1.63		0.058	114.8	1.65	5040			
DYE PENETRANT		AMB	AMB	TDT–1	V	0.322	0.228		1.60		0.058	114.0	1.90	4180			
				TDL–1	V	0.323	0.240		1.61		0.059	113.8	2.74	2280			
METHYL ALCOHOL (DILUTE)		AMB	AMB	TMDT–1	V	0.323	0.232		1.59		0.058	118.5	2.0l	3800			
				TMDL–1	V	0.324	0.226		1.61		0.058	118.3	3.27	145C			
METHYL ALCOHOL KETONE		AMB	AMB	TMET–1	V	0.321	0.228		1.60		0.058	138.5	1.64	5400			
				TMEL–1	V	0.324	0.228		1.61		0.058	138.3	1.64	4990			
ETHYL ALCOHOL (PURE)		AMB	AMB	TET–1	V	0.323	0.232		1.63		0.058	137.5	1.66	5320			
				TEL–1	V	0.324	0.228		1.61		0.059	137.3	1.68	5180			
ETHYL ALCOHOL (DILUTE)	LIQUID	AMB	AMB	TEDT–1	V	0.325	0.236		1.62		0.059	119.5	1.81	4800			
				TEDL–1	V	0.323	0.228	1.50	1.60		0.059	119.3	2.22	3250			

$\boxed{1}$ SUSTAINED GROWTH OUT OF PLANE

| | | SURFACE FLAWED SPECIMEN DATA | | | | | | | | | | | | | |
| | | SPECIMEN DETAILS | | | | | | TEST DATA | | | | | | | |
LENGTH, a_f (inch)	LOAD TO EFFECT JAW DISPLACEMENT (pounds)	IDENTIFICATION	CONFIGURATION (Figure Number)	THICKNESS (inch)	WIDTH (inch)	INITIAL FLAW DEPTH, a_i (inch)	INITIAL FLAW LENGTH, $2c_i$ (inch)	LOADING MEDIUM	GROSS STRESS (ksi)	TEST DURATION (hours)	FLAW DEPTH AFTER TEST RUN, a_f (inch)	FLAW LENGTH AFTER TEST RUN, $2c_f$ (inch)	FLAW DEPTH AFTER FATIGUE MARKING, a_{cr} (inch)	FLAW LENGTH AFTER FATIGUE MARKING, $2c_{cr}$ (inch)	AMBIENT TEMP. FAILURE LOAD (kips)
.63	5140														
.75	4950														
1	–														
.65	1250														
.66	5120														
.65	5040														
.90	4180														
.74	2280														
.01	3800														
.27	1450														
.64	5400														
.64	4990														
.66	5320														
.68	5180														
.81	4800														
2.22	3250														

157

FOLDOUT FRAME 2

Table B1: COMPLIANCE DATA FOR 2219 ALUMINUM DCB SPECIMENS

CONDITION	TEST TEMP (^{o}F)	SPECIMEN NUMBER	SIDE GROOVE SHAPE	DEPTH	CRACK LENGTH (IN.)	COMPLIANCE IN/LB X 10^6	a_0 (IN.)	(K_z) CRIT KSI $\sqrt{IN.}$
BASE METAL	72	AR20-1	SEMI-CIRCULAR	0.10	1.77 2.00 2.26 2.52 2.77 3.00	5.00 6.45 8.27 10.68 12.94 15.67	0.86 0.89 0.90 0.95 0.94 0.97	32.2
		AR20-2	SEMI-CIRCULAR	0.10	1.75 2.00 2.25 2.50 2.80	4.86 6.64 8.28 10.42 13.26	0.85 0.90 0.91 0.94 0.94	
		AR20-2A	SEMI-CIRCULAR	0.10	1.70	4.66	0.86	31.6
	-320	AR20-3	SEMI-CIRCULAR	0.10	1.74	4.40	0.88	38.4
		AR20-4	SEMI-CIRCULAR	0.10	1.75	4.29	0.81	37.7
WELD METAL	72	AW-1	VEE	0.10	1.65	4.70	0.90	–
		AW-3	VEE	0.10	1.68	4.68	0.87	–
		AW-2	VEE	0.10	1.62	4.60	0.89	–
	-320	AW-5	VEE	0.10	1.65	4.48	0.90	–

NOTE: BASE METAL SPECIMENS 1.00 INCH THICK
WELD METAL SPECIMENS 0.95 INCH THICK

PRECEDING PAGE BLANK NOT FILMED

Table B2: COMPLIANCE DATA FOR 5Al-2.5 Sn (ELI) TITANIUM 0.375-INCH THICK DCB SPECIMENS

CONDITION	TEST TEMP (°F)	SPECIMEN NUMBER	SIDE GROOVE		CRACK LENGTH (IN.)	COMPLIANCE IN/LB X 10^6	a_0 (IN.)	K_Q KSI $\sqrt{\text{IN.}}$
			SHAPE	DEPTH				
BASE METAL	72	TV20-1	VEE	0.038	1.77 2.00 2.25	7.80 9.92 12.45	0.75 0.75 0.75	—
		TR30-1	SEMI-CIRCULAR	0.056	1.77 2.05 2.30	8.12 10.71 13.48	0.79 0.79 0.79	—
		TV30-1	VEE	0.056	1.66 1.94	6.49 9.54	0.69 0.77	—
	-320	TR30-2	SEMI-CIRCULAR	0.056	1.77 2.10	6.57 9.05	0.65 0.63	
		TV20-2	VEE	0.038	1.77	7.09	0.73	67.6

Table B3: COMPLIANCE DATA FOR 5Al-2.5 Sn (ELI) TITANIUM 0.350-INCH THICK DCB SPECIMENS

CONDITION	TEST TEMP (°F)	SPECIMEN NUMBER	SIDE GROOVE		CRACK LENGTH (IN.)	COMPLIANCE IN/LB X 10^6	a_0 (IN.)	K_Q KSI $\sqrt{\text{IN.}}$
			SHAPE	DEPTH				
BASE METAL	72	T-5	VEE	0.053	1.62 1.85 2.11	7.22 9.34 12.09	0.77 0.78 0.78	—
		T-1	VEE	0.053	1.60	7.18	0.79	115
		T-2	VEE	0.053	1.63	7.29	0.77	—
	-320	T-3	VEE	0.053	1.61	6.64	0.77	59
	-423	THE-4	VEE	0.053	1.65	7.00	0.80	51
WELD METAL	72	TW2	VEE	0.053	1.61	7.87	0.75	—
		TW3	VEE	0.053	1.67	8.79	0.80	—
	-320	TW1	VEE	0.053	1.66	7.46	0.72	81.7
	-423	TW4	VEE	0.053	1.67	7.43	0.78	58.0

Table B4: COMPARISON OF MICROMETER AND CLIP GAGE DISPLACEMENT MEASUREMENTS FOR ALUMINUM BASE METAL DCB SPECIMENS

LOAD (LBS)	WHEN PIN LOADED IN TEST MACHINE		WHEN WEDGE LOADED IN VISE	
	CLIP GAGE READING (IN.)	MICROMETER READING (IN.)	CLIP GAGE READING (IN.)	MICROMETER READING (IN.)
0	0	0	0	0
1,000	0.0062	0.0057	0.0072	0.0068
2,000	0.0124	0.0117	0.0131	0.0121
3,000	0.0186	0.0176	0.0190	0.0178
4,000	0.0248	0.0237	0.0250	0.0235
0	0	0	0	0

161

Table C1: SUMMARY OF TEST SPECIMENS

PROGRAM PHASE	MATERIAL	TEST		SPECIMEN TYPE	SPECIMEN CONFIG (FIGURE NO.)
		TYPE	TEMP (°F)		
I	A1-2219-T87 BASE METAL	MECHANICAL PROPERTY SUSTAINED LOAD SUSTAINED LOAD	ALL ALL ALL	TENSILE DCB SF	C10a C8 C1
	A1-2219-T87 WELD METAL	MECHANICAL PROPERTY SUSTAINED LOAD SUSTAINED LOAD	ALL ALL ALL	TENSILE DCB SF	C10a C8 C2
	Ti-5A1-2.55N BASE METAL	MECHANICAL PROPERTY SUSTAINED LOAD (SL) SUSTAINED LOAD (SL) SL VARIABLE THICKNESS SL VARIABLE THICKNESS SL VARIABLE THICKNESS	ALL ALL 72 72 -320 -423	TENSILE DCB SF SF SF SF	C9a C8 C3 C5 C6 C7
	Ti-5A1-2.55N WELD METAL	MECHANICAL PROPERTY SUSTAINED LOAD SUSTAINED LOAD	ALL ALL 72 -320 -423	TENSILE DCB SF SF SF	C9a C8 C4 C5 C6
II	ALL ALUMINUM ALLOYS	MECHANICAL PROPERTY PROOF OVERLOAD SUSTAINED LOAD	ALL ALL ALL	TENSILE SF SF	C10a C11 C11
	Ti-6A1-4V Ti-5A1-2.55N	MECHANICAL PROPERTY MECHANICAL PROPERTY	ALL ALL	TENSILE TENSILE	C10b C9
	ALL TITANIUM ALLOYS	SUSTAINED LOAD	ALL	SF	C12